ANALYTICAL INVESTIGATION OF AASHTO LRFD RESPONSE MODIFICATION FACTORS AND SEISMIC PERFORMANCE LEVELS OF CIRCULAR BRIDGE COLUMNS

A THESIS SUBMITTED TO
THE GRADUATE SCHOOL OF NATURAL AND APPLIED SCIENCES
OF
MIDDLE EAST TECHNICAL UNIVERSITY

BY

ARDA ERDEM

IN PARTIAL FULFILLMENT OF THE REQUIREMENTS
FOR
THE DEGREE OF MASTER OF SCIENCE
IN
CIVIL ENGINEERING

APRIL 2010

Approval of the thesis:

ANALYTICAL INVESTIGATION OF AASHTO LRFD RESPONSE MODIFICATION FACTORS AND SEISMIC PERFORMANCE LEVELS OF CIRCULAR BRIDGE COLUMNS

submitted by **ARDA ERDEM** in partial fulfillment of the requirements for the degree of **Master of Science in Civil Engineering Department, Middle East Technical University** by,

Prof. Dr. Canan Özgen
Dean, Graduate School of **Natural and Applied Sciences** _______________

Prof. Dr. Güney Özcebe
Head of Department, **Civil Engineering** _______________

Asst. Prof. Dr. Alp Caner
Supervisor, **Civil Engineering Dept., METU** _______________

Examining Committee Members:

Prof. Dr. Polat Gülkan
Civil Engineering Dept., METU _______________

Asst. Prof. Dr. Alp Caner
Civil Engineering Dept., METU _______________

Assoc. Prof. Dr. Uğurhan Akyüz
Civil Engineering Dept., METU _______________

Assoc. Prof. Dr. Murat Altuğ Erberik
Civil Engineering Dept., METU _______________

Yeşim Esat (Civil Engineer, M.S)
Vice General Director, _______________
Division of Bridge Survey and Design,
General Directorate of Highways

Date: 09.04.2010

I hereby declare that all information in this document has been obtained and presented in accordance with academic rules and ethical conduct. I also declare that, as required by these rules and conduct, I have fully cited and referenced all material and results that are not original to this work.

Name, Last name : Arda Erdem

Signature :

ABSTRACT

ANALYTICAL INVESTIGATION OF AASHTO LRFD RESPONSE MODIFICATION FACTORS AND SEISMIC PERFORMANCE LEVELS OF CIRCULAR BRIDGE COLUMNS

Erdem, Arda
M.S., Department of Civil Engineering
Supervisor: Asst. Prof. Dr. Alp Caner

April 2010, 193 pages

Current seismic design approach of bridge structures can be categorized into two distinctive methods: (i) force based and (ii) performance based. AASHTO LRFD seismic design specification is a typical example of force based design approach especially used in Turkey. Three different importance categories are presented as “Critical Bridges”, “Essential Bridges” and “Other Bridges” in AASHTO LRFD. These classifications are mainly based on the serviceability requirement of bridges after a design earthquake. The bridge’s overall performance during a given seismic event cannot be clearly described. Serviceability requirements specified for a given importance category are assumed to be assured by using different response modification factors. Although response modification factor is directly related with strength provided to resisting column, it might be correlated with selected performance levels including different engineering response measures.

Within the scope of this study, 27216 single circular bridge column bent models designed according to AASHTO LRFD and having varying column aspect ratio, column diameter, axial load ratio, response modification factor and elastic design spectrum data are investigated through a series of analyses such as response spectrum analysis and push-over analysis. Three performance levels such as “Fully

Functional", "Operational" and "Delayed Operational" are defined in which their criteria are selected in terms of column drift measure corresponding to several damage states obtained from column tests. Using the results of analyses, performance categorization of single bridge column bents is conducted. Seismic responses of investigated cases are identified with several measures such as capacity over inelastic demand displacement and response modification factor.

Keywords: Single Circular Bridge Column Bent, Seismic Design, AASHTO LRFD, Seismic Performance Level, Response Modification Factor

ÖZ

AASHTO LRFD DAVRANIŞ MODİFİKASYON FAKTÖRLERİNİN VE DAİRESEL KÖPRÜ KOLONLARININ PERFORMANS SEVİYELERİNİN ANALİTİK OLARAK İRDELENMESİ

Erdem, Arda

Yüksek Lisans, İnşaat Mühendisliği Bölümü

Tez Yöneticisi: Yrd. Doç. Dr. Alp Caner

Nisan 2010, 193 sayfa

Köprüler için mevcut sismik tasarım yöntemi iki belirgin başlık altında sınıflandırılabilir: (i) kuvvet esaslı ve (ii) performans esaslı. AASHTO LRFD sismik tasarım şartnamesi kuvvet esaslı tasarım yönteminin özellikle Türkiye'de kullanılan tipik bir örneğidir. Buna göre, "Kritik Köprüler", "Gerekli Köprüler" ve "Diğer Köprüler" olmak üzere üç farklı önem kategorisi tanımlanmıştır.Bu sınıflandırmalar, çoğunlukla tasarım depremi sonrasındaki kullanışlılık gereksinimleri gözönüne alınarak mesnetlendirilmiştir. Sismik olay boyunca köprünün genel performansı açık bir biçimde tanımlanamamıştır. Belirlenmiş önem kategorisi için tayin edilmiş kullanışlık gereksinimleri farklı davranış modifikasyon faktörlerinin kullanılmasıyla sağlanacağı kabul edilir. Davranış modifikasyon faktörü doğrudan doğruya direnç gösteren kolona sağlanan mukavemet ile ilintili olmasına rağmen,bu faktör farklı mühendislik tepki ölçüleri de dahil olmak üzere tayin edilmiş performans seviyeleri ile ilişkilendirilebilir.

Bu çalışma kapsamında, AASHTO LRFD 'ye göre tasarımlanmış ve değişken kolon boy/çap oranı, kolon çapı, eksenel yük oranı, davranış modifikasyon faktörü ve elastik tepki spekrum datasına sahip 27216 münferit dairesel köprü kolon modeli, tepki spektrum analizi ve artımsal itme analizi gibi bir dizi analiz aracığıyla irdelenmiştir. “Tam Fonsiyonel”, “İşlevsel” ve “Geciktirilmiş İşlevsel” olmak üzere kriterleri kolon deneylerinden gözlenmiş muhtelif hasar durumlarına tekabül eden kolon ötelenme ölçütüne göre seçilmiş üç farklı performans seviyesi tanımlanmıştır. Analiz sonuçları kullanılarak münferit köprü kolonlarının performans sınıflandırması yapılmıştır. İrdenlenmiş durumların sismik davranışları, inelastik deplasman kapasite istem oranı ve davranış modifikasyon faktörü gibi muhtelif ölçülere göre belirlenmiştir.

Anahtar Kelimeler: Münferit Dairesel Köprü Kolonu, Sismik Tasarım, AASHTO LRFD, Sismik Performans Seviyesi, Davranış Modifikasyon Faktörü

To the ones who love me…

ACKNOWLEDGEMENTS

I would like to express very special thanks to my supervisor Asst. Prof. Dr. Alp CANER for his guidance, support, advice and patience during this study.

I am indebted to my colleagues and friends Kamil ERGÜNER and Doğu BOZALİOĞLU for providing me help for analyses and computer aided drawings.

I am grateful to Murat BALLIOĞLU, head of the company I have worked recently, for his patience and tolerance he has provided me by exempting me from work so that I can study and complete my thesis.

I wish to thank all of my friends for their finite supports helping me get through the difficult times. Merih AÇIKEL deserves special thanks for revising the manuscript of the thesis.

I would like to thank sincerely my beloved parent especially my mother. Without her concrete conviction and patience, this thesis would never exist.

TABLE OF CONTENTS

LIST OF TABLES

TABLES

LIST OF FIGURES

FIGURES

CHAPTER 1

INTRODUCTION

Current seismic design approach of bridge structures can be categorized into two distinctive methods: (i) force-based and (ii) performance-based. In both methods, the weakest link is always envisioned to be columns of the bridge. Permitting flexural damages, bridge columns can minimize other types of damage that may occur at the superstructure or foundation level. In force-based design approach, the column moments calculated from elastic dynamic analysis are reduced by the appropriate response modification factor (R-factor) to allow acceptable flexural damage since the main feature of force-based design approach is the R-factor. Basis of R-factor is mainly by virtue of ductility at section and member level and energy absorption capacity of the columns [1]. Inelastic hinges are permitted where they can be readily inspected and/or repaired. Capacity protection design of structural members is proceeded to prevent brittle failure as shear.

In performance-based design, a different nomenclature of displacement-based design, the level of deformation imposed on the structure in conjunction with quantification of degree of damage is the main issue [2]. Performance objective defined in design is in line with a desired level of service and repair effort. Strength of the structural member is determined optimally so that a given performance objective related to a defined level of damage, under a specific level of seismic intensity, is achieved [3]. This process requires quantification of the damage level in terms of engineering demand measures for a presumed performance objective. It is generally selected to be concrete and steel strains, drift and displacement ductility demand. Displacement-based design approach provides uniform risk, in other words, the degree of protection provided against damage under a given seismic intensity is supposed to be uniform [3].

1.1. Background on AASHTO [4] and AASHTO LRFD [5]

For the seismic design of bridge structures, AASHTO [4] and AASHTO LRFD [5] specifications are commonly used all over the world especially in Turkey. AASHTO [4] seismic design guidelines define acceleration coefficient, site coefficient, importance classification and seismic performance category. Bridges are classified as “Essential” and “Other” in terms of importance classification that affects seismic performance category at the end. According to the 1998 Commentary [4], essential bridges are defined as “Those that must continue to function after an earthquake”. Its classification is recommended according to Social/Survival and Security Defense requirements. For example, transportation routes to critical facilities such as hospitals, police and fire stations and communications centers must continue to function and bridges required for this purpose should be classified as “Essential”. Instead of defining damage level, it mostly mentions serviceability of the bridge after a 475-year return period of earthquake, which corresponds to 10% probability of exceedance in 50 years. This classification does not imply more than does “Life Safety or Collapse Prevention” as a performance level. The only consequence of entitling a bridge as “Essential” is observed in seismic performance category (SPC) D in which acceleration coefficient is larger than 0.29 for a given site. It should be noted that SPC C and D have the same requirements for minimum support length, column transverse reinforcement, confinement at plastic hinges and seismic detailing issues except several recommendations on foundation design as liquefaction, settlement and rocking.

Contrary to AASHTO [4], there are several differences in terms of seismic design in AASHTO LRFD [5]. Concerning Commentary C.3.10.1 [5], the principles used for the development of these specifications are;

- Small to moderate earthquakes should be resisted within the elastic range of the structural components without significant damage.
- Realistic seismic ground motion intensities and forces should be used in the design procedure.
- Exposure to shaking from large earthquakes should not cause collapse of all or part of the bridge. Where possible, damage that does occur should be readily detectable and accessible for inspection and repair.

Even though AASHTO LRFD [5] gives more satisfactory explanations on performance level of the bridge, it mainly results in "Minimal or Fully Functional" for a design earthquake and "Life Safety or Collapse Prevention" for a large earthquake as a performance level. Importance categories are divided into three as "Critical Bridges", "Essential Bridges" or "Other Bridges". According to Commentary C3.10.3 [5], essential bridges are generally those that should, as a minimum, be open to emergency vehicles and for security/defense purposes immediately after the design earthquake, i.e., a 475-year return period event. However, some bridges must remain open to all traffic after the design earthquake and be usable by emergency vehicles and for security/defense purposes immediately after a large earthquake, e.g., a 2500-year return period event. These bridges should be regarded as critical structures. Although seismic hazard map used in specification is prepared for a 475-year return period event, it is required to have a usable bridge after a 2500-year return period event. Given the fact that there is no seismic hazard map for a 2500-year return period event in AASHTO LRFD [5], the only way to have a design for a large earthquake is to manipulate the response modification factor for different importance category. Instead of having a higher spectral acceleration for a large earthquake, substructure is designed for higher flexural strength using a lower R-factor. As shown in the Table 1.1, bridges designated as "Critical" are to be designed with R-factor of *1.5* for a single column substructure that is the focus of this thesis. It is lower than the value of *3.0*, which is proposed in AASHTO [4] regardless of importance category.

Table 1.1 Response Modification Factors-Substructures [5]

Substructure	Importance Category		
	Critical	Essential	Other
Wall-type piers-larger dimension	1.5	1.5	2.0
Reinforced concrete pile bents			
- Vertical piles only	1.5	2.0	3.0
- With batter piles	1.5	1.5	2.0
Single columns	1.5	2.0	3.0
Steel or composite steel and concrete pile bents			
- Vertical piles only	1.5	3.5	5.0
- With batter piles	1.5	2.0	3.0
Multiple column bents	1.5	3.5	5.0

1.2. Aim and Scope of the study

In force-based seismic design approach, focus is on flexural strength of the bridge column. Therefore, the bridge's overall performance during a given seismic event cannot be clearly described [6]. Performance levels other than "Life Safety or Collapse Prevention" are paid very little attention. Although bridge importance categories specified in AASHTO LRFD [5] mainly touch upon the serviceability issue of the bridge after the design earthquake, they do not mention corresponding performance level in terms of damage level and repair effort. Nevertheless, R-factor, which is known to be based on consensus, engineering judgement and the performance of highway bridges in previous earthquakes seems to be a key design parameter to assure serviceability corresponding to a specified bridge importance category. In the light of these facts, the purpose of this study can be summarized with the following items;

- To assess performance level of an idealized single degree of freedom (SDOF) circular bridge column designed optimally according to AASHTO LRFD [5] for varying R-factor, column aspect ratio, column diameter, normalized axial load level, acceleration coefficient and soil site classification.

- To relate statistical results of response modification factors either with selected performance levels or with varying bridge importance categories.
- To develop a better understanding of any correlation between R-factor and specified performance levels.

Within the scope of this study, two groups of analysis are undertaken. An Excel VBA (Visual Basic for Applications) code is developed due to loaded analysis requirements as optimum section design, moment curvature analysis, pushover analysis and interaction among them. In the first group of analysis, single bridge columns seismically designed with respect to predefined range of R-factor are statistically studied. Several conclusions for stiffness modification factor, yield curvature, moment magnification factor, response modification factor and displacement ductility are drawn. In the second group of analysis, upper bound value of the R-factor is estimated for presumed performance level with several modifications of the analysis tool developed for the first group of analysis. In addition to R-factor, capacity over elastic and inelastic displacement is studied in terms of column aspect ratio and period of vibration. Expressions are derived corresponding to given performance level to be used in seismic design preliminarily.

Following this introduction, background information on force based design rudiments and response modification factor are given in Chapter 2. In addition, several concepts related to performance based design approach are introduced. Performance criteria, limit states and related demand parameters are discussed comprehensively. Besides, inelastic displacement coefficients are examined considering soil site effects. In Chapter 3, analysis tool developed for the parametric studies is explained in details that include analysis assumptions, input parameters, theory and formulations followed by specification. Results of moment curvature analysis, second order effect and optimum section design in terms of longitudinal reinforcement are verified with commercially available softwares. Definitions of related engineering measures studied in this study are also introduced within the content of this chapter. Chapter 4 is devoted to analysis results and findings. Lastly, limitations and conclusions of the study are given in Chapter 5.

CHAPTER 2

LITERATURE REVIEW

2.1. Background on Force-Based Design and Response Modification Factor

To understand the basis of response modification factor, it is required to review the force-based design procedure as it is currently applied in seismic design codes.

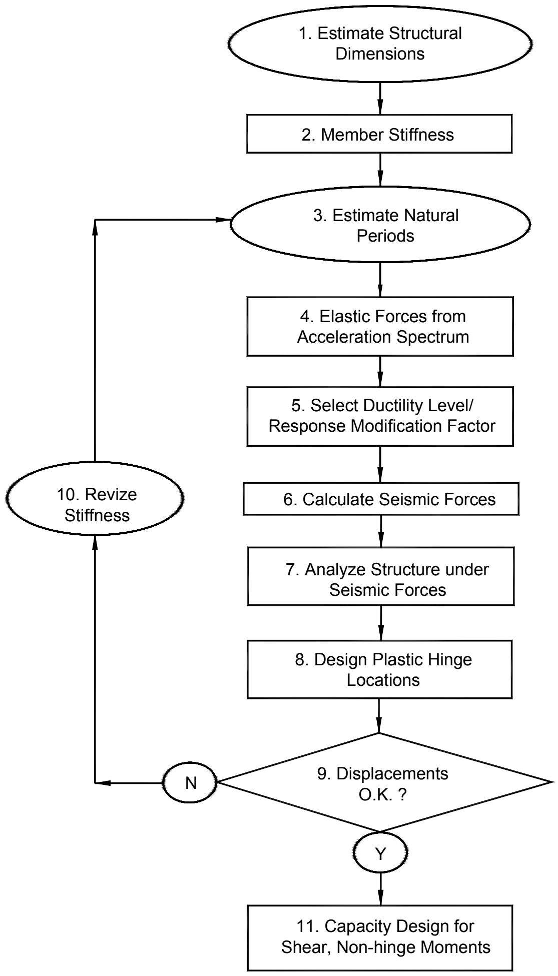

Figure 2.1 Sequence of Operations for Force-Based Design [3]

Per Figure 2.1, elastic seismic forces are computed for a given unreduced acceleration spectrum. Seismic flexural forces are reduced by response modification factor to provide a guaranteed uniform ductility based on the assumption of “Equal Displacement Rule”. Elastic displacement of structure determined from elastic dynamic analysis is believed to be equal to inelastic displacement determined from non-linear time history analysis. Therefore, ductility reduction factor, R_μ, becomes equal to displacement ductility, μ_Δ, defined in Eq.(2.2) and Eq.(2.4), respectively. However, equal-displacement approximation is inappropriate for both very short and very long-period structures, and is also of doubtful validity for medium period structures when the hysteretic character of the inelastic system deviates significantly from elasto-plastic response per Priestley et al. [3].

Designing a bridge responding elastically to large earthquakes can result in uneconomical solutions. By taking advantage of the inherent energy dissipation capacity of the structural elements, inelastic deformation in column can be achieved by dividing the elastically computed flexural force effects by an appropriate R-factor shown in Figure 2.2. Ductility capacity is attained by restrictive detailing requirements for structural components expecting to yield during strong ground motion.

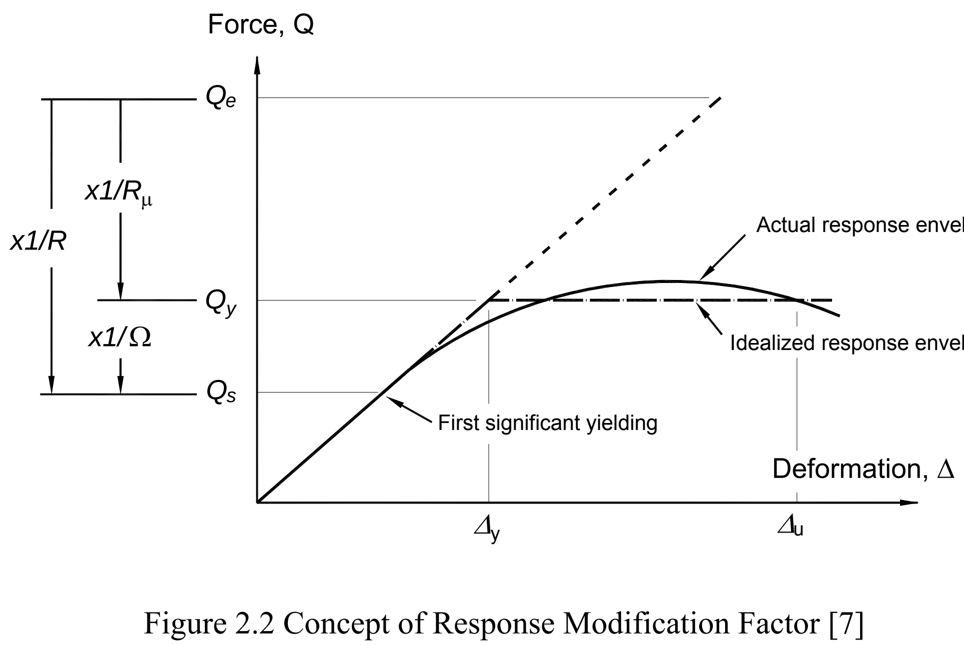

Figure 2.2 Concept of Response Modification Factor [7]

Definitions shown in Figure 2.2 are explained below;

Q_e : Elastic force level

Q_s : Design seismic force level

R : Response modification factor

$$R = \frac{Q_e}{Q_s} \tag{2.1}$$

Q_y : Yielding force level

R_μ : Ductility reduction factor

$$R_\mu = \frac{Q_e}{Q_y} \tag{2.2}$$

Ω : Overstrength factor

$$\Omega = \frac{Q_y}{Q_s} \tag{2.3}$$

Δ_y : Yield displacement of idealized response envelope

Δ_u : Maximum inelastic displacement capacity

μ_Δ : Displacement ductility

$$\mu_\Delta = \frac{\Delta_u}{\Delta_y} \tag{2.4}$$

R-factor given in AASHTO LRFD [5] is higher than ductility reduction factor, R_μ , which will be shown in subsequent chapters. This difference is mostly related to additional reserve capacity of structural member. Elnashai and Mwafy [8] summarized the main sources of reserve strength reviewed on other studies (Uang,1991; Mitchell and Paulter, 1994; Humar and Ragozar, 1996; Park, 1996). These sources were; (1) difference between the actual and the design material strength; (2) conservatism in design procedure and ductility requirements; (3) load factors and multiple load cases; (4) serviceability limit state provisions; (5) participation of nonstructural elements; (6) effect of structural elements not considered in predicting the lateral load capacity; (7) minimum reinforcement and member sizes that exceed the design requirements; (8) redundancy; (9) strain hardening; (10) actual confinement effect; and (11) utilizing the elastic period to obtain the design forces.

Although R-factor design procedure is used for both seismic codes for buildings and bridge designs, one major difference in use of R-factor should observed. For building design, R-factor is applied at the system level. All beam and column forces constituting shear and bending moment, are reduced with the same R-factor. On the contrary, for bridge design, the R-factor is applied at component level. For instance, different R-factors are used for columns and connections. Additionally, only elastic moments are divided by an R-factor for column design. Shear design is performed according to either elastic shear forces (R=1) or shear forces corresponding to plastic hinging moment of the column.

Most of the design specifications provide R-factors including overstrength in itself and utilizes "*Equal Displacement Rule*", without paying attention to soil condition, period range and displacement ductility. Many researchers have studied the relationship between displacement ductility and ductility reduction factor. Some of them are discussed below.

2.1.1. Newmark and Hall [9]

Newmark and Hall [9] divided elastic spectra into spectral regions. Then different factors were proposed to be reduced from elastic spectra. In the long period range, equal displacement rule was applied. For mid range, equal energy rule was proposed.

Ductility reduction factors are given in Eq.(2.5).

$$
\begin{aligned}
R_\mu &= 1 && \text{when } T < 0.03 \text{ s} \\
R_\mu &= \sqrt{2\mu - 1} && \text{when } 0.12 \text{ s} < T < 0.5 \text{ s} \\
R_\mu &= \mu && \text{when } T > 1 \text{ s}
\end{aligned}
\tag{2.5}
$$

2.1.2. Riddell, Hidalgo and Cruz [10]

A SDOF system with elasto-plastic hysteretic behavior was analyzed at 5 percent damping level under four different earthquake records. Ductility reduction factor is calculated using Eq.(2.6).

$$
\begin{aligned}
R_\mu &= 1 + \frac{R^* - 1}{T^*} T && \text{for } 0 \le T \le T^* \\
R_\mu &= R^* && \text{for } T^* \le T
\end{aligned}
\tag{2.6}
$$

Where the value of T^* is proposed to vary between 0.1 and 0.4 seconds for ductility ratios between 2 and 10, and the value of R^* is proposed to be equal to μ for $2 \le \mu \le 5$, and smaller than μ for $5 \le \mu \le 10$ [11].

2.1.3. Nassar and Krawinkler [12]

In this study, 15 ground motions recorded in the Western United States were studied for response of SDOF nonlinear systems. Although the records used in study were obtained at alluvium and rock sites, the influence of site conditions was not explicitly considered. Ductility reduction factor is given in Eq.(2.7).

$$
\begin{aligned}
R_\mu &= \left[c(\mu - 1) + 1 \right]^{1/c} \\
c(T, \alpha) &= \frac{T^a}{1 + T^a} + \frac{b}{T}
\end{aligned}
\tag{2.7}
$$

Where α is the post-yield stiffness as percentage of the initial stiffness of the system, and the parameters *a* and *b* come from regression analysis that is a function of α.

2.1.4. Miranda [13]

Ductility reduction factors were calculated for 5% damped bilinear SDOF systems for a displacement ductility range between 2 and 6, using a group of 124 ground motions recorded on a wide range of soil condition. Soil types were classified in three groups: being rock, alluvium and very soft soil deposits. It was shown that soil conditions might have a great influence on ductility reduction factor. Influence of magnitude and epicentral distance was negligible effect on ductility reduction factor [11]. In Eq.(2.8), mean ductility reduction factors are given.

$$R_\mu = \frac{\mu - 1}{\Phi} + 1 \geq 1 \tag{2.8}$$

Where Φ is a function of displacement ductility, μ, elastic period of the structure, T, and the soil conditions at the site, and is given in Eq.(2.9).

$$\begin{aligned}
&\textit{For rock sites} && \Phi = 1 + \frac{1}{10T - \mu T} - \frac{1}{2T}\exp\left[-\frac{3}{2}\left(\ln T - \frac{3}{5}\right)^2\right] \\
&\textit{For alluvium sites} && \Phi = 1 + \frac{1}{12T - \mu T} - \frac{2}{5T}\exp\left[-2\left(\ln T - \frac{1}{5}\right)^2\right] \\
&\textit{For soft soil sites} && \Phi = 1 + \frac{T_g}{3T} - \frac{3T_g}{4T}\exp\left[-3\left(\ln\frac{T}{T_g} - \frac{1}{4}\right)^2\right]
\end{aligned} \tag{2.9}$$

Where T_g is the predominant period of the ground motion, defined as the period at which the maximum relative velocity of a 5% damped linear elastic system is maximum throughout the whole period range.

2.2. Background on Performance-Based Design Approach

SEAOC [14] Vision 2000 Committee defines performance-based engineering as "consisting of the selection of design criteria, appropriate structural systems, layout, proportioning, and detailing for a structure and its structure and its nonstructural components and contents, and the assurance and control of construction quality and long-term maintenance, such that at specified levels of ground motions and with defined levels of reliability, the structure will not be damaged beyond certain limiting states or other usefulness limits." Current seismic bridge design codes require that strength of the structural elements exceed the nominal demands addressed in "Collapse Prevention" and "Life Safety" performance levels while providing very little indication of actual state of structure. After an earthquake, structure may still stand but damage to structural and nonstructural members may require costly repairs. Included indirect economic losses as production interruption and loss of occupancy may increase repair costs [15]. In addition to lack of multiple levels of performance, multiple earthquake design levels are not taken into account current codes. Design earthquake corresponds to an event with a return period of 475 years. In other words, for a seismic event with a greater return period, assurance of life safety will be controversial. Due to aforementioned drawbacks in current seismic design approach, the development of a performance based design approach has become necessary. This approach is supposed to predict the seismic performance of a structure based on a given level of design earthquake within a certain level of confidence so that economic losses, loss of life and the emergency services necessary for the post-earthquake operation diminish [6].

In Figure 2.3, methodology for performance-based seismic design of bridges is shown. At the beginning of the design process, selection of performance objective is required. For a given design earthquake level, design ground motion or design spectra are selected. In design, either force-based or displacement-based methods can be used. Generally, force-based approach is used in practice even though there is no restriction in current codes. Structural design is checked with respect to quantitative engineering measure corresponding to performance level. There are two crucial steps in performance based design approach; constitution of performance matrix and quantitative engineering demand parameters relating to damage level, respectively.

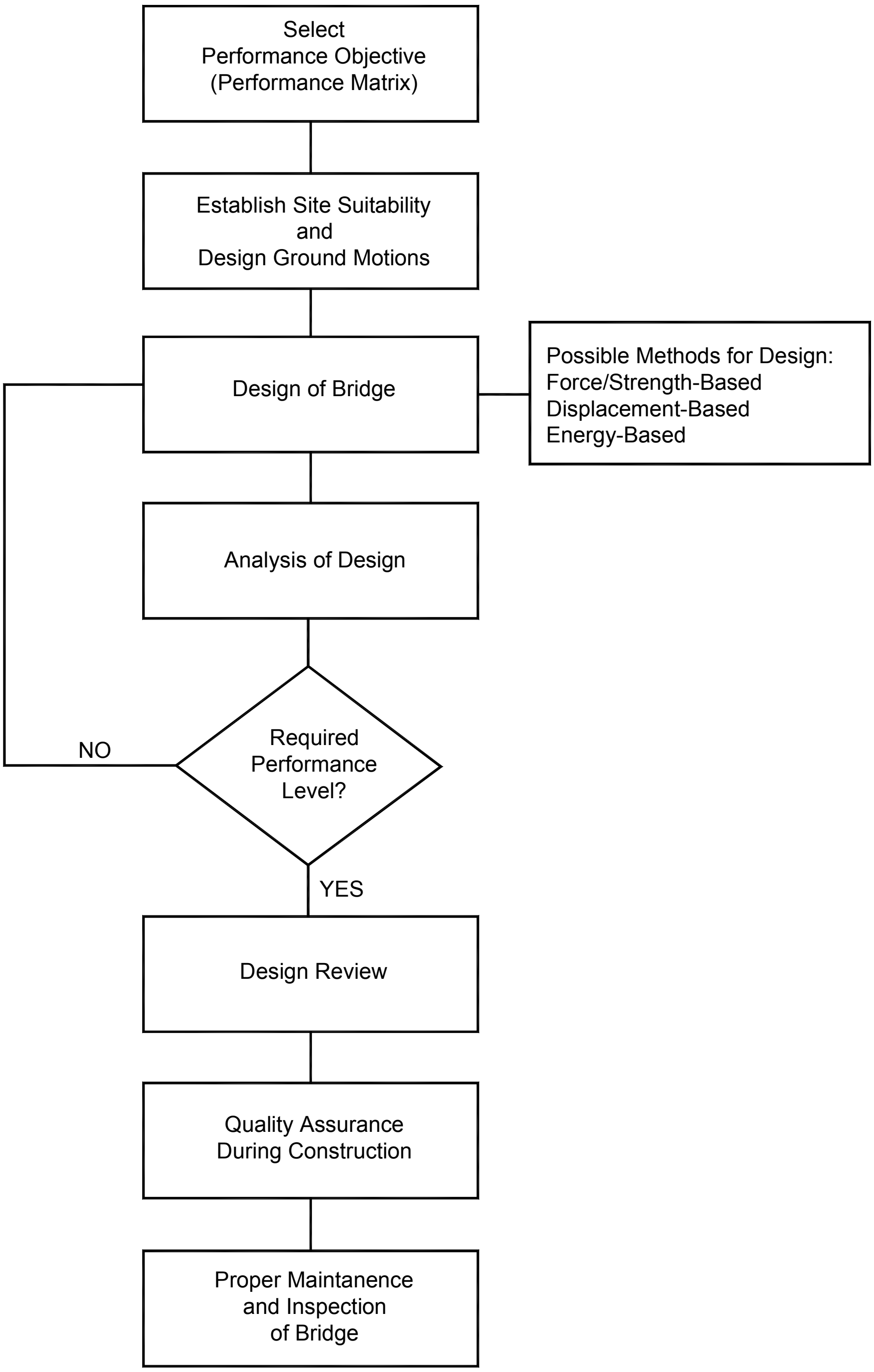

Figure 2.3 Methodology for Performance-Based Seismic Design of Bridges [6]

2.3. Background on Performance Criteria

A performance matrix defined by a target damage and serviceability state, and a seismic hazard specification, which can be defined in terms of ground shaking for a given return period. For bridge structures, importance category is implemented in performance matrix based on economic impact on society and availability for emergency use. ATC 32 [16] proposes two levels of performance objective as a function of ground motion at site and importance category of bridge.

Table 2.1 ATC 32 Performance Criteria [16]

Ground Motion at Site		Ordinary Bridges	Important Bridges
Functional Evaluation	Service Level Damage Level	Immediate Repairable	Immediate Minimal
Safety Evaluation	Service Level Damage Level	Limited Significant	Immediate Repairable

The terms used in Table 2.1 are described as follows:

Ground Motion Levels

Functional Evaluation Earthquake (FEE): Probabilistically assessed ground motion that has 60 % probability of not being exceeded during the useful life of the bridge.
Safety Evaluation Earthquake (SEE): Deterministically assessed ground motion from maximum credible earthquake or probabilistically assessed ground motion with a long return period (approximately 1000 to 2000 years).

Service Levels

Immediate : Full access to normal traffic available almost immediately.
Limited : Limited access possible within days; full service restorable within months.

Damage Levels

Minimal : Essentially elastic performance.

Repairable : No collapse. Damage that can be repaired with a minimum risk of losing functionality.

Significant : A minimum risk of collapse, but damage that would require closure for repair.

Importance Definitions

Important bridge is defined as any bridge satisfying one or more of the following:

- Required to provide post earthquake life safety.
- The time for restoration of functionality after closure would create a major economic impact.
- Formally designated as critical by a local emergency plan.

All bridges are considered *Ordinary* unless they have been designated as *Important.*

In Caltrans Seismic Design Methodology document [17], performance objectives are almost the same with the recommendations of ATC 32 [16]. In this document, Functional Evaluation Earthquake may be assessed either deterministically or probabilistically. The determination of this event is to be reviewed by a Caltrans-approved consensus group. It also states that an explicit Functional Evaluation is not required for Ordinary Bridges if they meet Safety Evaluation performance criteria and the requirements contained in Caltrans-SDC [18].

In AASHTO Guide Specifications for LRFD Seismic Bridge design (AASHTO-Seismic) [19], although performance matrix is not specified, it is mandated that bridges shall be designed for a life safety performance objective considering a seismic hazard corresponding to a 7% probability of exceedance in 75 years. (1000-year return period event) It aims to limit damage during moderate seismic event and to prevent collapse during rare, high amplitude earthquake. According to AASHTO-seismic [19], performance levels other than life safety should be established and authorized by of the bridge owner. Life safety for the design event implies having a low probability of collapse. A significant damage and disruption to service (reduced lanes, light emergency traffic) may be expected. Therefore, partial or complete replacement may be required. As a damage level, significant damage includes permanent offsets and damage consisting of cracking, reinforcement yielding, major spalling of concrete, extensive yielding and local buckling of steel columns, global and local buckling of steel braces, and cracking in the bridge deck slab at shear studs.

Floren and Mohammadi [6] presented performance-based design criteria for bridges inspired by The Vision report (SEAOC 1995) developed for building structures (Figure 2.4). Two service levels were defined: Immediate and limited. As shown in Table 2.2, full access of normal traffic almost immediately after an earthquake is assured in immediate service level. Accordingly, inspection of bridge for damage is allowed for a 24-h period. Nevertheless, limited service permits use of bridge within 3 days of the earthquake with a reduced access due to lane closures or restrictions of emergency traffic only. Full service is expected within months. Damage levels proposed are based on the criteria of ATC 32 [16]. Descriptions of three damage levels are given in Table 2.2.

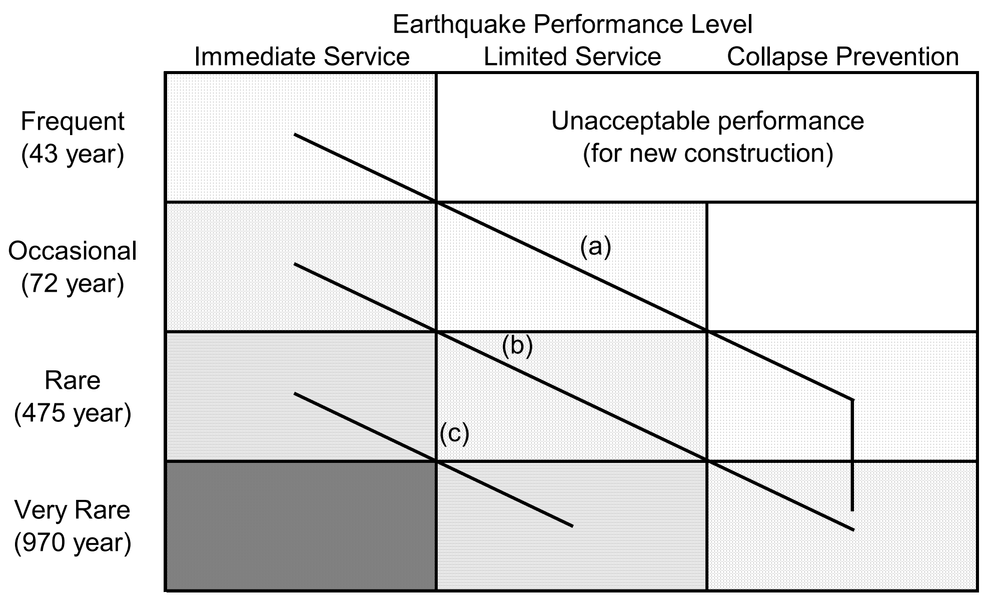

Figure 2.4 Performance Matrix for Bridges; Lines Identify Performance Objectives for: (a) Ordinary Bridges; (b) Important Bridges; (c) Critical Bridges [6]

Table 2.2 Proposed Seismic Performance Levels for Bridges [6]

Designation (1)	Description (2)
Immediate service (Operational without interruption to traffic flow)	Minimal damage has occured. Minor inelastic response may occur. Damage is restricted to narrow flexural cracking in concrete and permanent deformations are not apparent.
Limited service (Operational with minor damage)	Some structural damage has occured. Concrete cracking, reinforcement yield, and minor spalling of cover concrete is evident due to inelastic response. Limited damage is such that the structure can be essentially restored to its pre-earthquake condition.
Collapse prevention	Significant damage has occured.Concrete cracking, reinforcement yield, and major spalling may require closure for repair. Permanent offsets may occur. Partial or complete replacement may be required.

2.4. Background on Performance Limit States

Performance criteria do not provide distinctive damage state definition for a specified performance level. Avşar [20] defined limit state as “the ultimate point beyond which the bridge structure can no longer satisfy the specified performance level.” It is not sufficient for implementing performance based design approach for engineering purposes unless quantitatively predicted deformations in structural members are linked with a particular damage state. An effort to provide quantitative link between deformation measure and specific damage limit is necessitated by various researchers.

Hose et al. [21] specified five levels of performance and corresponding damage descriptions. Repair and socio-economic descriptions was related to specified five performance levels (Table 2.3). They provided qualitative and quantitative performance descriptions corresponding to the five performance levels in Table 2.4. For each performance level, quantitative guidelines were given in terms of crack widths, crack angles and regions of spalling.

Table 2.3 Bridge Damage Assessment [21]

Level	Damage Classification	Damage Description	Repair Description	Socio-economic Description
I	NO	Barely visible cracking	NO REPAIR	FULLY FUNCTIONAL
II	MINOR	Cracking	POSSIBLE REPAIR	OPERATIONAL
III	MODERATE	Open cracks Onset of spalling	MINIMUM REPAIR	LIFE SAFETY
IV	MAJOR	Very wide cracks Extended concrete spalling	REPAIR	NEAR COLLAPSE
V	LOCAL FAILURE / COLLAPSE	Visible permanent deformation Buckling / Rupture of reinforcement	REPLACEMENT	COLLAPSE

Table 2.4 Bridge Seismic Performance Assessment [21]

Level	Performance Level	Qualitative Performance Description	Quantitative Performance Description
I	CRACKING	Onset of hairline cracks.	Cracks barely visible.
II	YIELDING	Theoretical first yield of longitudinal reinforcement.	Crack widths < 1mm
III	INITIATION OF LOCAL MECHANISM	Initiation of inelastic deformation. Onset of concrete spalling. Development of diagonal cracks.	Crack widths 1-2mm. Length of spalled region > 1/10 cross-section depth.
IV	FULL DEVELOPMENT OF LOCAL MECHANISM	Wide crack widths/spalling over full local mechanism region.	Crack widths > 2mm. Diagonal cracks extend over 2/3 cross-section depth. Length of spalled region > 1/2 cross-section depth.
V	STRENGTH DEGRADATION	Buckling of main reinforcement. Rupture of transverse reinforcement. Crushing of core concrete.	Crack widths > 2mm in concrete core. Measurable dilation > 5% of original member dimension.

In Caltrans-SDC [18], minimum design requirements to meet performance goals specified for ordinary bridges are given in terms of displacement ductility demand in a quantitative manner.

Table 2.5 Maximum Displacement Ductility Demand Requirements for Bridges on Fixed Foundations [18]

Single column bents supported on fixed foundation		$\mu_D \leq 4$
Multi-column bents supported on fixed or pinned footings		$\mu_D \leq 5$
Pier walls supported on fixed or pinned footings	Weak direction	$\mu_D \leq 5$
	Strong direction	$\mu_D \leq 1$

Displacement ductility demand is defined in Eq.(2.10).

$$\mu_D = \Delta_D / \Delta_Y \tag{2.10}$$

Where;

Δ_D : Estimated global displacement demand

Δ_Y : Global yield displacement

In addition to displacement ductility demand, it is entailed that each bridge or frame shall satisfy global displacement criteria as shown in Eq.(2.11).

$$\Delta_C > \Delta_D \tag{2.11}$$

Where;

Δ_C : Global displacement capacity

Δ_D : Global displacement demand

To ensure dependable rotational capacity in plastic hinge regions, each ductile member shall have a minimum local displacement ductility demand capacity of μ_c=3. The local displacement ductility capacity for a particular member is defined in Eq.(2.12).

$$\mu_c = \Delta_c / \Delta_Y^{col} \tag{2.12}$$

Where;

Δ_c : Displacement capacity measured from the point of maximum moment to the contra-flexure point

Δ_Y^{col} : Yield displacement measured from the point of maximum moment to contra-flexure point

In AASHTO-Seismic [19], quantitative response measure is given in terms of displacement ductility demand identical with Caltrans-SDC [18]. Expected performance level is presumed as “Life Safety” for a design earthquake having a probability of exceedance 7% in 75 years. This may result in a significant damage consisting of cracking, reinforcement yield and major spalling of concrete for reinforced concrete elements. Ductility demand requirements are given in Table 2.6.

Table 2.6 Maximum Displacement Ductility Demand Requirements for Bridges on Fixed Foundations [19]

Single column bents		$\mu_D \le 5$
Multi-column bents		$\mu_D \le 6$
Pier walls	Weak direction	$\mu_D \le 5$
	Strong direction	$\mu_D \le 1$

$$\mu_D = 1 + \Delta_{pd} / \Delta_{yi} \tag{2.13}$$

Where;

Δ_{pd} : Plastic displacement demand

Δ_{yi} : Idealized yield displacement corresponding to idealized yield curvature

Kowalsky [22] considered two limit states: “serviceability” and “damage control” for circular reinforced concrete columns. Qualitative description of serviceability limit state implies that repair is not required after the earthquake, while damage control implies that only repairable damage occurs. Quantitative measures of limit states were given in terms of concrete compression and steel tension strain limits. These limits are listed in Table 2.7. The serviceability concrete compression strain was defined as the strain at which crushing is expected to begin, while the serviceability steel tension strain was defined as the strain at which residual crack widths would exceed 1 mm, thus likely requiring repair and interrupting serviceability. According to Priestley et al. [23], a residual crack width of 1 mm is taken as the maximum width than can be tolerated in normal environmental conditions without requiring remedial actions. The damage control concrete compression strain was defined as the compression strain at which the concrete is still repairable. It was stated that energy balance approach developed by Mander et al. [24] could be utilized to estimate the ultimate concrete crushing strain. It was believed that when a spiral fracture strain capacity of 12% was assumed, energy balance approach becomes conservative by 50% or more. Steel tension strain at the damage control level was related to the point at which incipient buckling of reinforcement occurs.

Table 2.7 Quantitative Damage Limit State Definitions [22]

Limit state	*Concrete strain limit*	*Steel strain limit*
Serviceability	0.004 (compression)	0.015 (tension)
Damage control	0.018 (compression)	0.060 (tension)

Avşar [20] determined several damage states of the relevant bridge components to develop fragility curves. Three damage limit states employed in this study were termed as “serviceability” (LS-1), “damage control” (LS-2) and “collapse prevention” (LS-3). Three damage limits and their corresponding damage states are marked on a force-deformation curve in Figure 2.5. Quantitative engineering demand parameter for serviceability damage limit state was obtained from section yield point determined from bilinear moment-curvature curve. It was envisioned that crack widths should be sufficiently small and member functionality should not be impaired. Damage-control limit state was assumed to be obtained when spalling of the concrete cover occurs. It was mostly agreed that spalling of the concrete cover is an indication of significant damage due to sudden strength loss, possible fracture of transverse reinforcement and buckling of longitudinal reinforcement. Damage-control limit state was quantified with a curvature limit that is calculated when the extreme fiber of the unconfined concrete attains a compressive strain of 0.003. Author thinks that assumed compressive concrete strain for spalling is very conservative according to experimental program performed by Calderone et al. [25]. In their study, concrete spalling did not occur until the inferred compression strain in the concrete at the level of the spiral reinforcement exceeded 0.008.

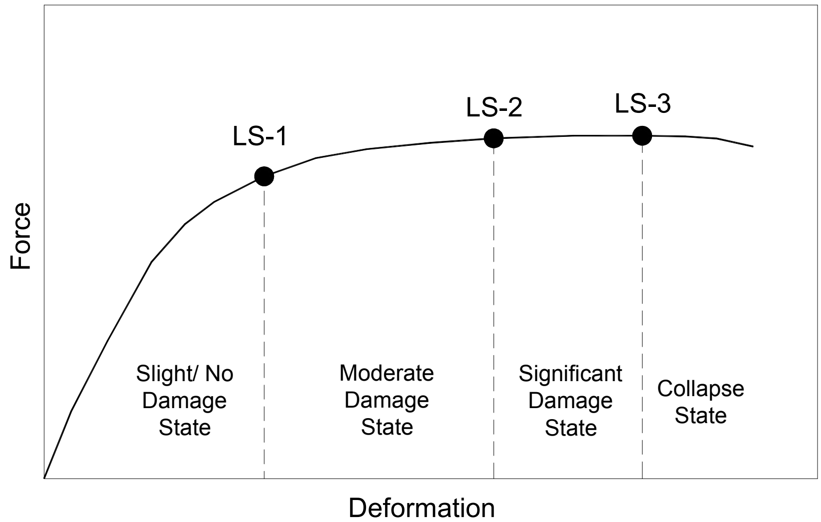

Figure 2.5 Damage States and Damage Limits on a Force–Deformation Curve [20]

For collapse-prevention limit state, results of experimental data were used to determine the ultimate curvature that satisfies performance without occurrence of complete failure. For this purpose, an empirical equation for the column displacement ductility capacity based on the results of previous column experiments proposed by Erduran and Yakut [26] was used to quantify given limit state. Corresponding relationship is given in Eq.(2.14).

$$\mu_u = 0.6\ln\left[\left(\frac{\rho_s}{N/N_o}\right)^2\right] + 7.5 \tag{2.14}$$

Where;

μ_u : Ultimate displacement ductility

ρ_s : Transverse reinforcement ratio

N/N_o : Axial load ratio

2.4.1. Reinforced Concrete Bridge Column Performance States and Demand Parameters

Although qualitative descriptions of damage states are agreed in general, a widely accepted quantitative damage limit state definitions are not readily available. Engineering demand parameters required for implementation of performance-based design procedure, can be expressed in global structural level as drift or displacement ductility, or local level as concrete compression and steel tension strain, and curvature. Previous studies mentioned above quantified damage limit states using either concrete and steel strain or displacement ductility. In order to develop a consistent performance-based design methodology, laboratory observations of bridge column performance that provide link between deformation and specific damage states are essential.

Lehman et al. [2] prepared an experimental program to obtain performance data for circular bridge columns having details of those currently in use in regions of high seismicity in the United States. The columns were assumed to be fixed to a stiff foundation and were designed so that flexural dominant response would be observed during lateral loading. The column dimensions were selected to represent typical column dimensions scaled to one-third of full scale. Ten columns were tested with varying longitudinal reinforcement, aspect ratio, axial load ratio, spiral spacing and confinement length. It was concluded that sequence of damage was similar for all columns. The most notable observations in sequence of first occurrence were concrete cracking, longitudinal reinforcement yielding, initial spalling of the concrete cover, complete spalling of the concrete cover, spiral fracture, longitudinal reinforcement buckling, and reinforcement fracture as shown in Figure 2.6.

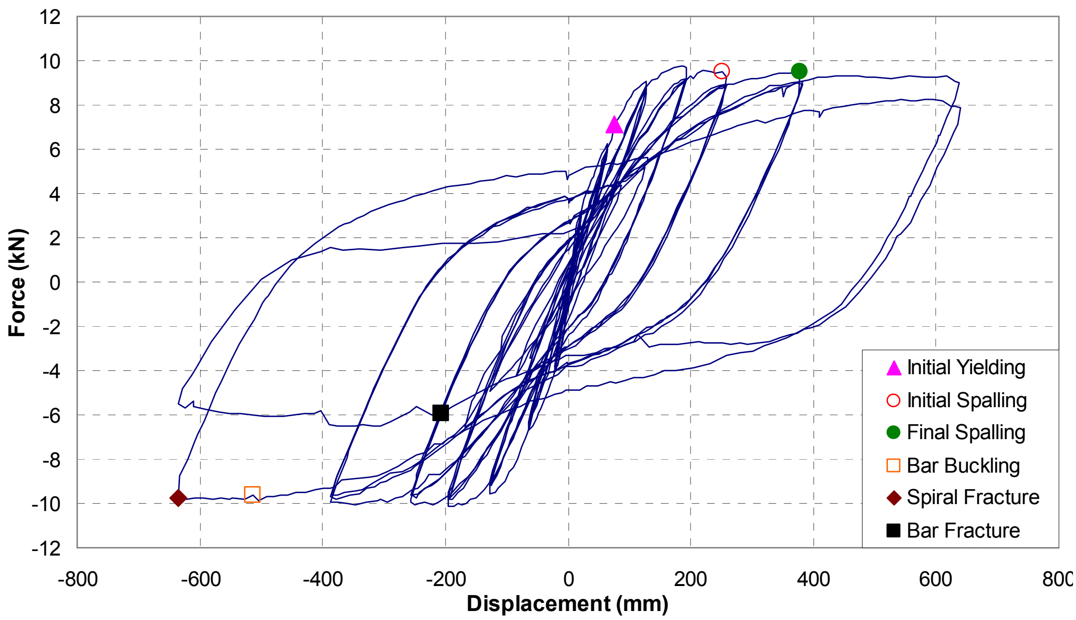

Figure 2.6 Force-Displacement Response of Column 1015 [2]

Concrete cracking pattern shown in Figure 2.7 has an importance in the context of damage state since open residual cracks may determine whether repair by epoxy injection is required during remedial action. Further repair effort is required when concrete cover spalls and core concrete begins to crush. Column shown in Figure 2.8 requires more costly, time consuming and possibly disruptive repair effort, which is an indication of moderate performance state. Buckling and fracture of longitudinal steel reinforcement may be postulated as ultimate damage state (Figure 2.9 & Figure 2.10). The onset of this type of damage induces significant loss of lateral load strength without imminent collapse. In this case, bridge is needed to be closed to traffic and replacement is required.

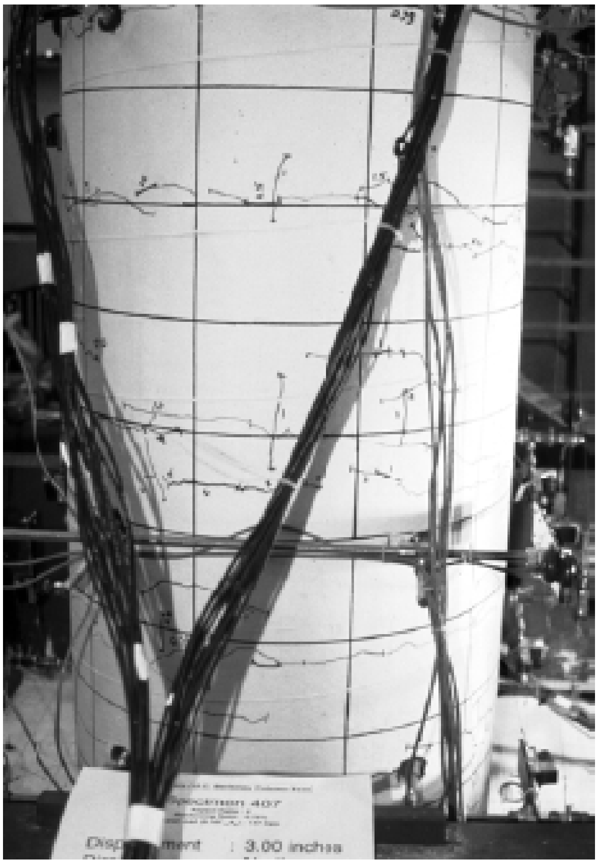

Figure 2.7 Crack Patterns of Column 407 [27]

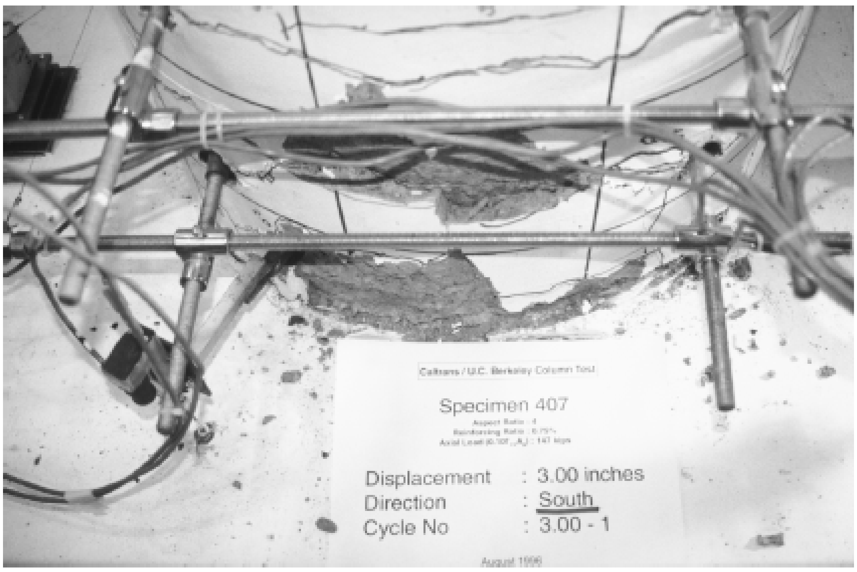

Figure 2.8 Cover Spalling of Column 407 [27]

Figure 2.9 Bar Buckling and Bar Fracture of Column 407 [27]

Figure 2.10 Final Damage State of Column 407 [27]

Table 2.8 ACI-341 Performance States [28]

I. Fully Functional: This damage state is characterized by residual cracks that are small enough that no repair is required. The cracks are due to flexure and shrinkage, not shear or bond.
II. Operational: This damage state is characterized by limited damage to structural components that does not affect their structural integrity. Potential damage includes settlement of approach slabs, pounding at expansion joints, yielding of restrainer cables, and spalling of concrete cover. Some yielding of reinforcement is acceptable, but nothing approaching buckling or fracture. Closure of the bridge may be required until an inspection is completed, and partial lane closures may be required to repair damage. Repairs should be completed in the days and weeks following an earthquake.
III. Delayed Operation: This damage state is characterized by severe damage to structural components, such as buckling or fracture of longitudinal reinforcement or fracture of transverse reinforcement. Some loss of core concrete may occur. Ductile details allow the components to maintain their gravity load carrying capacity. Complete replacement of the structure is not anticipated, but repair and replacement of components requires closure to all but emergency traffic.
IV. Collapse Prevention: This limit state includes extensive crushing of the concrete core, buckling and fracture of longitudinal steel reinforcement, extensive fracture of transverse reinforcement, and the partial or total collapse of the structure. The bridge is closed to traffic, and complete replacement is required.

In this study, ACI Committee 341 [28] performance states were used. They are named as "*Fully Functional*", "*Operational*" and "*Delayed Operational*". The degree of damage and disruption to service associated with limit states are described in Table 2.8. First three possible limits states were considered for performance based design since forth limit state "Collapse Prevention" should never be a design objective.

In ACI Committee 341 [28] draft report, it is stated that use of local engineering parameters is difficult for two reasons: (1) most researchers do not report values of local parameters corresponding to a given damage state as compressive strain related to concrete spalling, and (2) current models that are used in practice do not provide reliable estimates of local engineering parameters. Lehman et al. [2] concluded that limit state criteria according to compressive strain at which the hoop reinforcement ruptures were based on models developed from the pure compressive tests of confined concrete cross sections in which hoop rupture due to concrete dilation was a predominant failure mode. However, hoop rupture was dominated by local strains due to longitudinal buckling and bearing against the hoops under reversed cyclic loading. Therefore, using compressive strain limits for performance based design approach requires new models and significant attention. Although displacement ductility is a better engineering measure than concrete or steel strain related to given damage state, it includes some level of uncertainty associated with estimates of the yield displacement. Berry and Eberhard [15] studied for recommendations of concrete compressive strain, plastic rotation, drift ratio and displacement ductility at the onset of a particular damage to be implemented easily in practice. It was concluded that although coefficient of variations of the ratios of measured displacements to calculated displacements are similar for all deformation measures, the drift-based equations are recommended for their simplicity in use [15]. In the light of these facts, drift ratio equations corresponding to the onset of particular damage states are utilized [28]. Application of these correlations are limited to tests in which the distance to the point of contraflexure does not vary, the axial load does not vary, there is only uniaxial bending and effects of cycling on damage cannot be taken into account [29]. Regardless of limitations, the drift ratio equations are the simplest since no additional analysis is required to estimate the displacements and these equations are as accurate as the more complex methods. Therefore, author of this thesis chose drift ratio equations as the most suitable tool for correlating damage states at particular levels of column deformation.

Berry and Eberhard [15] evaluated the influence of key parameters such as column geometry, longitudinal and transverse reinforcement and axial load ratio on the drift ratio, displacement ductility, plastic rotation and longitudinal strain corresponding to specific damage states in reinforced concrete columns. In their study, longitudinal bar buckling and concrete cover spalling in flexure-dominant reinforced concrete columns were predicted. They employed a database containing the results of cyclic lateral-load tests on reinforced concrete columns assembled at the University of Washington with the support of the National Science Foundation through the Pacific Earthquake Engineering Research Center (PEER). The database contained the results of 274 tests of rectangular columns and 160 tests of spiral-reinforced columns as of January 2004. For each column test, the database provides the column geometry;

material, reinforcement, and loading properties; test results; and a reference. The test results include the digital force-displacement history and the maximum recorded tip deflections before the onset of the particular damage states [30]. To be included in the analysis, the column tests should satisfy the following criteria:

- Flexural-critical column, as defined by Camarillo [31]
- An aspect of 1.95 or more
- Longitudinal reinforcement is not spliced
- Normalized axial load level of 0.3 or less
- Longitudinal reinforcement ratio of 0.04 or less
- Effective confinement ratio of 0.05 or more (defined for Eq.(2.16))

Table 2.9 provides the number of rectangular and spiral-reinforced column tests that met the screening criteria, and in which the tip displacements at the onset of longitudinal bar buckling and concrete cover spalling were reported.

Table 2.9 Number of Tests for Which Damage Displacement Was Available [15]

	Bar Buckling	Cover Spalling
Rectangular Columns	62	102
Spiral-Reinforced Columns	42	40

The drift ratio at the onset of a particular damage state was defined as Δ_{damage} / L, where Δ_{damage} is the maximum reported tip deflection before the onset of a particular damage state, and L is the distance from the column base to the point of contraflexure.

<u>Proposed cover spalling equation:</u>

A simple equation was developed by Berry and Eberhard [15] to estimate the mean drift ratio at the onset of cover spalling based on column tests that reported cover spalling drift measure. The proposed equation is as follows;

$$\frac{\Delta_{spall\_calc}}{L}(\%) = 1.6\left(1 - \frac{P}{A_g f_c^{'}}\right)\left(1 + \frac{L}{10D}\right) \tag{2.15}$$

Where;

L : Column length

D : Column diameter

P : Axial load

A_g : Gross area of cross section

$f_c^{'}$: Concrete compressive strength

Table 2.10 Statistics of Δ_{spall} / Δ_{spall_calc} for Design Equation [15]

		Statistics of Δ_{spall} / Δ_{mean_DRIFT}				Statistics of Δ_{spall} / Δ_{calc}			
	Number of Tests	min	max	mean	CoV	min	max	mean	CoV
Rectangular-Reinforced	102	0.09	1.98	1.00	47.6%	0.17	1.93	0.97	43.3%
Spiral- Reinforced	62	0.27	1.97	1.00	44.2%	0.48	1.93	1.07	35.2%

By using Eq.(2.15) to estimate the mean drift ratios at the onset of cover spalling, the coefficient of variation (CoV) of Δ_{spall} / Δ_{spall_calc} was 43.3% for rectangular columns and 35.2% for spiral-reinforced columns were obtained. Δ_{spall} / Δ_{spall_calc} is the ratio of the observed displacement from column database to the displacement calculated with Eq.(2.15) at the onset of concrete cover spalling. Similarly, Δ_{spall} / Δ_{mean_DRIFT} is the ratio of the observed displacement from column database to the displacement associated with the mean drift calculated from column database at the onset of concrete cover spalling.

Proposed bar buckling equation:

An empirical equation was developed to estimate the mean drift ratio at the onset of bar buckling based on column tests that reported bar buckling drift measure [15]. The proposed equation is as follows;

$$\frac{\Delta_{bb\_calc}}{L}(\%) = 3.25\left(1 + k_e \rho_{eff}\frac{d_b}{D}\right)\left(1 - \frac{P}{A_g f_c^{'}}\right)\left(1 + \frac{L}{10D}\right) \tag{2.16}$$

Where;

k_e : 50 for rectangular columns 150 for spiral-reinforced concrete

$\rho_{eff} = \rho_s \frac{f_{ys}}{f_c^{'}}$: Effective confinement ratio

ρ_s : Volumetric transverse reinforcement ratio

f_{ys} : Yield stress of transverse reinforcement

d_b : Diameter of longitudinal reinforcing bars

By using Eq. (2.16) to estimate the mean drift ratios at the onset of bar buckling, the coefficient of variation (CoV) of Δ_{BB} / Δ_{BB_calc} was 26.3% for rectangular columns and 24.6% for spiral-reinforced columns were obtained. Δ_{BB} / Δ_{BB_calc} is the ratio of the observed displacement from column database to the displacement calculated with Eq.(2.16) at the onset of bar buckling. Similarly, Δ_{BB} / Δ_{mean_DRIFT} is the ratio of the observed displacement from column database to the displacement associated with the mean drift calculated from column database at the onset of bar buckling.

Table 2.11 Statistics of Δ_{BB} / Δ_{BB_calc} for Design Equation [15]

		Statistics of Δ_{BB} / Δ_{mean_DRIFT}				Statistics of Δ_{BB} / Δ_{calc}			
	Number of Tests	min	max	mean	CoV	min	max	mean	CoV
Rectangular-Reinforced	62	0.34	1.73	1.00	33.3%	0.42	1.56	1.00	26.3%
Spiral- Reinforced	42	0.34	2.19	1.00	42.0%	0.47	1.50	0.97	24.6%

As stated before, buckling of longitudinal bars may be regarded as significant damage state that requires partial replacement of column(s) resulting in closure of bridge to all but emergency vehicle. Kunnath et al. [32] performed series of column test to verify the behavior of bridge piers responding in flexure to a random displacement input such as those typically experienced under earthquake loading. Test observations indicated two potential failure modes: low cycle fatigue of longitudinal reinforcing bars and confinement failure due to rupture of confining spirals. Due to complex series of interrelated mechanism of failure mode related to bar buckling, biaxial lateral loading and earthquake-induced displacement histories are expected to have a significant effect on the drift capacity at bar buckling. According to Eurocode 8 –Part 3 [33], the chord rotation capacity corresponding to significant damage may be assumed as to be 3/4 of the ultimate chord rotation. Since rotation is directly related to displacement, drift limit calculated using Eq. (2.16) was reduced by 20% with the recommendation of ACI Committee 341 [28].

In Table 2.8, Fully Functional Performance Level is characterized by limited residual crack that indicates if epoxy or other material must be used to restore the tensile strength. In other words, bridge designed to meet this performance level is supposed to respond essentially in the elastic range. According to Lehman and Moehle [27], residual crack width should be limited to 0.02 in (0.50 mm). They concluded that the residual crack widths of 0.01 in (0.25 mm) or less correspond to displacement ductility demand less than 1.5 and the residual crack widths of 0.02 in (0.50 mm) or less corresponds to displacement ductility less than 2. The author of this thesis assumes displacement ductility demand less than 1.5 for fully functional performance level.

In this study, three performance limits states of “Fully Functional”, “Operational” and “Delayed Operational” were used. Drift limits corresponding to given performance limit sates are summarized as below:

- The drift limit corresponding to *Fully Functional limit state* (FF) was estimated as 1.5 times the effective yield displacement, Δ'_y, based on flexural deformation. Details of calculation shall be given in Section 3.9.

- *The Operational limit state* (O) was assumed to correlate to cover concrete spalling and the corresponding mean drift limit was estimated based on Eq.(2.15).
- *The Delayed Operational limit state* (DO) was assumed to correlate to the onset of bar buckling and the corresponding mean drift limit was estimated based on Eq.(2.16) with a 20% reduction.

2.5. Background on Inelastic Displacement Ratio

In current seismic design approach, it is generally agreed that the seismic design of new structures and the seismic evaluation of existing structures requires the explicit consideration of lateral deformation demand for a selected performance limit state [34]. It brings on the necessity of simplified analysis procedure to estimate inelastic displacement demand of structure exposed to earthquake ground motion. Regular way of succeeding this is to have a nonlinear acceleration time history analyses, which is very sensitive to selected earthquake ground motion and unpractical for everyday design situation. A possible simplified approach is to estimate the maximum inelastic displacement demand using linear analysis [35].

Many seismic design criteria contain an implicit assumption known as the *equal displacement rule.* This assumption is an approximation that states that an upper bound to the peak displacement of a ductile system, having strength V_y less than the strength V_e required for elastic response, is given by the peak displacement of elastic system, Δ_e as shown in Figure 2.11 (a). Priestley et al. [3] stated that equal-displacement approximation is inappropriate for both very short and very long-period structures, and is of doubtful validity for medium period structures when the hysteretic character of the inelastic system deviates significantly from elasto-plastic. Therefore, a noniterative so-called displacement coefficient method is used in which the maximum inelastic deformation is estimated from the maximum elastic deformation by using a modifying factor C_μ, shown in Figure 2.11 (b). C_μ corresponds to the expected ratio of maximum inelastic displacement to the maximum elastic displacement taking account of elastic vibration period, level of inelastic behavior, soil conditions and earthquake characteristics as magnitude and distance. Previously, many researchers studied on inelastic displacement ratios for SDOF system over ensembles of ground motions including effects of soil condition, stiffness and strength degradation of structural system. Three of them are introduced below in details and the ones selected for this study is discussed with its reasons.

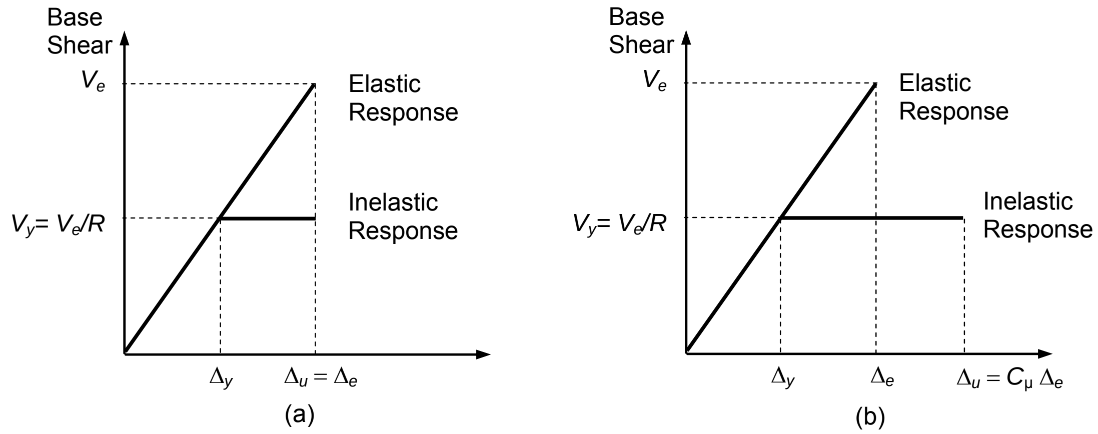

Figure 2.11 (a) Equal Displacement Approximation, (b) Inelastic Displacement Coefficient Method [28]

2.5.1. Miranda [36]

In this study, 264 acceleration time histories recorded on firm sites during various earthquake ground motions were used to compute approximate mean inelastic displacement ratios for single-degree-of-freedom (SDOF) systems undergoing different levels of inelastic deformation. The inelastic displacement ratio C_μ is defined as the maximum lateral inelastic displacement demand $\Delta_{inelastic}$ divided by the maximum lateral elastic displacement demand $\Delta_{elastic}$ on a system with the same period when the system is exposed to the same earthquake ground motion. Mathematical expression is given in Eq.(2.17).

$$C_\mu = \frac{\Delta_{inelastic}}{\Delta_{elastic}} \tag{2.17}$$

Inelastic displacement ratios were computed for SDOF systems having a viscous damping ratio of 5% and a nonlinear elastoplastic hysteretic behavior. For each earthquake record and target displacement ductility ratio ranging between 1.5 and 6, inelastic displacement ratios were computed for a set of 50 periods of vibration between 0.05 and 3.0 s. Earthquake ground motions used in the study were divided into three groups according to the soil conditions at the recording station. The first group consisted of ground motions recorded on stations located on rock with average shear-wave velocities higher than 760 m/s. The second group consisted of records obtained on stations very dense soil or soft rock with average shear-wave velocities between 360 m/s and 760 m/s and the third group consisted of ground motions recorded on stations on stiff soil with average shear-wave velocities between 180 m/s and 360 m/s. Recording stations on the first group correspond to site classes A and B according to recent design provisions [16], and recording stations on the second and third group correspond to site classes C and D, respectively. Using mean inelastic displacement ratios corresponding to all earthquake ground motions (for site classes A, B, C and D), nonlinear regression analyses were done. The resulting equation is given by;

$$C_{\mu} = \left[1 + \left(\frac{1}{\mu} - 1 \right) \exp\left(-12 T \mu^{-0.8} \right) \right]^{-1} \tag{2.18}$$

Where;

μ : Displacement ductility ratio

T : Period of vibration

Figure 2.12 shows inelastic displacement ratios computed with Eq.(2.18). Without the need of estimating a characteristic or corner period for the site, Eq.(2.18) can be used for all sites with average shear-wave velocities larger than 180 m/s. In spite of its simplicity, this approach brings erroneous results for individual soil site classification. It is realized that mean inelastic displacement ratios of site A, B and C is less than the one with all soil site. In other words, Eq.(2.18) overestimates in the range of 10-15% in average. For inelastic displacement ratios of soil site D, Eq.(2.18) underestimates in the range of 10-15% in average. Although there seems to be negligible effect on inelastic displacement demand of SDOF system, author of this thesis thinks that 10-15% error might affect performance categorization of the given column in the dataset of this study.

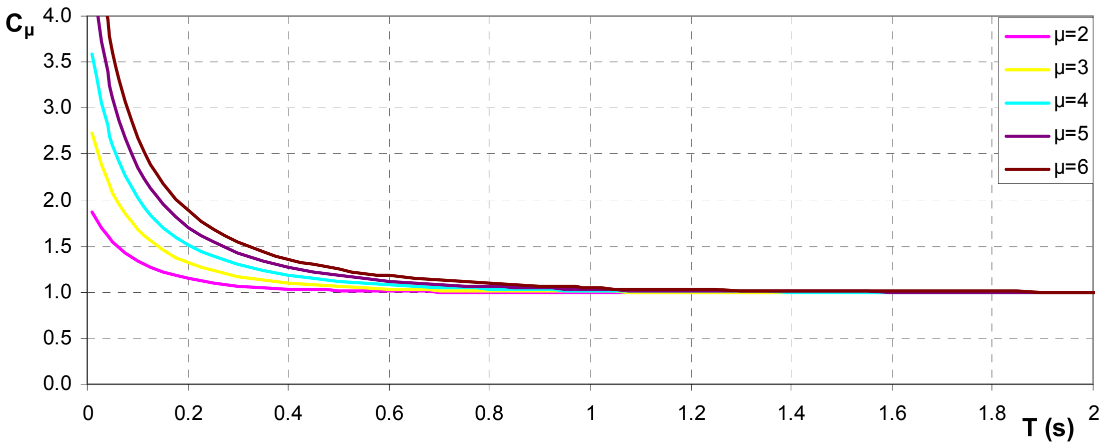

Figure 2.12 Inelastic Displacement Ratios for Sites A, B, C and D Computed with Eq.(2.18)

2.5.2. Chopra and Chintanapakdee [37]

In this study, median of the inelastic deformation ratio for 214 ground motions organized into 11 ensembles of ground motions, representing large or small earthquake magnitude and distance, and National Earthquake Hazards Reduction Program (NEHRP) site classes B, C, and D; near-fault ground motions were presented. Two sets of results for bilinear nondegrading systems over the complete range of elastic vibration period, T_n, were presented: C_μ for systems with known displacement ductility, μ, and C_R for systems with ductility reduction factor, R_μ. Contrary to Miranda [36], equations for C_μ and C_R were given as a function of T_n / T_c and μ and R_μ where T_c is the period separating the acceleration- and velocity-sensitive regions. The resulting equations are given by;

$$C_\mu = 1 + \left[\left(L_\mu - 1 \right)^{-1} + \left(\frac{a}{\mu^b} + c \right) \left(\frac{T_n}{T_c} \right)^d \right]^{-1} \tag{2.19}$$

$$C_R = 1 + \left[\left(L_R - 1 \right)^{-1} + \left(\frac{a}{R_\mu^b} + c \right) \left(\frac{T_n}{T_c} \right)^d \right]^{-1} \tag{2.20}$$

Where;

$$L_\mu : \frac{\mu}{1 + (\mu - 1)\alpha} \tag{2.21}$$

$$L_R : \frac{1}{R_\mu} \left(1 + \frac{R_\mu - 1}{\alpha} \right) \tag{2.22}$$

α : Postyield stiffness ratio (for elastoplastic system α=0)

The numerical parameters *a*, *b*, *c* and *d* being independent of postyield stiffness ratio is given with an underestimation of inelastic displacement ratio computed with Eq. (2.15): *a*=105, *b*=2.3, *c*=1.9, *d*=1.7 using the data for four (LMSR, LMLR, SMSR, and SMLR) ensembles. Figure 2.13 shows inelastic displacement ratios computed with Eq.(2.19).

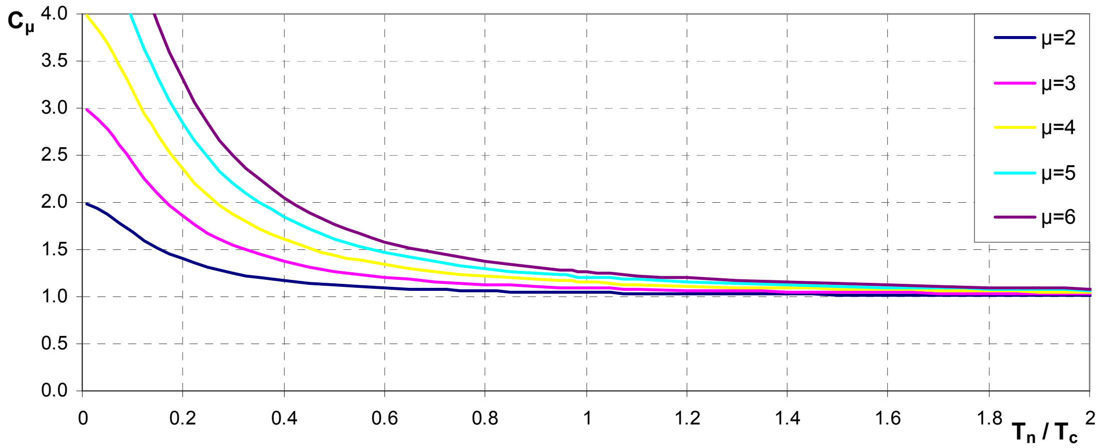

Figure 2.13 Inelastic Displacement Ratios for Four Ensembles (α=0) Computed with Eq. (2.19)

2.5.3. Garcia and Miranda [38] & [39]

In this study, median inelastic displacement ratios for SDOF systems undergoing six levels of inelastic deformation when subjected to 116 earthquake ground motions recorded on bay-mud site of San Francisco Bay Area and on sites in the former lake-bed zone of Mexico City were computed. Low shear-wave velocities, high water contents and high plasticity indices characterize these soft soils. Site classes of E and F of current design provisions address soft soil conditions. This classification corresponds to soil profiles with more than 3 m of soft clay defined as soils with plasticity indices higher than 20, water contents higher than 40% or soil profiles with average shear-wave velocities lower than 180 m/s in the upper 30 m of the soil profile. During the analysis, 5% damping ratio was used. Two types of hysteretic behavior were chosen: elastic-perfectly plastic model and modified Clough model to represent stiffness-degrading behavior. As it was assumed by Chopra and Chintanapakdee [37], inelastic displacement ratios were computed for 50 normalized periods of vibration, T/T_g. Predominant period of the ground motion, T_g, corresponds to the period of maximum ordinate in the relative velocity spectrum computed for a elastic system having 5% ramping ratio. From 116 records, two sets of ground motion were considered. The first set includes 16 acceleration time histories recorded at stations on bay mud sites in the San Francisco Bay Area (SFBA). The second set includes 100 acceleration time histories recorded at stations in the soft soil zone of Mexico City (MEXC). The general equation is given by;

$$C_\mu = 1 + (\mu - 1)\left[\theta_1 + \theta_2\left(\frac{T}{T_g} + 1.8\right)^{-4.2}\right] + \theta_3(\mu - 1)^{0.5}\left(\frac{T_g}{T}\right)$$
$$\exp\left[\left(2.3 - \frac{32}{\mu}\right)\left(\ln\left\{\frac{T}{T_g}\right\} - 0.1\right)^2\right] - 0.08(\mu - 1) \qquad (2.23)$$
$$\left(\frac{T_g}{T}\right)\exp\left[-70\left(\ln\left(\frac{T}{T_g} + 0.67\right)\right)^2\right]$$

Where;

T : Period of vibration

$\theta_1, \theta_2, \theta_3$: Constants, which depend on the type of hysteretic behavior and the ground motion ensemble

θ_1= 0.04, θ_2= 10.5 and θ_3= -0.68 was chosen for the Mexico City ground motion set with elastic- perfectly plastic hysteretic behavior. Figure 2.14 shows inelastic displacement ratios computed with Eq.(2.23).

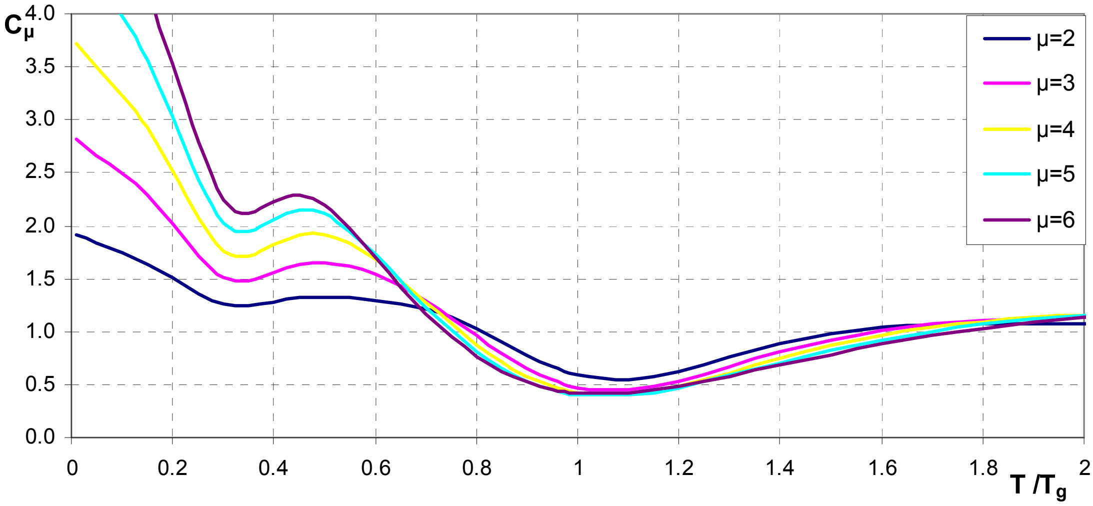

Figure 2.14 Inelastic Displacement Ratios for MEXC Ensemble of Elastic-Perfectly Plastic Model Computed with Eq.(2.23)

2.5.4. Inelastic Displacement Ratios Used in This Study

Previously mentioned studies consider soil condition effect. To achieve this, use of predominant period of ground motion is suggested in Eq.(2.19) and Eq.(2.23) for firm and soft soil sites respectively. In this study, all soil types specified in AASHTO LRFD [5] are used to investigate soil type variability in performance of the column. Soil profile type I, II and III corresponds to NEHRP site classes of A, B, C and D. In addition, soil type IV corresponds to NEHRP site classes of E and F, which stands for soft soil condition. Therefore, to calculate inelastic displacement demand of structure located in soil types I, II and III, Eq.(2.19) is used. For calculation of inelastic demand located in soil type IV, Eq.(2.23) suggested by Garcia and Miranda [39] is used. It should be noted that both equations use displacement ductility that is a direct measure of capacity of circular bridge column estimated by pushover analysis. The characteristic period of ground motion, T_c in Eq.(2.19) and T_g in Eq.(2.23) is assumed to be approximately equal to corner period located at the transition from the "constant acceleration" portion of elastic response spectrum to the "constant velocity" portion of spectrum. The necessity of using different inelastic displacement ratios for firm and soft sites is shown for ductility levels of 2, 4 and 6 in Figure 2.15. In soft soil sites, inelastic displacement may be expected less than elastic displacement in the range of normalized structural period of 1 s.

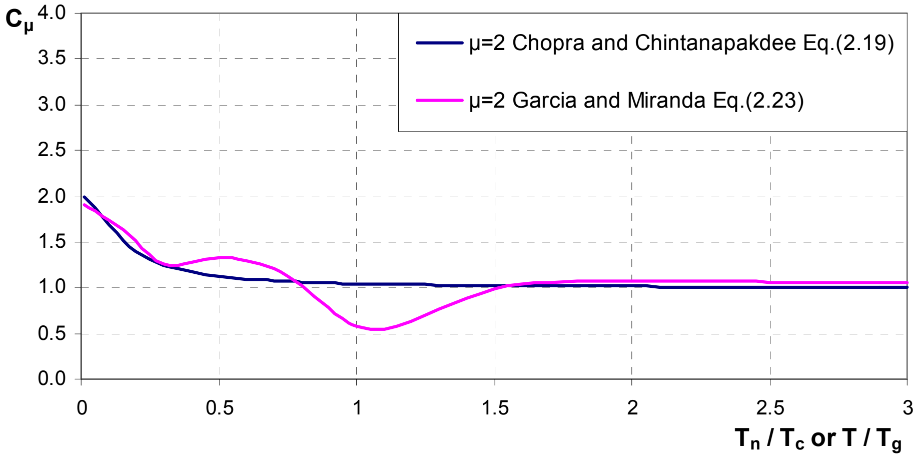

(a)

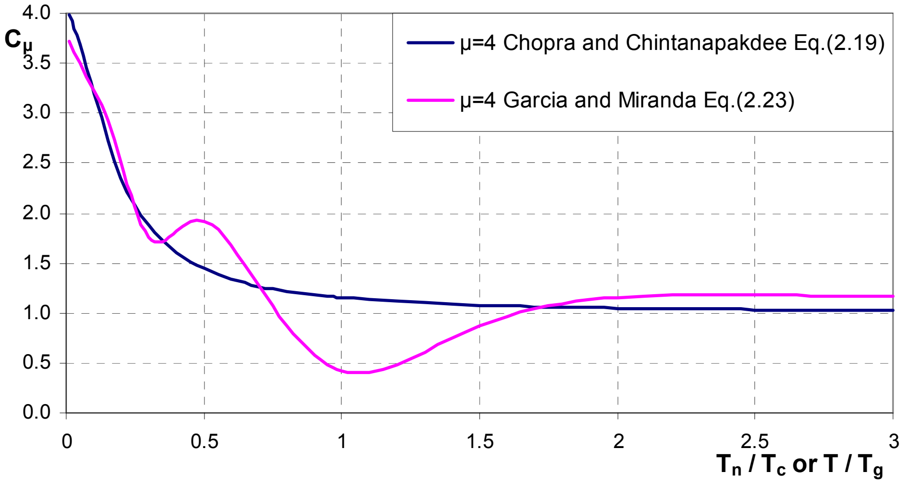

(b)

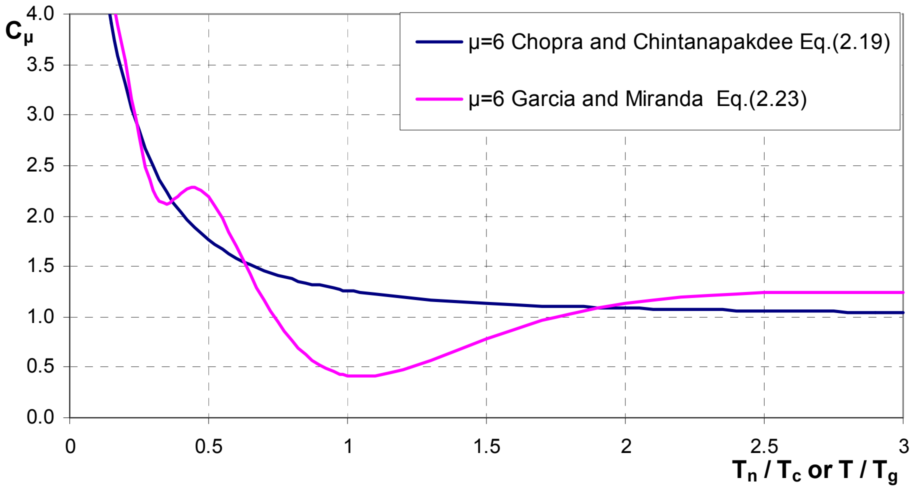

(c)

Figure 2.15 Comparison of Inelastic Displacement Ratios for Firm and Soft Sites Computed with Eq.(2.19) and Eq.(2.23), for (a) μ=2, (b) μ=4, (c) μ=6

CHAPTER 3

DEVELOPING THE ANALYSIS TOOL

3.1. Purposes of the Analysis Tool and Outline of Design Procedure

Analysis tool developed in this study is used for two purposes. In the first part, for given structural properties as column aspect ratio, diameter and design axial load ratio, performance assessments of circular bridge columns designed according to various R-factors, acceleration coefficients and soil conditions are conducted by comparing inelastic demand drift with performance drift. This chapter mainly focuses on analysis routines of a regular design process with a known R-factor. In the second part of this study, an R-factor satisfying Fully Functional and Operational performance drift demand is estimated within a given error tolerance. Since it only requires several modifications of the analysis tool developed for the first part, details of modifications are explained in Section 3.10.

Flowchart of seismic design procedure for the purpose of performance assessment is shown in Figure 3.1. AASHTO LRFD [5] seismic provisions are applied for design of bridge columns in this study. Noticing that minimum requirements necessary to provide public safety are intended to be specified in the code, several advancements are involved during the analysis process. Primarily, instead of using uncracked section for flexural rigidity, $(EI)_{gross}$, effective flexural rigidity, $(EI)_{eff}$, is utilized for dynamic analysis, slenderness effect embedded in P-Δ calculation and elastic displacement demand. Although AASHTO LRFD [5] does not refer to use of cracked section in dynamic analysis except in consideration of slenderness effect in P-Δ analysis, it is a fundamental basis of R-factor used in design of columns. Taking this into account, a stiffness modification factor, α_{gross} is defined in Eq.(3.1).

$$\alpha_{gross} = \frac{EI_{eff}}{EI_{gross}} \tag{3.1}$$

Where;

EI_{eff} : Effective flexural rigidity of cracked section estimated from the slope of linear portion of bilinearized moment curvature graph (Discussed in Section 3.7)

EI_{gross} : Flexural rigidity of uncracked section

It is obvious that α_{gross} is dependent on longitudinal reinforcement ratio and design axial load ratio. Since longitudinal reinforcement demand changes with respect to design forces that is a function of α_{gross}, iterative solution for α_{gross} is necessitated. It is initially assumed as 0.4 to avoid maximum reinforcement ratio to be exceeded so that given case is not discarded from dataset. Although lower stiffness results in a lower spectral acceleration compared to the one calculated with uncracked stiffness, a higher moment magnification factor due to P-Δ effect might be expected. This may cause maximum reinforcement criterion not to be satisfied. Therefore, initial assumption of 0.4 for α_{gross} is selected carefully to minimize data loss due to this fact. After having performed moment curvature analysis, initially assumed stiffness modification factor is checked according to relative error ε=1% (0.01) given in Eq.(3.2).

$$\left| \frac{\alpha_{gross}^{cal} - \alpha_{gross}}{\alpha_{gross}} \right| \le \varepsilon \tag{3.2}$$

Where;

α_{gross}^{cal}: Stiffness modification factor obtained after moment curvature analysis is performed for previously calculated α_{gross}

If Eq.(3.2) is not satisfied, new stiffness modification factor to be used in dynamic analysis and so on is calculated as given in Eq.(3.3).

$$\alpha_{gross} = \frac{\alpha_{gross}^{cal} + \alpha_{gross}}{2} \tag{3.3}$$

Most of the cases converge to the given relative error within 5 to 10 iterations. Since moment curvature analyses and section design modules are included within the loop of stiffness modification factor, they both have to iterate 5 to 10 times. Although there are several commercial softwares performing section design and moment curvature analysis separately, due to integrated nature of problem and high amount of numerical operations, an analysis tool is necessitated. Source code of the analysis tool developed in Excel VBA environment is given in APPENDIX A. In following sections, components of software are explained in details.

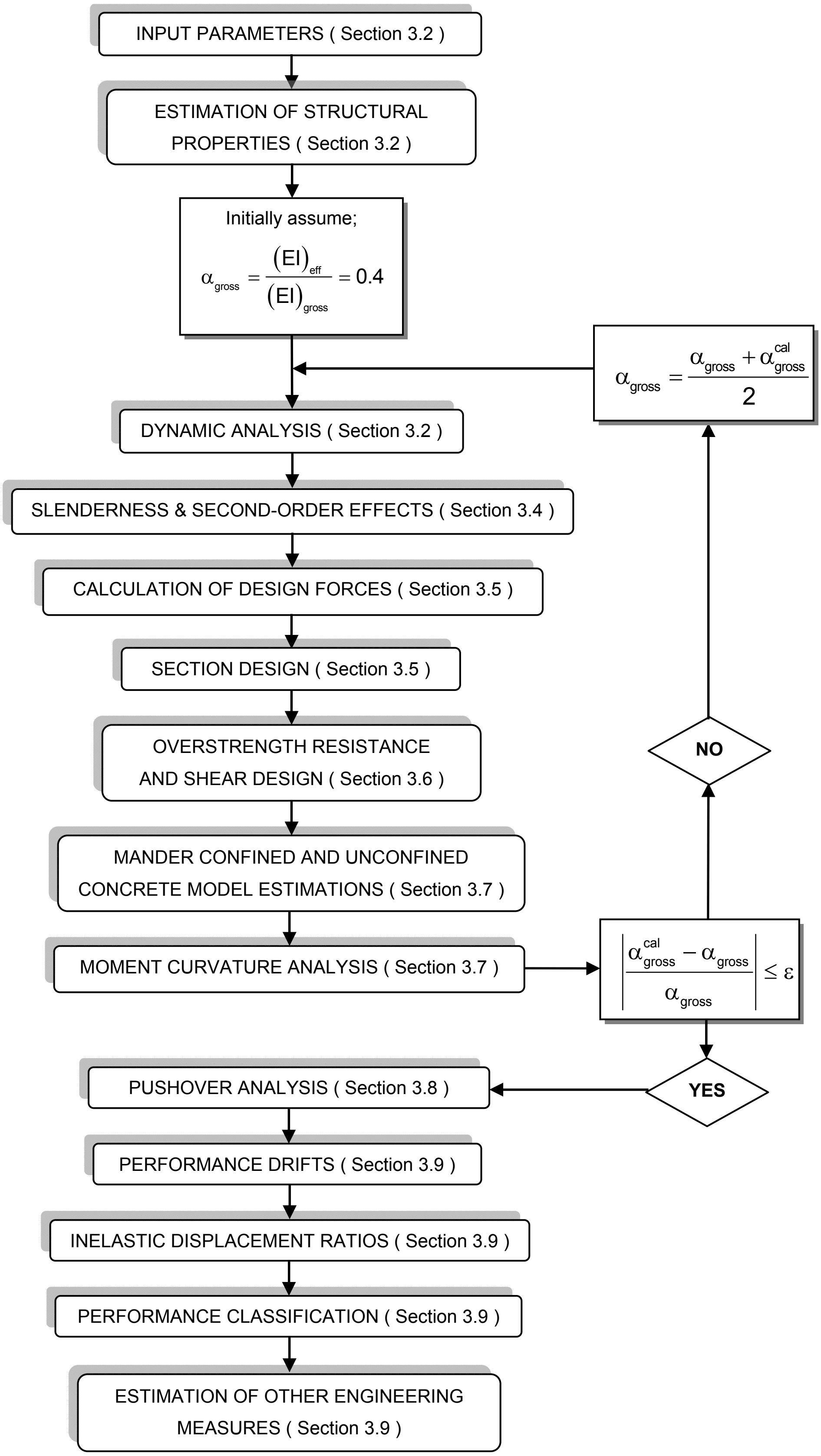

Figure 3.1 Seismic Design Procedure Flowchart

3.2. Input Parameters and Estimation of Structural Properties

Three input parameters are considered regarding to SDOF circular column as aspect ratio (L/D), diameter (D) and design axial load ratio ($P_u/A_g f_c$). For seismic design, response modification factor (R) varying from 1 to 5 is employed to examine variability of R-factor in selected performance levels. Range of selected parameters is shown in Figure 3.2. It is believed that ranges of structural inputs cover mostly preferred design practice in Turkey. For a given acceleration coefficient and soil condition for generating elastic response spectrum, 7x9x3x9=1701 analyses are performed. For four types of soil condition and acceleration coefficient, 27216 analyses are employed totally. Analysis results shall be given in Chapter 4.

PREPARATION OF DATA SET

L/D	D(m)	$P_u / (A_g x f_c)$	R
2.5	1	0.1	1
3	1.25	0.2	1.5
4	1.5	0.3	2
5	1.75		2.5
6	2		3
7	2.25		3.5
8	2.5		4
	2.75		4.5
	3		5

PREPARE

# of data set = 1701

Figure 3.2 Input Parameters and Ranges

In Table 3.1, corresponding part of Excelsheet is shown. Definitions and related formulations are explained below.

L : Height of the column measured from the top of the foundation to the bottom of the cap beam (m)

P_u : Factored design axial load acting at the bottom of the column including superstructure, cap beam and column (kN)

P_{self} : Force acting at the bottom of column due to self-weight of the column (kN)

P_{mass} : Force corresponding to tributary mass lumped at the top of the column (kN)

m : Mass of the superstructure including cap beam and half of the column weight to be used in dynamic analyses (ton)

EI_{gross} : Unreduced flexural stiffness for a given diameter of the column and modulus of elasticity of concrete (kN m^2)

k_{eff} : Effective transverse stiffness to be used in calculation of effective period (kN/m)

Table 3.1 Part of Excelsheet Corresponding to Input Parameters and Structural Properties

INPUT PARAMETERS				STRUCTURAL PROPERTIES								
(-)	(m)	(-)	(-)	(m)	(kN)	(kN)	(kN)	(ton)	(kN m^2)	(-)	(kN m^2)	(kN/m)
L / D	D	P_u / (A_gxf_c)	R	L	P_u	P_{self}	P_{mass}	m	EI_{gross}	α_{gross}	EI_{eff}	k_{eff}
2.5	1.00	0.10	1	2.5	1963.50	49.09	1546.25	157.62	1178097.25	**0.40**	471238.90	90477.87
2.5	1.00	0.10	1.5	2.5	1963.50	49.09	1546.25	157.62	1178097.25	**0.63**	744991.65	143038.40
2.5	1.00	0.10	2	2.5	1963.50	49.09	1546.25	157.62	1178097.25	**0.48**	569779.66	109397.69
2.5	1.00	0.10	2.5	2.5	1963.50	49.09	1546.25	157.62	1178097.25	**0.40**	467036.57	89671.02
2.5	1.00	0.10	3	2.5	1963.50	49.09	1546.25	157.62	1178097.25	**0.33**	394074.95	75662.39
2.5	1.00	0.10	3.5	2.5	1963.50	49.09	1546.25	157.62	1178097.25	**0.33**	394074.95	75662.39
2.5	1.00	0.10	4	2.5	1963.50	49.09	1546.25	157.62	1178097.25	**0.33**	394074.95	75662.39
2.5	1.00	0.10	4.5	2.5	1963.50	49.09	1546.25	157.62	1178097.25	**0.33**	394074.95	75662.39
2.5	1.00	0.10	5	2.5	1963.50	49.09	1546.25	157.62	1178097.25	**0.33**	394074.95	75662.39

Circular bridge columns dealt in this study are simulated with SDOF oscillator model. It is assumed as a single column bent for both longitudinal and transverse direction of bridge. Mass of the superstructure is assumed to be lumped at the top of the column. Massless frame that only provides stiffness to the system resembles the design practice in Turkey. Current bridge design approach in Turkey is comprised of prestressed I girders placed on elastomeric bearings without shear connection between bearing and girder. Additionally, inverted T shaped cap beam is preferred to elongate length of the bridge. Continuity between sequential spans is guaranteed with in-situ slab in longitudinal direction. With the use of shear keys thought as the sacrificial element during the earthquake, integrity in transverse direction is ensured. Due to the presence of elastomeric bearings, it can be assumed that no moment is transferred from superstructure to substructure for both longitudinal and transverse direction. Stiffness of the elastomeric bearing is ignored since pounding phenomena between side of the girder and shear key in transverse direction and between front face of the girder and cap beam in longitudinal direction increases the stiffness of the bearing modeled as a spring dashpot analogy. In this case, equivalent stiffness of pier and bearing spring system that is similar to circuits connected in parallel is governed by stiffness of the pier. Therefore, SDOF system approximation for the calculation of structural properties as mass and effective stiffness of pier only seems to be reasonable. Modeling system as a cantilever column in both direction produces the identical predominant period of vibration. Foundation flexibility is ignored regardless of any soil condition. It is assumed as fixed based foundation. Columns are designed according to Extreme Event I load combination given in Eq.(3.4).

$$\gamma_p DL + \gamma_{EQ} LL + EQ \tag{3.4}$$

Load factor for permanent dead load, γ_p, is given as 1.25 considering maximum load effect. AASHTO LRFD [5] states that the load factor for live load in Extreme Event Load Combination I, γ_{EQ}, shall be determined on a project-specific basis Although γ_{EQ}=0.5 is thought to be reasonable according to Turkstra's rule [40], the possibility of partial live load with earthquake is not considered in this study.(γ_{EQ}=0). No additional axial load is created due to earthquake. In the light of these assumptions, Mass to be used in dynamic analysis is calculated according to Eq.(3.5).

$$m = \left(\frac{P_u}{1.25} - \frac{P_{self}}{2} \right) \Big/ 9.81 \tag{3.5}$$

Effective stiffness calculation to be used in analysis is given in Eq.(3.6) for a SDOF cantilever column.

$$k_{eff} = \frac{3EI_{eff}}{L^3} \tag{3.6}$$

3.3. Dynamic Analysis

Single-mode spectral approach is adopted in analyses. It is based on the assumption that earthquake design forces for structures respond predominantly in the first mode of vibration in either longitudinal or transverse direction. It holds true for simple bridge structures with relatively straight alignment, small skewness and well-balanced spans with equally distributed stiffness [5]. Natural period of SDOF mass-spring oscillator is calculated by a tributary mass originated from superstructure and structural stiffness corresponding to a single column bent. The base shear being equal to the product of spectral acceleration and the tributary mass is applied at the vertical centre of mass of the superstructure.

Elastic design spectra for four different soil profiles defined in AASHTO LRFD [5] are used for dynamic analyses. Normalized design coefficients are given in Figure 3.3. For each soil profile, four different acceleration coefficients (0.1, 0.2, 0.3 and 0.4) are selected for analyses. These values are obtained from seismic zoning map of Turkey [41] assuming that a normal construction, which has 50 years of economical life, may not be exposed larger than these expected maximum acceleration values with 90% probability (475-year return period event). In Table 3.2, corresponding part of Excelsheet is shown. Definitions and related formulations are explained below.

T_{eff} : Fundamental period of SDOF column (second)

S_{a_eff} : Spectral acceleration corresponding to T_{eff} for given a soil profile and acceleration coefficient (g)

V, M : Base shear and moment respectively (kN), (kNm)

M_x, M_y : Design moments of orthogonal direction (kNm)

$$T_{eff} = 2\pi \sqrt{\frac{m}{k_{eff}}} \tag{3.7}$$

$$V = m \cdot S_{a\_eff}$$
$$M = V \cdot L \tag{3.8}$$

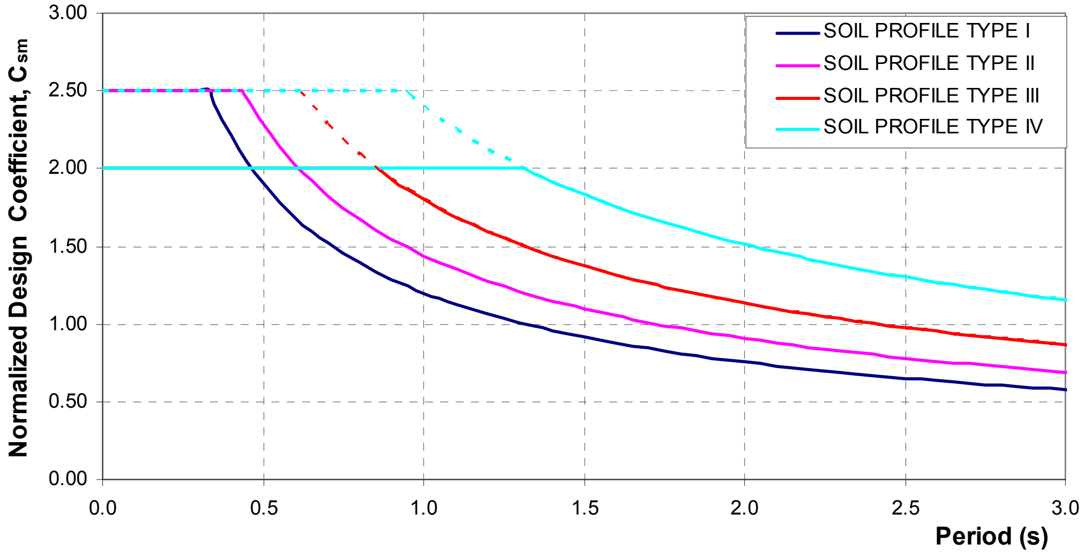

Figure 3.3 Normalized Design Coefficients for Different Soil Profiles [5]

Table 3.2 Part of Excelsheet Corresponding to Dynamic Analysis

				LC1 = EQX +0.3 EQY	
DYNAMIC ANALYSIS					
(sec)	(g)	(kN)	(kN m)	(kN m)	(kN m)
T_{eff}	S_{a_eff}	V	M	M_x	M_y
0.26	1.00	1546.25	3865.63	3865.63	1159.69
0.21	1.00	1546.25	3865.63	3865.63	1159.69
0.24	1.00	1546.25	3865.63	3865.63	1159.69
0.26	1.00	1546.25	3865.63	3865.63	1159.69
0.29	1.00	1546.25	3865.63	3865.63	1159.69
0.29	1.00	1546.25	3865.63	3865.63	1159.69
0.29	1.00	1546.25	3865.63	3865.63	1159.69
0.29	1.00	1546.25	3865.63	3865.63	1159.69
0.29	1.00	1546.25	3865.63	3865.63	1159.69

3.4. Slenderness and Second-Order Effects

There are two sources that comprise of geometric nonlinearity. The first one is P-Δ due to member chord rotation effect and the second one is P-δ due to member curvature effect [42]. White and Hajjar [43] stated that the P-Δ effect reduces the element flexural stiffness against sidesway. The P-δ effect reduces the element flexural stiffness in both sidesway and non-sidesway modes of deformation. Therefore, force effects caused by both sidesway and non-sidesway frame action are superposed to be as shown in Eq.(3.9) according to AASHTO LRFD [5]. The effects of deflection on forces are approximated by single-step adjustment method known as moment magnification.

$$M_c = \delta_b M_{2b} + \delta_s M_{2s} \tag{3.9}$$

$$\delta_b = \frac{C_m}{1 - \dfrac{P_u}{\phi_K P_e}} \geq 1.0 \tag{3.10}$$

$$\delta_s = \frac{1}{1 - \dfrac{\sum P_u}{\phi_K \sum P_e}} \tag{3.11}$$

Where;

M_{2b} : Moment on compression member due to factored gravity loads that result in no appreciable sidesway calculated by conventional first-order elastic frame analysis

M_{2s} : Moment on compression member due to factored lateral or gravity loads that result in, Δ, greater than $l_u/1500$, calculated by conventional first-order elastic frame analysis

ϕ_K : Stiffness reduction factor; 0.75 for concrete members and 1.0 for steel and aluminum members

P_e : Euler buckling load given in Eq.(3.12)

$$P_e = \frac{\pi^2 EI}{\left(Kl_u\right)^2} \tag{3.12}$$

Where;

K : Effective length factor in the plane of bending (In the case of having a cantilever column, it is taken as 2.)

l_u : Unsupported length of a compression member

EI : Flexural stiffness. In the lieu of a more precise calculation, greater of Eq.(3.13) and Eq.(3.14) shall be used in determining P_e,

$$EI = \frac{\frac{E_c I_g}{5} + E_s I_s}{1+\beta_d} \tag{3.13}$$

$$EI = \frac{\frac{E_c I_g}{2.5}}{1+\beta_d} \tag{3.14}$$

Where;

E_c : Modulus of elasticity of concrete

I_g : Moment of inertia of the gross concrete section about the centroidal axis

E_s : Modulus of elasticity of longitudinal steel

I_s : Moment of inertia of longitudinal steel about the centroidal axis

β_d : Ratio of maximum factored permanent load moments to maximum factored total load moment.

In defining the critical load P_e, the choice of flexural stiffness, EI, that reasonably approximates the variations in stiffness due to cracking, creep, and nonlinearity of the concrete stress-strain curve has a crucial importance to take account of slenderness. Assuming that β_d =0, flexural rigidity to be used in Eq.(3.10) and Eq.(3.11) becomes 0.4x0.75=0.3 of EI_{gross} with inclusion of the stiffness reduction factor, ϕ_K. It might be thought as lower boundary value regardless of any sectional and design property. Realizing this, AASHTO LRFD [5] states that although moment magnification procedure outlined above is easy to use for practical design purposes, it is believed to be conservative. In this study, more refined second-order analysis is implemented into design routine of analysis tool. Table 3.3, corresponding part of Excelsheet is shown.

Table 3.3 Part of Excelsheet Corresponding to Second-Order Analysis

SLENDERNESS CALCULATIONS_ITERATIVE THEORETICAL SOLUTION							
	1st Iteration		Unbalanced Forces		2nd Iteration		
$\delta_{s\_THEORETICAL}$	$\Delta_{2,1}$	$\theta_{2,1}$	V_{un}	M_{un}	$\Delta_{2,2}$	$\theta_{2,2}$	M_{P_Δ}
1.009	0.0171	0.0103	14.09	3.36	0.00018	0.00011	3899.54
1.006	0.0108	0.0065	8.91	2.12	0.00007	0.00004	3887.00
1.007	0.0141	0.0085	11.66	2.78	0.00012	0.00008	3893.63
1.009	0.0172	0.0103	14.22	3.39	0.00018	0.00011	3899.85
1.011	0.0204	0.0123	16.85	4.01	0.00026	0.00016	3906.26
1.011	0.0204	0.0123	16.85	4.01	0.00026	0.00016	3906.26
1.011	0.0204	0.0123	16.85	4.01	0.00026	0.00016	3906.26
1.011	0.0204	0.0123	16.85	4.01	0.00026	0.00016	3906.26
1.011	0.0204	0.0123	16.85	4.01	0.00026	0.00016	3906.26

To take account of second-order effect, the geometric stiffness approach is implemented. It is derived from principles of virtual work, assuming interpolation of shape functions for the member's displacements [42]. In second-order frame analysis, structural stiffness matrix given in Eq. (3.15) is updated in each load increment considering the change in structural geometry.

$$[K]=[K_E]+[K_G] \tag{3.15}$$

Where;

$[K_E]$: Elastic stiffness matrix

$[K_G]$: Geometric stiffness matrix

The geometric stiffness used in Eq.(3.15) has ability to reflect the effect of P-Δ exactly, but in general, it only approximates the P-δ effect. Nevertheless, it is sufficient to capture the geometric nonlinear behavior of SDOF column under consideration of this study. In Figure 3.4, degrees of freedom, deflected shape including forces acting on the column and member local forces are shown. Each step is examined in details.

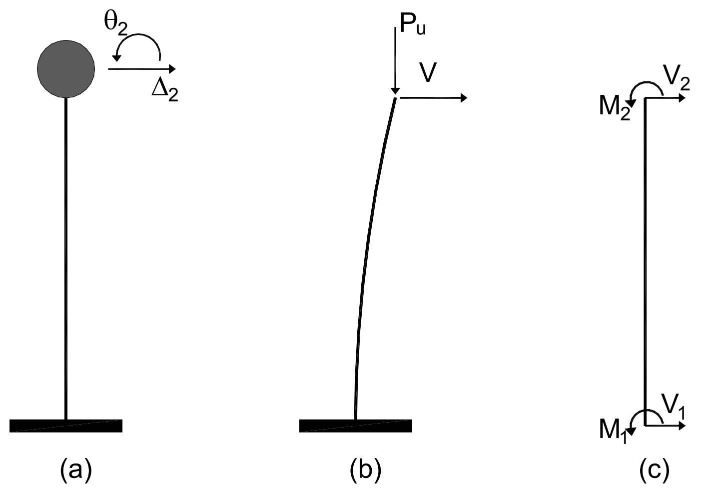

Figure 3.4 (a) Degrees of Freedom, (b) Deflected Shape, (c) Member Local Forces

In analysis procedure mentioned below, geometry of deflected shape is not updated in structural stiffness matrix, since it requires loads to be applied incrementally with consideration for the changes in stiffness after each increment, as well as discretization of structural member. Single step loading is used with geometric stiffness matrix given in McGuire et al. [44].

- Elastic and geometric stiffness matrices are constructed for degrees of freedom shown in Figure 3.4 (a). In elastic stiffness matrix, EI_{eff} is utilized to take account of slenderness due to nonlinear behavior of member. As mentioned before, instead of having a constant value of EI_{eff}, it is estimated in each case within a confidence level performing moment-curvature analysis. For compression forces, P_u is taken as negative in Eq.(3.16).

$$K_E = \begin{bmatrix} \frac{12EI_{eff}}{L^3} & \frac{-6EI_{eff}}{L^2} \\ \frac{-6EI_{eff}}{L^2} & \frac{4EI_{eff}}{L} \end{bmatrix} \qquad K_G = \frac{P_u}{L}\begin{bmatrix} \frac{6}{5} & \frac{-L}{10} \\ \frac{-L}{10} & \frac{2L^2}{15} \end{bmatrix} \tag{3.16}$$

- Elastic displacements, $\Delta_{2,1}$and $\theta_{2,1}$, are calculated for design shear force, V.

$$\left[K_E\right]\begin{bmatrix} \Delta_{2,1} \\ \theta_{2,1} \end{bmatrix} = \begin{bmatrix} V \\ 0 \end{bmatrix} \tag{3.17}$$

- Unbalanced forces,V_{un} and M_{un}, caused by second-order effect are calculated in Eq.(3.18) and Eq.(3.19).

$$\left[K_E + K_G\right]\begin{bmatrix} \Delta_{2,1} \\ \theta_{2,1} \end{bmatrix} = \begin{bmatrix} V_0 \\ M_0 \end{bmatrix} \tag{3.18}$$

$$\begin{aligned} V_{un} &= V - V_0 \\ M_{un} &= -M_0 \end{aligned} \tag{3.19}$$

- Displacements, Δ and θ, caused by unbalanced forces, V_{un} and M_{un}, are calculated in Eq.(3.20).

$$\left[K_E + K_G\right]\begin{bmatrix} \Delta \\ \theta \end{bmatrix} = \begin{bmatrix} V_{un} \\ M_{un} \end{bmatrix} \tag{3.20}$$

- Elastic deformations, $\Delta_{2,1}$and $\theta_{2,1}$, are summed up with Δ and θ caused by unbalanced forces in Eq.(3.21).

$$\begin{aligned} \Delta_{2,2} &= \Delta + \Delta_{2,1} \\ \theta_{2,2} &= \theta + \theta_{2,1} \end{aligned} \tag{3.21}$$

- Member stiffness matrices are constructed to calculate member end forces.

$$K_E = \begin{bmatrix} \frac{12EI_{eff}}{L^3} & \frac{6EI_{eff}}{L^2} & \frac{-12EI_{eff}}{L^3} & \frac{6EI_{eff}}{L^2} \\ & \frac{4EI_{eff}}{L} & \frac{-6EI_{eff}}{L^2} & \frac{2EI_{eff}}{L} \\ & & \frac{12EI_{eff}}{L^3} & \frac{-6EI_{eff}}{L^2} \\ & & & \frac{4EI_{eff}}{L} \end{bmatrix} \qquad K_G = \frac{P_u}{L}\begin{bmatrix} \frac{6}{5} & \frac{L}{10} & \frac{-6}{5} & \frac{L}{10} \\ & \frac{2L^2}{15} & \frac{-L}{10} & \frac{-L^2}{30} \\ & & \frac{6}{5} & \frac{-L}{10} \\ & & & \frac{2L^2}{15} \end{bmatrix} \tag{3.22}$$

- Member end forces, V_1, M_1, V_2 and M_2 shown in Figure 3.4(c), is given in Eq.(3.23).

$$\left[K_E + K_G\right]\begin{bmatrix} 0 \\ 0 \\ \Delta_{2,2} \\ \theta_{2,2} \end{bmatrix} = \begin{bmatrix} V_1 \\ M_1 \\ V_2 \\ M_2 \end{bmatrix} \tag{3.23}$$

Amplified base moment to be used in section design is M_1 obtained from Eq.(3.23). Moment magnification factor is calculated as in Eq.(3.24).

$$\delta_s = \frac{M_1}{M} \tag{3.24}$$

To compare the results of moment magnification factor with commercially available software programs as SAP2000 [45] and LARSA 4D [46], a generic study is conducted. Parameters are tabulated in Table 3.4. Lateral force acting on the cantilever column is assumed as 40% of design axial load, P_u. Stiffness modification factor, α_{gross}, is taken as 0.4 to be consisted with AASHTO LRFD [5] approximate procedure for slenderness consideration. Although geometry of the deflected shape is not updated in structural stiffness matrix necessitating incremental force approach, results of the implemented procedure are in good agreement with software solutions.

Table 3.4 Comparisons of Moment Magnification Factors

	(m)	(m)		(kN)		(kN)	(kNm^2)	SAP2000	LARSA4D	THEORETICAL
L / D	D	L	P_u / (A_gxf_c)	P_u	α	$V_b = \alpha \times P_u$	$EI_{eff} = 0.4xEI_{gross}$	δ_s (Moment Magnification Factor)		
5	3.00	15.00	0.10	17671.46	0.40	7068.58	37613699.79	1.037	1.037	1.037
5	3.00	15.00	0.20	35342.92	0.40	14137.17	37613699.79	1.076	1.077	1.077
5	3.00	15.00	0.30	53014.38	0.40	21205.75	37613699.79	1.118	1.120	1.121
6	3.00	18.00	0.10	17671.46	0.40	7068.58	37613699.79	1.054	1.054	1.054
6	3.00	18.00	0.20	35342.92	0.40	14137.17	37613699.79	1.112	1.115	1.116
6	3.00	18.00	0.30	53014.38	0.40	21205.75	37613699.79	1.177	1.183	1.186
7	3.00	21.00	0.10	17671.46	0.40	7068.58	37613699.79	1.074	1.075	1.075
7	3.00	21.00	0.20	35342.92	0.40	14137.17	37613699.79	1.159	1.163	1.166
7	3.00	21.00	0.30	53014.38	0.40	21205.75	37613699.79	1.255	1.267	1.276
8	3.00	24.00	0.10	17671.46	0.40	7068.58	37613699.79	1.099	1.100	1.101
8	3.00	24.00	0.20	35342.92	0.40	14137.17	37613699.79	1.216	1.225	1.230
8	3.00	24.00	0.30	53014.38	0.40	21205.75	37613699.79	1.356	1.380	1.401

3.5. Calculation of Design Forces and Section Design

According to AASHTO LRFD [5], seismic design forces obtained for global orthogonal directions are combined. This is due to accounting for uncertainty in the direction of an earthquake motion. Load combinations to combine two orthogonal earthquake force effects are given below;

Load Combination 1 (LC1): 1.0 EQ_X + 0.30 EQ_Y

Load Combination 2 (LC2): 1.0 EQ_Y + 0.30 EQ_X

Where;

EQ_X : Response value in longitudinal direction (X)

EQ_Y : Response value in transverse direction (Y)

It is assumed that earthquake analysis in transverse direction does not yield a response value in longitudinal direction and vice versa. This assumption seems to be reasonable for non-skewed regular bridges. Therefore, LC1 and LC2 yield same response values in terms of base shear and turning moment. Dynamic analysis in vertical direction is out of the scope of this study. Hence, the effect of vertical response is ignored in LC1 and LC2. As stated in section 3.2, Extreme Event Load Combination I governs the design. No axial load is induced during earthquake loading since axial force couple due to multiple bent column behavior is not expected. Furthermore, no bending moment in orthogonal directions are caused owing to dead load analysis. If it is needed to write Eq.(3.4) in complete form;

COMB1 (longitudinal direction) : 1.25 DL + 1.0 EQX + 0.3 EQY
COMB2 (longitudinal direction) : 1.25 DL - 1.0 EQX - 0.3 EQY
COMB3 (transverse direction) : 1.25 DL + 1.0 EQY + 0.3 EQX
COMB4 (transverse direction) : 1.25 DL - 1.0 EQY - 0.3 EQX

Since all combinations given above produce same result, it is sufficient to design circular column section according to COMB1. Design moments are established by dividing the elastically computed force effects by the appropriate R-factor assuming inelastic behavior is allowed. In addition to that, factored moments are increased to reflect effects of deformations due to slenderness and second-order effect. To do that, moment magnification factor, δ_s, explained in section 3.4 is multiplied with factored moments of orthogonal directions. In Table 3.5, corresponding part of Excelsheet is shown. Definitions and related formulations are explained below.

Table 3.5 Part of Excelsheet Corresponding to Design Forces and Section Design

COMB1 =1.25 DL + LC1							
DESIGN FORCES AND SECTION DESIGN							
(kN)	(kN)	(kN m)	(kN m)	(kN m)		(%)	
P_d	V_e	M_x	$0.3 \times M_y$	M_d	ϕ	ρ	ε_t
1963.50	**1546.25**	3899.54	1169.86	**4071.24**	0.700	**MAX.**	-
1963.50	**1546.25**	2591.33	777.40	**2705.43**	0.700	**3.28**	0.0055
1963.50	**1546.25**	1946.81	584.04	**2032.53**	0.700	**2.09**	0.0069
1963.50	**1546.25**	1559.94	467.98	**1628.62**	0.700	**1.42**	0.0085
1963.50	**1546.25**	1302.09	390.63	**1359.42**	0.700	**1.00**	0.0102
1963.50	**1546.25**	1116.08	334.82	**1165.22**	0.700	**1.00**	0.0102
1963.50	**1546.25**	976.57	292.97	**1019.56**	0.700	**1.00**	0.0102
1963.50	**1546.25**	868.06	260.42	**906.28**	0.700	**1.00**	0.0102
1963.50	**1546.25**	781.25	234.38	**815.65**	0.700	**1.00**	0.0102

P_d : Design axial load acting at the bottom of the column (kN)

V_e : Elastic design base shear (kN)

M_x : Design bending moment in longitudinal direction calculated according to COMB1 (kN.m) (See Eq.(3.25))

M_y : Design bending moment in transverse direction calculated according to COMB1 (kN.m) (See Eq.(3.26))

M_d : Uniaxial design bending moment calculated according to Eq.(3.27) (kN.m)

ϕ : Resistance factor to determine factored resistances by multiplying both P_n and M_n

ρ : Optimum longitudinal reinforcement ratio (%)

ε_t : Net tensile strain in the extreme tension steel

$$M_x = M\delta_s / R \tag{3.25}$$

$$M_y = M\delta_s / R \tag{3.26}$$

$$M_d = \sqrt{M_x^2 + \left(0.3M_y\right)^2} \tag{3.27}$$

In Eq.(3.27), design moment, M_d, is calculated by taking square root of sum of squares of design moments in orthogonal directions. This is due to having equally distributed longitudinal reinforcement and circular cross section. This produces equal flexural strength regardless of direction in column cross section. Resistance factor, ϕ, to be used in calculation of factored resistance is given according to seismic zone category and strain condition at the cross section on the contrary to AASHTO [4] in which magnitude of resistance factor is given in terms of the type of loading. Seismic performance zones are presented in Table 3.6.

Table 3.6 Seismic Performance Zones [5]

Acceleration Coefficient	Seismic Zone
$A \le 0.09$	1
$0.09 < A \le 0.19$	2
$0.19 < A \le 0.29$	3
$0.29 < A$	4

In AASHTO LRFD [5], resistance factors are defined separately for tension-controlled and compression controlled reinforced concrete sections. A lower ϕ-factor is used for compression-controlled sections than is used for tension controlled sections because the later one have less ductility and are more sensitive to variations in concrete strength. For seismic zone 2, resistance factor is taken as 0.9 regardless of design axial load ratio. For seismic zones 3 and 4, further reduction in nominal strength is proposed according to design axial load ratio. To estimate resistance factor for seismic zones 3 and 4, it is firstly required to have a section analysis for a given longitudinal reinforcement ratio under pure bending (P=0). From Figure 3.5, resistance factor is found in accordance with net tensile strain in extreme tension steel, ε_t, obtained from section analysis. Secondly, resistance factor obtained from Figure 3.5 is further reduced according to design axial load ratio interpolating from ϕ_P=0 to 0.5. This interpolation is demonstrated figuratively in Figure 3.6. It should be stated that design axial load ratio higher than 0.2 results in resistance factor of 0.5 regardless of ε_t.

For sections subjected to axial load with flexure, factored resistances are determined by multiplying both nominal strengths P_n and M_n by single value of ϕ. It is obvious that longitudinal reinforcement ratio that is directly dependent on resistance factor is not known at the beginning of design procedure. Therefore, it requires iteration to find resistance factor corresponding to longitudinal reinforcement ratio just satisfying design forces. In this study, resistance factor calculation is initially based on the assumption of tension-controlled section for pure bending case. After having optimum longitudinal reinforcement design, it is checked whether ε_t is greater than limiting value of 0.005 for tension-controlled section. It is observed that all designs satisfy initial assumption without any exception.

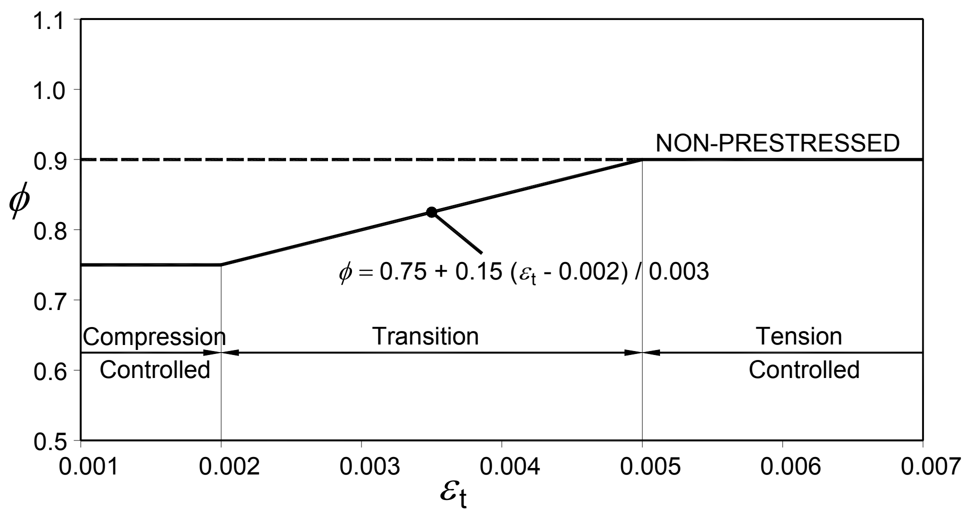

Figure 3.5 Variation of ϕ with Net Tensile Strain ε_t for Grade 420 Reinforcement [5]

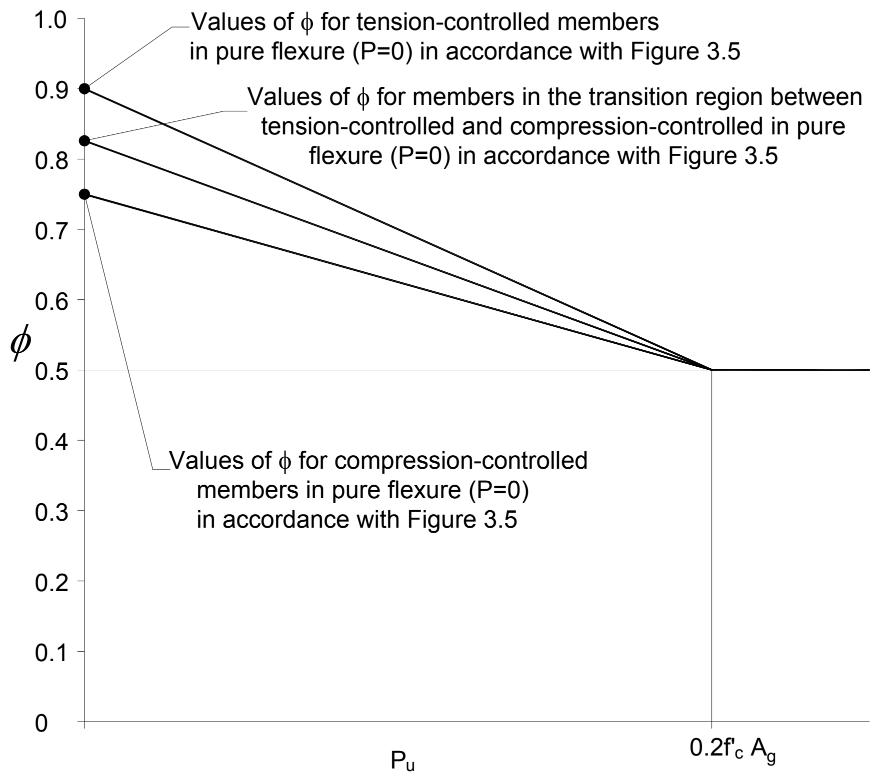

Figure 3.6 Variation of Resistance Factor in Seismic Zones 3 and 4 [5]

SECTION DESIGN DATA

CONCRETE		STEEL	
f_c (Mpa)=	25	f_y (Mpa)=	420
γ_{conc} (kN/m^3)=	25	E_s (Mpa) =	200000
E_c (Mpa) =	24000	ε_y =	0.0021
ε_{cu} =	0.003		

GENERAL			
cover (mm) =	100	ε_{axial} (%) =	0.1
ρ_{min} (%) =	1	ε_{moment} (%) =	0.1
ρ_{max} (%) =	4	Spacing (mm) =	150

Figure 3.7 Section Design Data

Material properties and input data related to section design given in Figure 3.7 are explained below;

f_c : Specified compressive strength of concrete for use in design (Mpa)

γ_{conc} : Density of concrete (kN/m^3)

E_c : Modulus of elasticity of concrete (Mpa)

ε_{cu} : Failure strain of concrete in compression (mm/mm)

f_y : Specified minimum yield strength of reinforcing bars (Mpa)

E_s : Modulus of elasticity of reinforcing bars (Mpa)

ε_y : Yield strain of reinforcing steel (mm/mm)

$cover$: Distance from extreme concrete fiber to centroid of the longitudinal reinforcing bars (mm)

$\rho_{\min}$: Minimum ratio of longitudinal reinforcement to gross cross-section area (%)

$\rho_{\max}$: Maximum ratio of longitudinal reinforcement to gross cross-section area (%)

ε_{axial} : Tolerance between factored resistance and design axial load (%)

ε_{moment} : Tolerance between factored resistance and design bending moment (%)

spacing : Spacing between longitudinal reinforcing bars (mm)

Although AASHTO LRFD [5] allows maximum area of longitudinal reinforcement up to 6% times the gross cross-section area, reinforcement ratio is limited to 4% in order to avoid congestion of reinforcing bars and to permit anchorage of the longitudinal steel. In addition to that, it is tried to be consistent with column test criteria used in developing Eq.(2.15) and Eq.(2.16). Assumptions used in determining longitudinal reinforcement ratio are given below;

- The analysis and design of the reinforced concrete section conforms to the provisions of the Strength and Extreme Event Limit State requirements specified in AASHTO LRFD [5]
- All conditions of strength satisfy the applicable conditions of equilibrium and strain compatibility. (Figure 3.8)
- Strain in the concrete and in the reinforcement is directly proportional to the distance from the neutral axis. (Figure 3.8)
- The maximum usable (ultimate) strain at the extreme concrete compression fiber, ε_{cu}, is assumed equal to 0.003. (Figure 3.8)
- Uniform rectangular concrete stress block approach is used. The maximum uniform concrete compressive stress is $0.85f_c$ and the block depth is $\beta_1 c$, where f_c denotes the concrete strength, c is the distance from the extreme compression fiber to the neutral axis and β_1 is described in Eq.(3.28). (Figure 3.8)

$$\begin{aligned}&\text{If } f_c \leq 28 \text{ Mpa}\\&\beta_1 = 0.85\\&\text{If } f_c > 28 \text{ Mpa}\\&\beta_1 = 0.85 - 0.05\left(f_c - 28\right)/7 \leq 0.65\end{aligned} \tag{3.28}$$

- Concrete displaced by the reinforcement in compression is not deducted from the compression block.

- Reinforcing bars are equally distributed around the periphery of cross-section (Figure 3.8). It is experienced that assumed spacing of 150 mm between longitudinal reinforcing bars do not alter moment capacities significantly.
- For the reinforcing steel, the elastic-plastic stress-strain distribution is used. Stress in the reinforcing steel below the yield strength, f_y, is directly proportional to the strain. For strains greater than that corresponding to the yield strength, the reinforcement stress remains constant and equal to f_y.
- Tensile strength of concrete is neglected.
- Stress in the reinforcement is computed based on the strain at the centroid of each reinforcing bar.
- All moments are referenced to the geometric centroid of the gross cross-concrete section.

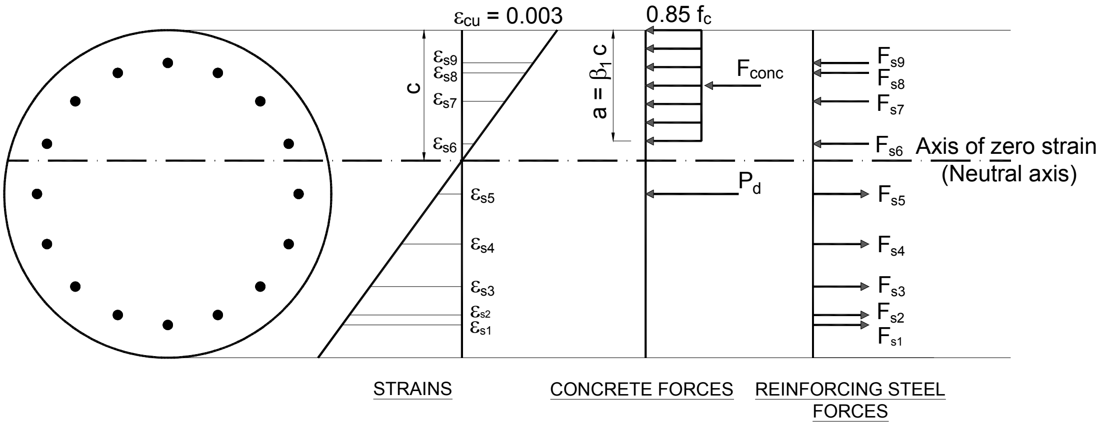

Figure 3.8 Strain Compatibility and Force Diagrams of Cross-Section

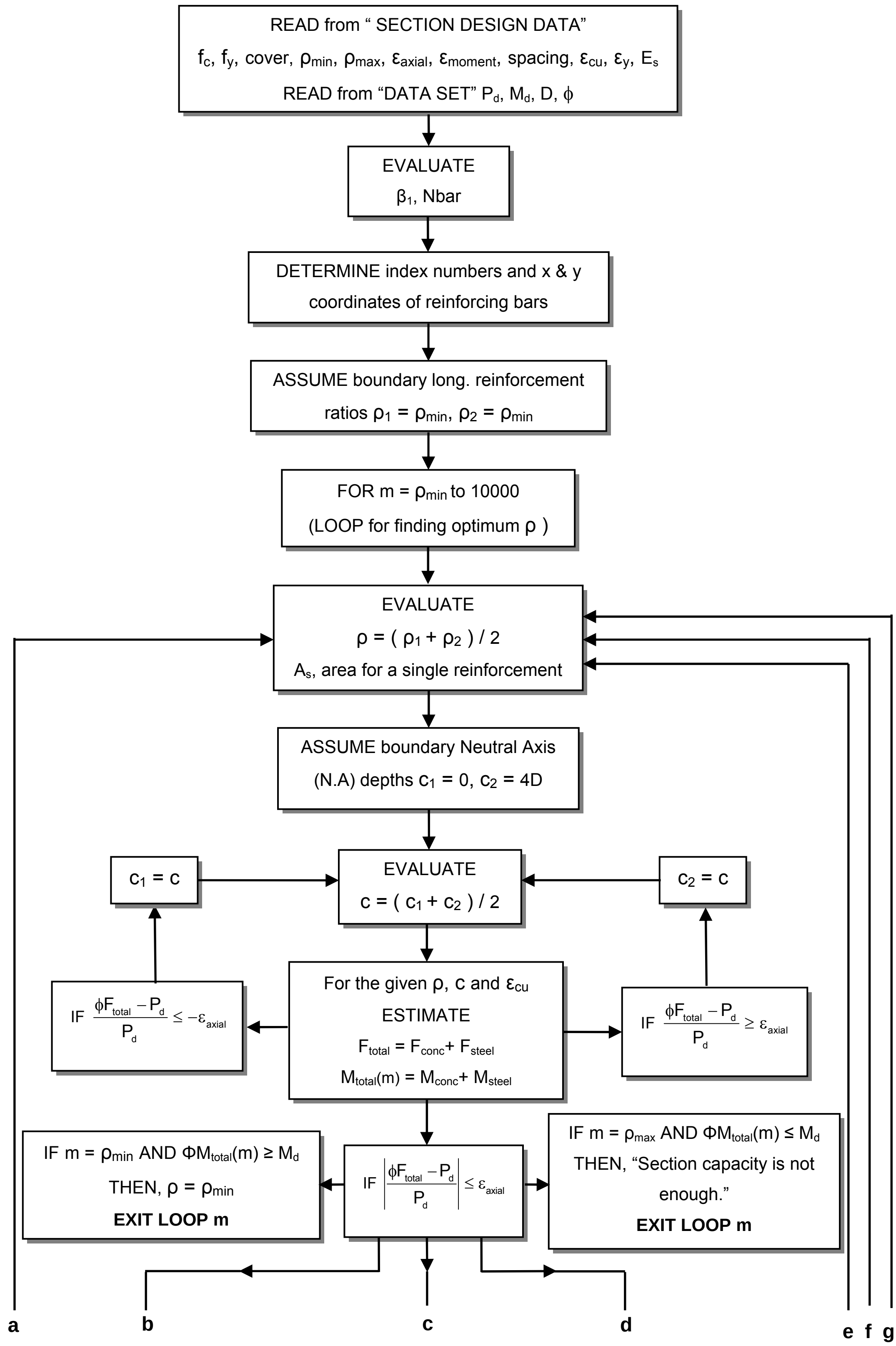

Figure 3.9 Section Design Flowchart

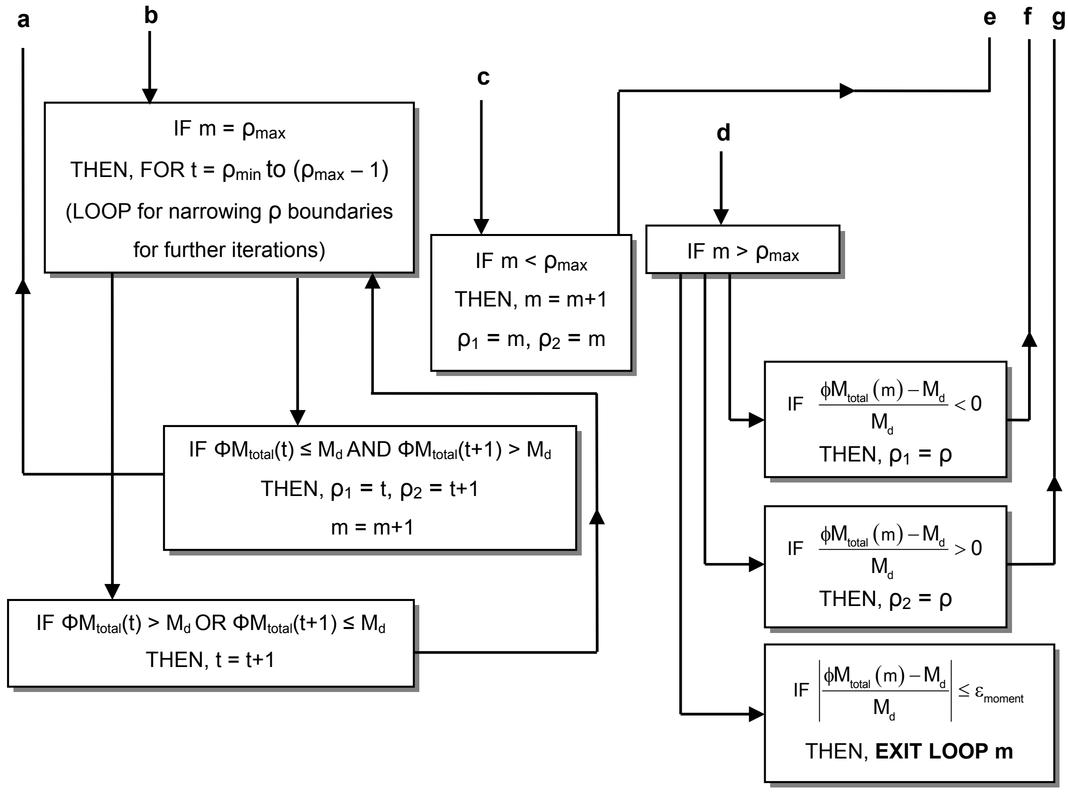

Figure 3.9 Section Design Flowchart (continued)

Section design flowchart is illustrated in Figure 3.9. (See APPENDIX A for source code) Underlying logic of design algorithm is comprised of nested iterations for finding neutral axis depth, c, to satisfy force equilibrium and for finding optimum steel ratio to provide required moment capacity simultaneously. Since the nature of the problem necessitates much iteration and there are more than 27000 analyses to be performed, run times become more of an issue for the efficiency and the stability of the program. Therefore, binary search algorithm is utilized for longitudinal reinforcement ratio iteration (LOOP m in Figure 3.9) and neutral axis depth iteration. In computer science, a binary search is an algorithm for locating the position of an element in a sorted list [47]. It inspects the middle element of the sorted list: if equal to the sought value, then the position has been found; otherwise, the upper half or lower half is chosen for further searching based on whether the sought value is greater than or less than the middle element. However, further searching for sought value requires reasoning behind the problem that should always hold true. For instance, if factored axial load resistance, ϕF_{total} in Figure 3.9, is less than axial load demand, P_d, neutral axis depth should always be increased or vice versa. Furthermore, if factored moment resistance, $\phi M_{total}(m)$ in Figure 3.9, is less than moment demand, M_d, longitudinal reinforcement ratio should always be increased or vice versa. Since these two facts hold true without any exceptions, binary search algorithm does not give rise to convergence problem during iterations. As a further advancement in design procedure, before starting with binary search for optimum reinforcement ratio, boundary conditions are tested initially to determine whether minimum or maximum reinforcement requirements are governed for the given cross-section. After that, successive integer values of trial reinforcement ratio starting from minimum to maximum steel ratio are tried so that range of sorted list is narrowed without a significant effort. This can be seen in Figure 3.9. Below, further definitions utilized in Figure 3.9 are given below.

N_{bar} : Number of reinforcing bars to be used in section design

A_s : Area of a single reinforcement bar calculated for assumed longitudinal reinforcement ratio (mm^2)

ρ_1, ρ_2 : Lower and upper limits for optimum reinforcement ratio, respectively (%)

c_1, c_2 : Lower and upper limits for neutral axis depth, respectively (mm)

F_{conc}, F_{steel} : Internal rectangular concrete stress block and reinforcing steel forces for a given ρ, c and ε_{cu}, respectively (kN)

M_{conc}, M_{steel} : Internal concrete and reinforcing steel moments referenced to the geometric centroid of the gross cross-concrete section, respectively (kN.m)

In order to compare results of section design with commercially available software program as PCACOL [48], back analyses are conducted for varying diameter, D, design forces, N_d and M_d, and resistance factor, ϕ as shown in Table 3.7. The longitudinal reinforcement ratios found in section design are back substituted in PCACOL [48] and corresponding factored moment resistance, ϕM_n, is obtained. For sections, conforming minimum reinforcement ratio (1%), ϕM_n / M_d is expected to be greater than unity. Additionally, for sections, exceeding maximum reinforcement ratio (4%), ϕM_n / M_d is expected to be less than unity. In between, it is supposed to be close to unity. As shown in Table 3.7, section design algorithm developed for this study is confirmed substantially.

Table 3.7 Comparison of Factored Moment Capacities

					PCACOL	
D (m)	P_d (kN)	M_d (kN.m)	ϕ	ρ (%)	ϕM_n (Kn.m)	ϕM_n / M_d
1.00	3926.99	1648.17	0.50	2.27	1615.40	0.980
1.25	3067.96	3953.64	0.70	1.98	3920.30	0.992
1.50	8835.73	27097.09	0.50	MAX.	8004.30	0.295
1.75	6013.20	5394.28	0.70	MIN.	7669.20	1.422
2.00	15707.96	18609.60	0.50	3.55	18191.20	0.978
2.25	19880.39	20361.12	0.50	2.20	20005.00	0.983
2.50	36815.54	55908.72	0.50	MAX.	35167.20	0.629
2.75	29697.87	33580.92	0.50	1.75	33099.80	0.986
3.00	17671.46	23006.88	0.70	MIN.	39535.90	1.718

3.6. Overstrength Resistance and Shear Design

Although elastic base shear is calculated in Table 3.5, forces resulting from inelastic hinging at the top and/or bottom of the column constitute as a basis for seismic design. The logic behind this fact is that the columns may have insufficient shear strength to enable a ductile flexural mechanism to develop due to potential overstrength in the flexural capacity of columns. Two procedures specified in AASHTO LRFD [5] are utilized for calculating plastic hinging forces of single column for the sake of comparison. The first procedure is explained below.

- Determination of the column overstrength moment resistance, is provided by a resistance factor, ϕ of 1.3 for reinforced concrete columns and 1.25 for structural steel column. For both materials, the applied axial load in the column is determined using Extreme Event Load Combination I.

- Using the overstrength moment resistance of column, $1.3M_n$, corresponding shear force is calculated by dividing with the height of the column, L.
- M_n in Table 3.8 represents nominal flexural resistance calculated according to assumptions in section 3.5.

Table 3.8 Part of Excelsheet Corresponding to Overstrength Resistance

OVERSTRENGTH RESISTANCE						
(kN m)	(kN m)		(kN)		(kN)	(kN)
M_n	M_p	M_p / M_n	V_p	Design Condition	V_d	V_d / ϕ
-	-	-	-	-	-	-
3761.70	4982.04	1.32	1992.82	Elastic	1546.25	1718.06
2755.53	3586.04	1.30	1434.42	Plastic	1434.42	1593.80
2164.98	2762.89	1.28	1105.16	Plastic	1105.16	1227.95
1787.67	2225.17	1.24	890.07	Plastic	890.07	988.97
1787.67	2225.17	1.24	890.07	Plastic	890.07	988.97
1787.67	2225.17	1.24	890.07	Plastic	890.07	988.97
1787.67	2225.17	1.24	890.07	Plastic	890.07	988.97
1787.67	2225.17	1.24	890.07	Plastic	890.07	988.97

A second procedure for finding forces resulting from plastic hinging is defined in APPENDIX B3 of AASHTO LRFD [5].

- Instead of implementing resistance factor greater than unity, actual material properties being greater than the minimum specified values are utilized for the overstrength resistance. Realistic values for f_c, f_y and ε_{cu} are tabulated in Figure 3.9. Increase in concrete strength reflects the effect of expected material strength and confinement provided by the transverse steel. Similarly, increase in reinforcement strength counts the effect of expected material strength and strain hardening.
- Plastic hinging moment, M_p in Table 3.8, is calculated by a uniform rectangular concrete stress block assumption mentioned in section 3.5 with material properties of Figure 3.9. The applied axial load in the column is determined using Extreme Event Load Combination I. Corresponding shear

force, V_p in Table 3.8 is calculated by dividing plastic hinging moment with the height of the column, L.

Table 3.9 Recommended Increased Values of Material Properties [5]

Increased f_y (minimum)	1.25 f_y
Increased f_c	1.5 f_c
Increased ε_{cu}	0.01

In this study, the second procedure is implemented. For the comparison of resistance factor of 1.3 proposed in the first procedure, with the results of latter procedure, statistical study of M_p/M_n is conducted. Sections ending up with minimum longitudinal reinforcement ratio (1%) are treated separately from whole dataset. Frequency distributions of M_p/M_n values are shown in Figure 3.10. Mean value of 11740 analyses corresponding to sections having minimum longitudinal reinforcement ratio is estimated as 1.248 with a standard deviation of 0.0204. This is obviously less than proposed resistance factor of 1.3 in AASHTO LRFD [5]. On the contrary, the mean value of 5854 analyses corresponding to sections having reinforcement ratio other than minimum is computed as 1.301 with a standard deviation of 0.033. This is in good agreement with AASHTO LRFD [5] for assumed values of increased material properties.

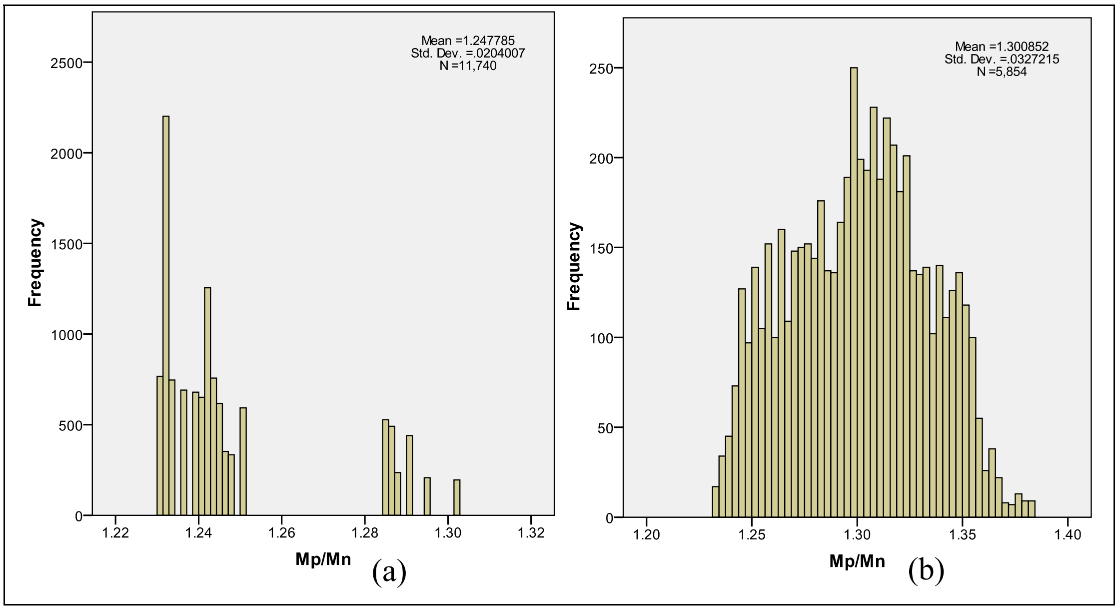

Figure 3.10 Histograms of M_p/M_n for (a) sections having minimum longitudinal reinforcement ratio, (b) sections having longitudinal reinforcement ratio other than minimum

Design shear force, V_d in Table 3.8, is the lesser of either the elastic design force, V_e in Table 3.5, determined from Extreme Event Limit State Load Combination I with R factor of 1 for the column, or the value corresponding to plastic hinging of the column. Instead of multiplying nominal shear strength with the resistance factor of 0.9 specified for shear and torsion, design load is increased by dividing with 0.9.

Table 3.10 Part of Excelsheet Corresponding to Shear Design

SHEAR DESIGN												
(mm)	(mm)	(kN)		(kN)	(kN)	(mm)	(mm^2)	(mm^2)			(mm^2)	(mm^2)
b_v	d_v	V_{n_max}	Shear Condition	V_c	V_s	s	A_{v_req}	A_{v_min}	ρ_{s_1}	ρ_{s_2}	A_{v_conf}	A_v
1000	679.2	-	-	-	-	100	-	-	-	-	-	-
1000	679.2	4244.89	Designable	405.88	1312.18	100	460.00	98.81	0.0071	0.0063	321.43	460.00
1000	679.2	4244.89	Designable	405.88	1187.92	100	416.44	98.81	0.0071	0.0063	321.43	416.44
1000	679.2	4244.89	Designable	405.88	822.07	100	288.19	98.81	0.0071	0.0063	321.43	321.43
1000	679.2	4244.89	Designable	405.88	583.09	100	204.41	98.81	0.0071	0.0063	321.43	321.43
1000	679.2	4244.89	Designable	405.88	583.09	100	204.41	98.81	0.0071	0.0063	321.43	321.43
1000	679.2	4244.89	Designable	405.88	583.09	100	204.41	98.81	0.0071	0.0063	321.43	321.43
1000	679.2	4244.89	Designable	405.88	583.09	100	204.41	98.81	0.0071	0.0063	321.43	321.43
1000	679.2	4244.89	Designable	405.88	583.09	100	204.41	98.81	0.0071	0.0063	321.43	321.43

Three complementary methods are given to evaluate shear resistance in AASHTO LRFD [5]. For concrete footings in which the distance from the point of zero shear to the face of the column, pier or wall is less than $3d_v$ with or without transverse reinforcement, and for other nonprestressed concrete sections not subjected to axial tension and containing at least the minimum reinforcement specified in Eq.(3.33), or having an overall depth of less than 400 mm, the following requirement of Method 1 may be used. In Table 3.10, corresponding part of Excelsheet related to shear design is tabulated. Definitions and formulations corresponding to Method 1 are explained below.

b_v: Effective web width. For circular sections, it can be taken as the diameter of the section (mm) (Figure 3.11)

d_v: Effective shear depth taken as distance, measured perpendicular to the neutral axis, between the resultants of the tensile and compressive forces due to flexure. Alternatively, d_v can be taken as 0.9 d_e.

d_e: Effective depth from extreme compression fiber to the centroid of the tensile force in the tensile reinforcement (mm)

$$d_e = \frac{D}{2} + \frac{D_r}{\pi} \tag{3.29}$$

D_r: Diameter of the circle passing through the centers of the longitudinal reinforcement (mm) (Figure 3.11)

V_{n_max}: Maximum nominal shear resistance (kN)

$$V_{n\_max} = 0.25 f_c b_v d_v \tag{3.30}$$

If maximum nominal shear resistance, V_{n_max}, is less than design force, V_d/ϕ, section is considered “Not Designable”. In this study, all analyses are “Designable” in terms of shear resistance.

V_c : Nominal shear resistance provided by tensile stresses in the concrete (kN)

$$V_c = 0.166\sqrt{f_c}\, b_v d_v \tag{3.31}$$

Since concrete contribution to shear resistance is doubtful within the plastic hinge zone, the concrete shear contribution is reduced for minimum factored axial compression force levels less than $0.1f_cA_g$ according to AASHTO LRFD [5]. For this case, V_c is decreased linearly from the value given in Eq.(3.31) to zero at zero compression force. Other than this, V_c is taken as that calculated in Eq.(3.31). Since maximum factor of 1.25 is used in Eq.(3.4), it needs to be converted to minimum factored axial compression force level with a factor of 0.9/1.25. Afterwards, related reduction in the concrete shear contribution is applied.

V_s : Shear resistance provided by shear reinforcement (kN)

$$V_s = V_d / \phi - V_c = \frac{A_v f_y d_v}{s} \tag{3.32}$$

s : Spacing of transverse reinforcement (mm)

According to seismic detailing provisions, transverse reinforcement for confinement is spaced not to exceed one-quarter of the minimum member dimension or 100 mm center to center. Therefore, spacing of spirals is taken as 100 mm. Furthermore, it is assumed that all required transverse reinforcement is supplied by two legs of spiral.

A_{v_req} : Total area of shear reinforcement within a distance, s, calculated according to Eq.(3.32) (mm^2)

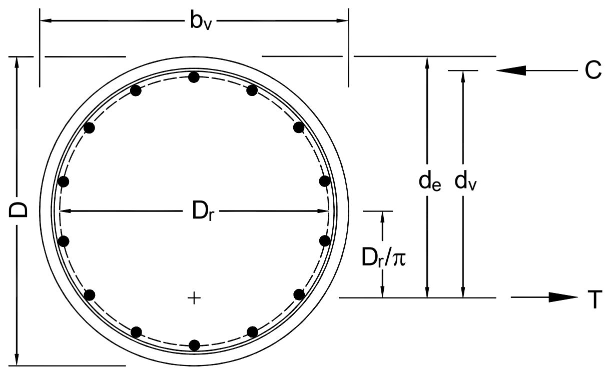

Figure 3.11 Illustration of Terms b_v, d_v and d_e for Circular Sections

A_{v_min} : Total area of minimum transverse reinforcement within a distance, s (mm^2)

$$A_{v\_min} \geq 0.083\sqrt{f_c}\frac{b_v s}{f_y} \tag{3.33}$$

ρ_{s_1}, ρ_{s_2} : Ratios of spiral reinforcement to total volume of column core for confinement in plastic hinge locations

$$\rho_{s\_1} \geq 0.12\frac{f_c}{f_y} \tag{3.34}$$

$$\rho_{s\_2} \geq 0.45\left(\frac{A_g}{A_c} - 1\right)\frac{f_c}{f_{yh}} \tag{3.35}$$

Where;

A_g : Gross area of concrete section (mm^2)

A_c : Area of core measured to the outside diameter of the spiral (mm^2)

f_c : Specified strength of concrete at 28 days, unless another age is specified (Mpa)

f_y : Yield strength of reinforcing bars (Mpa)

f_{yh} : Specified yield strength of spiral reinforcement (Mpa)

A_{v_conf} : Total area of transverse reinforcement required for confinement in plastic hinge locations within a distance, s (mm^2)

$$A_{v\_conf} = \frac{\max\left(\rho_{s\_1}, \rho_{s\_2}\right) d_s s}{2} \tag{3.36}$$

d_s : Diameter of spiral between bar centers (mm)

A_v : Total area of transverse reinforcement within a distance, s (mm^2)

$$A_v = \max\left(A_{v\_req}, A_{v\_\min}, A_{v\_conf}\right) \tag{3.37}$$

3.7. Moment Curvature Analysis

To provide a more realistic estimate for the displacement capacity of the structural members, calculations of yield and ultimate curvatures are based on expected (most probable) material properties. Following reasons are given below as of an origination of expected material properties according to Priestley et al. [49],

- The permissible range for yield strength of A706 steel is specified as 414 Mpa ≤ f_y ≤ 534 Mpa such that upper limit is 30% higher than the specified design value with an average increase of 12%.
- Typically, conservative concrete batch designs result in actual 28-day strengths of about 20 to 25 % higher than specified. Concrete also continues to gain strength with age. Test on cores taken from older California bridges built in the 1950s and 1960s have consistently yielded compression strength in excess of 1.5f'_c.

In this study, Caltrans-SDC [18] requirements are used for the calculation of expected material properties.

Expected unconfined concrete compressive strength, f'_{co} = 1.3 f_c (32.5 Mpa)

Expected yield strength of reinforcing steel, f_y = 475 Mpa

Expected ultimate tensile strength of reinforcing steel, f_{su} = 655 Mpa

The effect of strain hardening of reinforcing steel is combined with the increase of yield and tensile strength. Further enhancement in confined concrete strength and ultimate crushing strain owing to possible confinement provided by transverse reinforcement is taken into consideration by an appropriate concrete model.

Reinforcing Steel Model TEC [50]

Stress-strain relationship used for longitudinal and transverse reinforcing steel is shown in Figure 3.12 (b). Corresponding relations are given in Eq.(3.38).

$$f_s = \begin{cases} E_s \varepsilon_s & \varepsilon_s \le \varepsilon_y \\ f_s & \varepsilon_y < \varepsilon_s \le \varepsilon_{sh} \\ f_{su} - \left(f_{su} - f_y\right)\left[\left(\varepsilon_{su} - \varepsilon_s\right)/\left(\varepsilon_{su} - \varepsilon_{sh}\right)\right]^2 & \varepsilon_{sh} < \varepsilon_s \le \varepsilon_{su} \end{cases} \tag{3.38}$$

In this study, the strain at the onset of strain hardening, ε_{sh}, is taken as 0.008, the strain at ultimate stress, ε_{sh}, as 0.1 and modulus of elasticity, E_s, 200000 Mpa. In Figure 3.13, summary of longitudinal and transverse steel properties are represented.

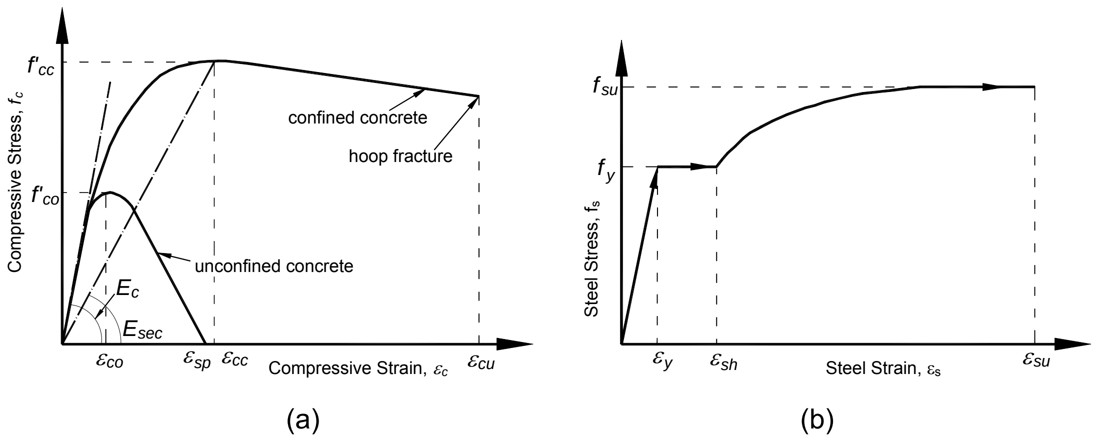

Figure 3.12 (a) Mander's [24] Confined and Unconfined Model (b) Reinforcing Steel Model [50]

MOMENT CURVATURE ANALYSIS DATA

CONCRETE

f'_{co} (Mpa) =	32.5
ε_{co} =	0.002
ε_{sp} =	0.005
cover_reinf. (mm) =	100
cover_conc (mm) =	50
strip_thick (mm) =	5

LONG. STEEL

f_y (Mpa) =	475
f_{su} (Mpa) =	655
E_s (Mpa) =	200000
ε_y =	0.002375
ε_{sh} =	0.008
ε_{su} =	0.1

TRANS. STEEL

f_y (Mpa) =	475
f_{su} (Mpa) =	655
E_s (Mpa) =	200000
ε_y =	0.002375
ε_{sh} =	0.008
ε_{su} =	0.1

GENERAL

inc_strain =	0.0002
ε_{axial} (%) =	0.1

Figure 3.13 Moment Curvature Analysis Data

Confined and Unconfined Concrete Model, Mander et al. [24]

Mander's material model is used for stress-strain relationship of both confined and unconfined concrete under uniaxial compression. Unconfined concrete parameters are shown in Figure 3.13.

Where;

f'_{co} : Unconfined concrete strength (Mpa) (Figure 3.12 (a))

ε_{co} : Unconfined concrete compressive strain at maximum compressive stress, taken as 0.002 (Figure 3.12 (a))

ε_{sp} : Ultimate unconfined concrete compressive strain corresponding to spalling, taken as 0.005 (Figure 3.12 (a))

In Table 3.11, related parts of Excelsheet corresponding to confined and unconfined concrete model calculations are shown. Definitions and related formulations for circular column confined with circular spirals are explained below.

Table 3.11 Part of Excelsheet Corresponding to Confined and Unconfined Concrete Model

MANDER CONFINED CONCRETE MODEL											MANDER UNCONFINED CONCRETE MODEL	
(mm)	(mm)			(Mpa)	(Mpa)	(Mpa)		(Mpa)			(Mpa)	
d_s	s'	ρ_s	k_e	f'_l	E_c	f'_{cc}	ε_{cc}	E_{sec}	r_{cc}	ε_{cu}	E_{sec}	r_{uncon}
900	100	-	-	-	-	-	-	-	-	-	-	-
900	100	0.0102	0.92	2.24	28504.39	45.9	0.0061	7500.40	1.36	0.0188	16250.00	2.33
900	100	0.0093	0.91	2.00	28504.39	44.6	0.0057	7784.43	1.38	0.0178	16250.00	2.33
900	100	0.0071	0.90	1.53	28504.39	42.1	0.0049	8506.89	1.43	0.0153	16250.00	2.33
900	100	0.0071	0.90	1.53	28504.39	42.0	0.0049	8518.86	1.43	0.0153	16250.00	2.33
900	100	0.0071	0.90	1.53	28504.39	42.0	0.0049	8518.86	1.43	0.0153	16250.00	2.33
900	100	0.0071	0.90	1.53	28504.39	42.0	0.0049	8518.86	1.43	0.0153	16250.00	2.33
900	100	0.0071	0.90	1.53	28504.39	42.0	0.0049	8518.86	1.43	0.0153	16250.00	2.33
900	100	0.0071	0.90	1.53	28504.39	42.0	0.0049	8518.86	1.43	0.0153	16250.00	2.33

Where;

d_s : Diameter of spiral between bar centers (mm)

s': Clear vertical spacing between spiral (mm)

ρ_s: Ratio of the volume of transverse confining steel to the volume of confined concrete core given in Eq.(3.39)

$$\rho_s = \frac{4A_s}{d_s s} \tag{3.39}$$

k_e : Confinement effectiveness coefficient for circular spirals given in Eq.(3.40)

$$k_e = \frac{1 - \dfrac{s'}{2d_s}}{1 - \rho_{cc}} \tag{3.40}$$

ρ_{cc} : Ratio of area of longitudinal reinforcement to the area of the core section

f_l' : Effective lateral confining stress on concrete for circular sections (Mpa) given in Eq.(3.41)

$$f_l^{'} = \frac{1}{2} k_e \rho_s f_{yh} \tag{3.41}$$

f_y : Yield strength of the transverse reinforcement (Mpa)

E_c : Tangent modulus of elasticity of the concrete (Mpa) given in Eq.(3.42) (Figure 3.12 (a))

$$E_c = 5000\sqrt{f_{co}^{'}} \tag{3.42}$$

$f_{cc}^{'}$: Compressive strength of confined concrete (Mpa) given in Eq.(3.43) (Figure 3.12 (a))

$$f_{cc}^{'} = f_{co}^{'}\left(-1.254 + 2.254\sqrt{1 + \frac{7.94 f_l^{'}}{f_{co}^{'}}} - 2\frac{f_l^{'}}{f_{co}^{'}}\right) \tag{3.43}$$

ε_{cc} : The maximum concrete strain corresponding to maximum concrete stress, $f^{'}_{cc}$, given in Eq. (3.44) (Figure 3.12 (a))

$$\varepsilon_{cc} = \varepsilon_{co}\left[1 + 5\left(\frac{f_{cc}^{'}}{f_{co}^{'}} - 1\right)\right] \tag{3.44}$$

$E_{\sec}$: Secant modulus of elasticity of the concrete (Mpa) given in Eq.(3.45) (Figure 3.12 (a))

$$E_{\sec} = \frac{f_{cc}^{'}}{\varepsilon_{cc}} \tag{3.45}$$

r : Parameter given in Eq.(3.46)

$$r = \frac{E_c}{E_c - E_{sec}} \tag{3.46}$$

Stress-strain relationship of confined concrete is given as;

$$f_c = \frac{f'_{cc} x r}{r - 1 + x^r} \tag{3.47}$$

Where;

$$x = \frac{\varepsilon_c}{\varepsilon_{cc}} \tag{3.48}$$

The unconfined concrete follows the same curve that the confined concrete does. With an effective lateral confining stress on concrete, f'_l =0, stress-strain relationship for unconfined concrete can be obtained. The part of the falling branch for strains larger than $2\varepsilon_{co}$ is assumed to be a straight line which reaches zero stress at the spalling strain, ε_{sp} .

ε_{cu} : Ultimate confined concrete compression strain given in Eq.(3.49) (Figure 3.12 (a))

$$U_{sh} = U_{cc} + U_{sc} - U_{co} \tag{3.49}$$

Where;

U_{sh} : The ultimate strain energy capacity of the confining reinforcement per unit volume of core

U_{cc} : Area under confined concrete stress-strain curve

U_{cc} : Area under unconfined concrete stress-strain curve

U_{sh} : Additional energy to maintain yield in the longitudinal steel in compression

Substituting in Eq.(3.49) gives;

$$\rho_s A_{cc} \cdot \int_0^{\varepsilon_{sf}} f_s d\varepsilon_s = A_{cc} \cdot \int_0^{\varepsilon_{cu}} f_c d\varepsilon_c + \rho_{cc} A_{cc} \cdot \int_0^{\varepsilon_{cu}} f_{sl} d\varepsilon_c - A_{cc} \cdot \int_0^{\varepsilon_{sp}} f_c d\varepsilon_c \qquad (3.50)$$

Where;

A_{cc} : Area of concrete core

ε_{sf} : Fracture strain of transverse reinforcement

f_s : Stress in transverse reinforcement

ε_s : Strain in transverse reinforcement

ε_{sf} : Fracture strain of transverse reinforcement

f_c : Longitudinal compressive stress in concrete

ε_c : Longitudinal compressive strain in concrete

f_{sl} : Stress in longitudinal reinforcement

The energy balance approach pointed out in Eq.(3.50), requires iterative solution to find ultimate crushing strain of the confined concrete. Instead of using this, an approximate and conservative approach proposed by Priestley et al. [3] is utilized.

$$\varepsilon_{cu} = 0.004 + \frac{1.4 \rho_s f_{yh} \varepsilon_{su}}{f'_{cc}} \qquad (3.51)$$

Where;

f_{yh} : Yielding stress of transverse reinforcement (Mpa)

Priestley et al. [3] state that Eq (3.51) is approximate for number of reasons:

- Simplified equation is based on pure axial compression of the core concrete. Under combined axial load and bending, the equation will predict conservatively low estimates for ε_{cu}.

- The additional confinement effect of adjacent member in critical section is not taken into consideration. A column supported by massive foundation will have additional restraint to lateral expansion that is probable to increase ultimate crushing strain of the confined concrete

When combined effects of these approximations are considered, ultimate compression strain calculated by Eq. (3.51) predicts the values by a factor of about 1.3 to 1.6. This conservatism may ensure an adequate margin of safety to allow for uncertainties in moment curvature analysis. Assumptions used in determining moment curvature relationship are given below;

- All conditions of strength satisfy the applicable conditions of equilibrium and strain compatibility. (Figure 3.14)
- Strain in the concrete and in the reinforcement is directly proportional to the distance from the neutral axis. (Figure 3.14)
- The maximum usable (ultimate) strain at the confined concrete compression fiber, ε_{cu}, is calculated according to Eq.(3.51). (Figure 3.14)
- Compression zone is divided into filaments for both confined and unconfined region to be taken into account separately. (Figure 3.14)
- Reinforcing bars are equally distributed around the periphery of cross-section. (Figure 3.14)
- For the reinforcing steel, strain hardening is considered. (Figure 3.12 (b))
- Tensile strength of concrete is ignored in analyses.
- Stress in the reinforcement is computed based on the strain at the centroid of each reinforcing bar.
- All moments are referenced to the geometric centroid of the gross cross-concrete section.
- Termination criteria of the analysis are assumed as either when the extreme fiber of confined concrete reaches the ultimate crushing strain of confined concrete, $\varepsilon_{cu,}$ or steel reaches the rupture strain, ε_{su}.

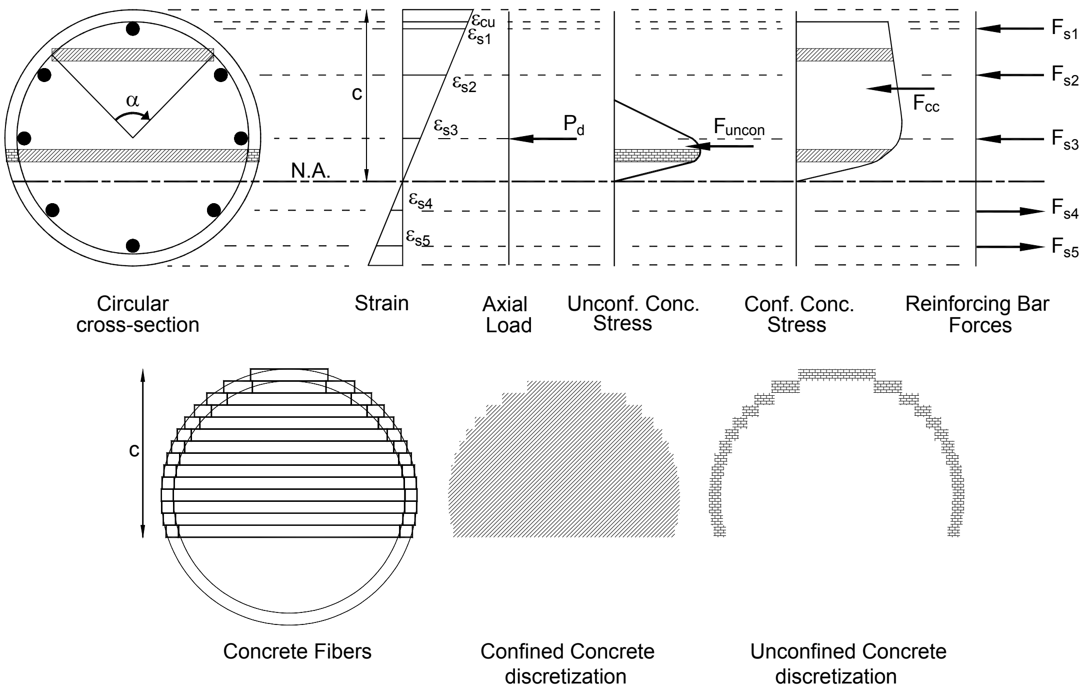

Figure 3.14 Strain Compatibility, Force Diagrams and Discretization of Cross-Section

Additional input data given in Figure 3.13 is explained below;

cover_reinf : Distance from extreme concrete fiber to centroid of the longitudinal reinforcing bars (mm)

cover_con : Distance of unconfined concrete region from extreme concrete fiber (mm)

strip_thick : Strip thickness to discretize the compression zone (mm)

inc_strain : Incremental strain at the extreme confined concrete fiber to be used in each curvature calculation

Flowchart of moment curvature analysis is illustrated in Figure 3.15. (See APPENDIX A for source code). The algorithm to evaluate the moment and curvature values for a given design axial load, P_d, and strain of extreme confined concrete fiber, ε_c, is as follows:

- Instead of selecting curvature values for uppermost extreme fiber of confined concrete for iteration, strain values from 0.0002 up to ε_{cu}, are selected to find corresponding curvature value.
- Before starting iteration for neutral axis depth, it is checked whether pure compression axial load capacity of the section for the given ε_c and longitudinal reinforcement ratio is enough or not. If it is not, convergence of iteration for neutral axis depth is not possible.
- For neutral axis depth iteration, binary search algorithm is benefited from as in section 3.5. Confined and unconfined concrete forces are integrated along the neutral axis depth.
- If the evaluated axial load, F_{total}, is equal to the design axial load, P_d, within a predetermined margin, ε_{axial}, the neutral axis is found and then the corresponding moment and curvature are evaluated. They are stored in the program memory as of M(count) and ϕ(count) for moment and curvature value corresponding to ε_c, respectively.
- In addition, extreme tension strain of reinforcing steel, ε_{s_extr}(count), and extreme compression strain of unconfined concrete, ε_{con}(count), are stored in order to calculate the first yield point,(ϕ'_y, M'_y), shown in Figure 3.16.

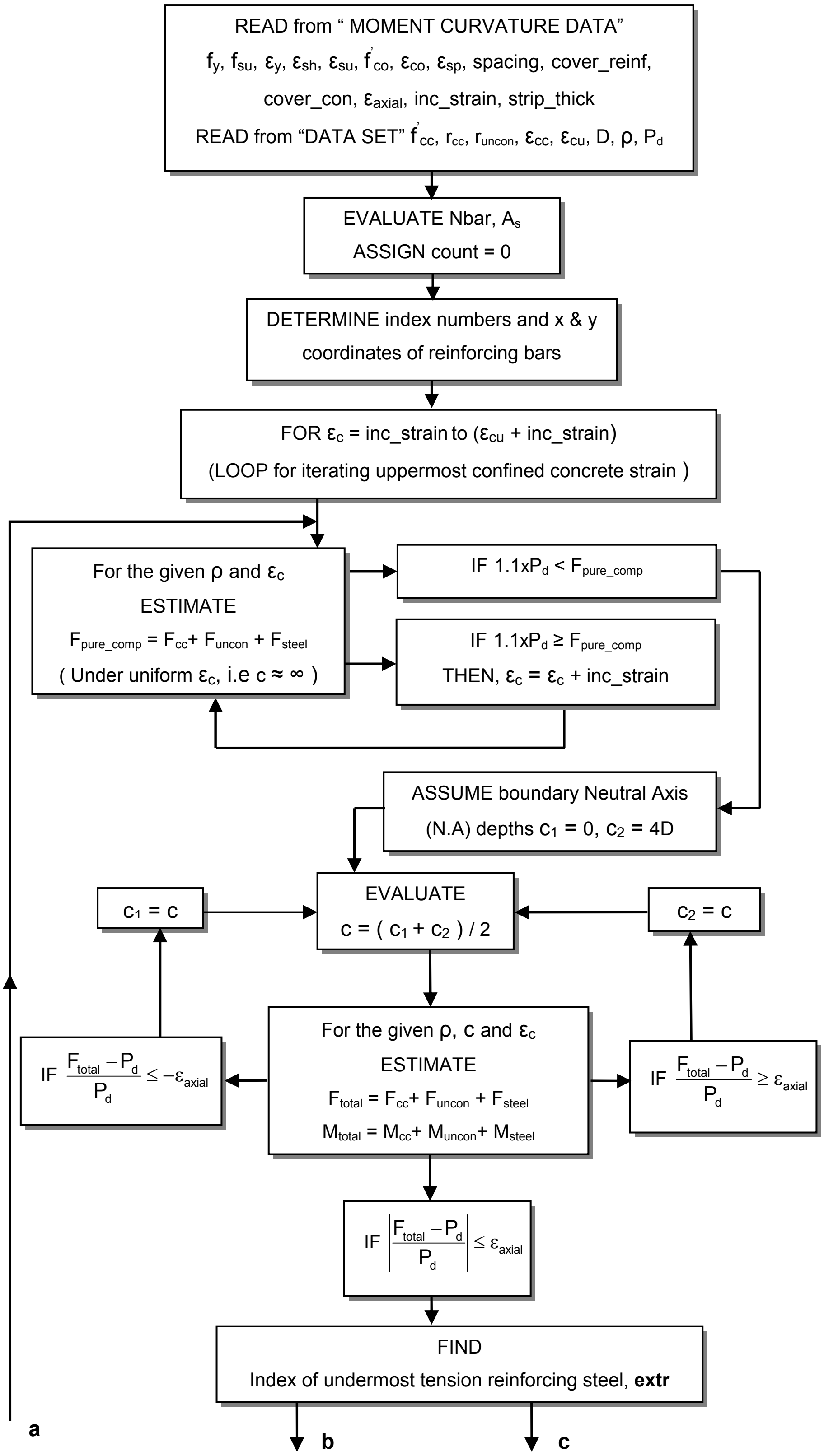

Figure 3.15 Moment Curvature Analysis Flowchart

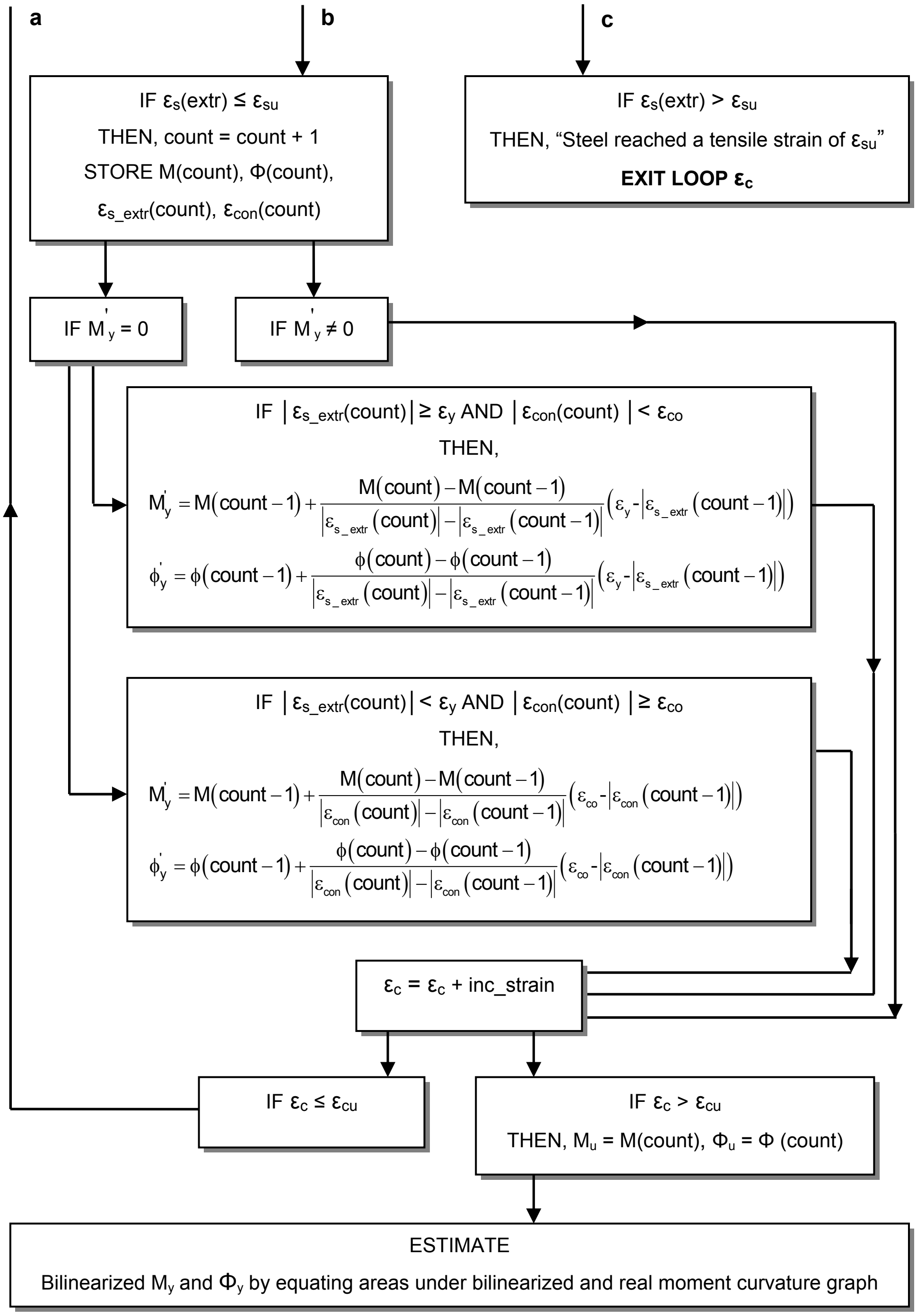

Figure 3.15 Moment Curvature Analysis Flowchart (continued)

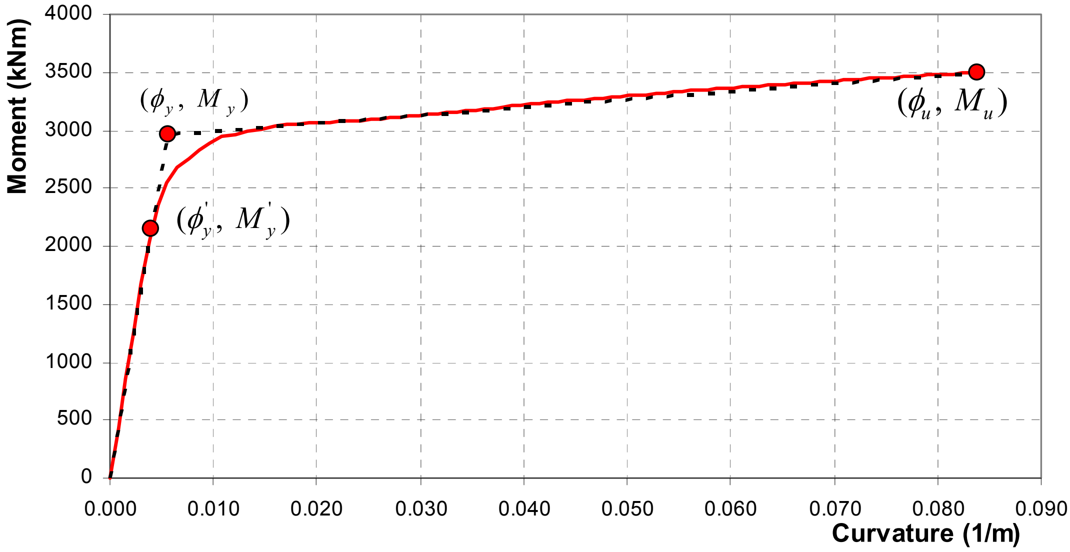

Figure 3.16 Bilinear Idealization of a Moment Curvature Diagram

The first yield point, (ϕ'_y, M'_y), is defined as the point when extreme tension reinforcement reaches yield strain, ε_y, or when the extreme unconfined concrete compression fiber reaches a strain of 0.002, ε_{co}, whichever occurs first. The first yield point is calculated by interpolating either ε_y or ε_{co} between stored moment and curvature values as formulized in Figure 3.15. The ultimate point, (ϕ_u, M_u), is the stopping point of original moment curvature diagram. The idealized yield moment and curvature, (ϕ_y, M_y), is obtained by balancing the areas between the actual and idealized moment-curvature curves. In Table 3.12, related parts of Excelsheet corresponding to moment curvature analysis are shown. Additional definitions and related formulations are explained below.

α_{gross}^{cal}: Stiffness modification factor obtained after moment curvature analysis is performed for previously calculated α_{gross}.

$$\alpha_{gross}^{cal} = \frac{M_y}{\phi_y} \tag{3.52}$$

μ_ϕ : Curvature ductility

$$\mu_\phi = \frac{\phi_u}{\phi_y} \tag{3.53}$$

Table 3.12 Part of Excelsheet Corresponding to Moment Curvature Analysis

MOMENT CURVATURE ANALYSIS						
(1/m)	(kN)	(1/m)	(kN)	(1/m)		
ϕ'_y	M_y	ϕ_y	M_u	ϕ_u	α^{cal}_{gross}	μ_ϕ
-	-	-	-	-	-	-
0.0046	4489.30	0.0060	5007.54	0.0688	0.64	11.49
0.0044	3236.48	0.0057	3615.47	0.0732	0.49	12.95
0.0042	2490.79	0.0054	2719.94	0.0712	0.39	13.23
0.0041	2022.18	0.0052	2190.94	0.0793	0.33	15.35
0.0041	2022.18	0.0052	2190.94	0.0793	0.33	15.35
0.0041	2022.18	0.0052	2190.94	0.0793	0.33	15.35
0.0041	2022.18	0.0052	2190.94	0.0793	0.33	15.35
0.0041	2022.18	0.0052	2190.94	0.0793	0.33	15.35

Since moment curvature analysis has a key role in capacity calculations as ultimate curvature and eventually ultimate displacement of the column members, the author of this thesis believes that reliability of the analysis tool developed for this study should be verified by other commercially and non-commercially available software packages. For this purpose, USC_RC [51] and XTRACT [52] are used for comparison of the results. UCS_RC [51] is developed by Asad Esmaeily as a freeware. It utilizes the same "dividing compression zone into filaments" analogy for calculation of confined and unconfined concrete forces. Although ultimate crushing strain of confined concrete, ε_{cu}, is estimated by energy balance approach, there is an option to set stopping criterion for the exceedance of ultimate strain for confined concrete. On the contrary, XTRACT [52] discretizes any arbitrary section into triangular fibers of user specified size created with user specified material as shown in Figure 3.17. Both softwares use same material models for confined and unconfined concrete as well as strain hardening steel model. In order to compare moment curvature curves of different softwares, a generic case is studied.

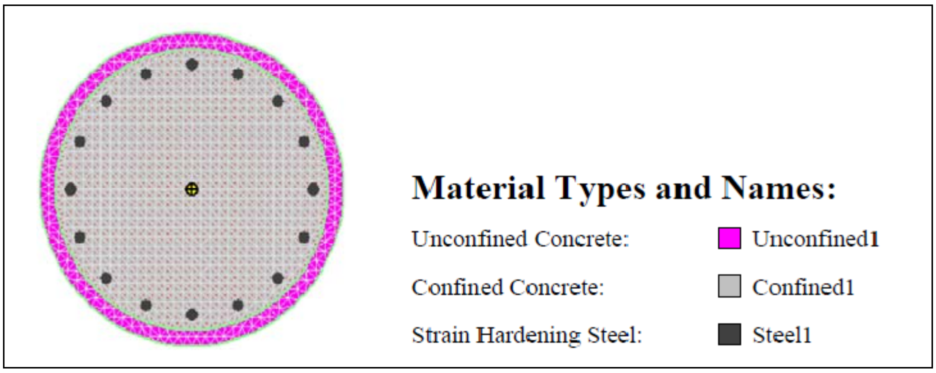

Figure 3.17 Discretization of Circular Cross-Section and Corresponding Material Types, XTRACT [52]

Comparison of moment curvature diagrams of circular cross-section having the diameter of D = 1 meter with varying longitudinal reinforcement ratios (1%, 2.074% and 2.957%) and design axial loads (1 kN, 2000 kN, 4000 kN, 6000 kN and 8000 kN) is shown in Figure 3.18. All have the same ultimate concrete crushing strain of ε_{cu}=0.0153 calculated according to Eq.(3.51). Compared to XTRACT [52] and this study, USC_RC [51] yields little higher moment and less ultimate curvature. XTRACT [52] and this study yield almost the identical diagrams. Therefore, moment curvature program developed for this study may be regarded as reasonable and satisfactory.

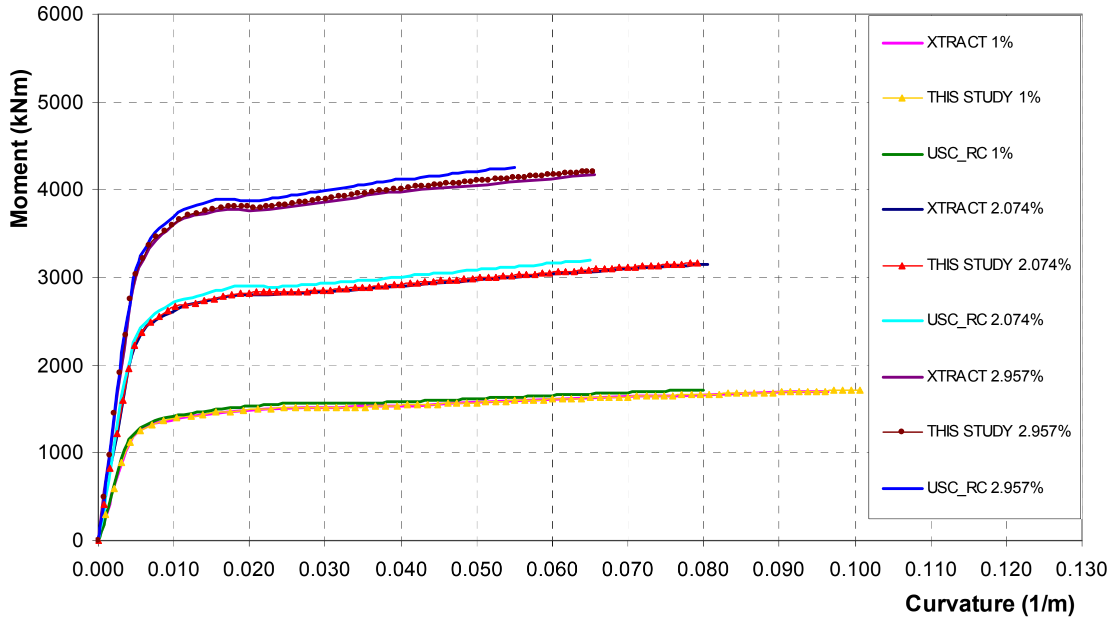

(a)

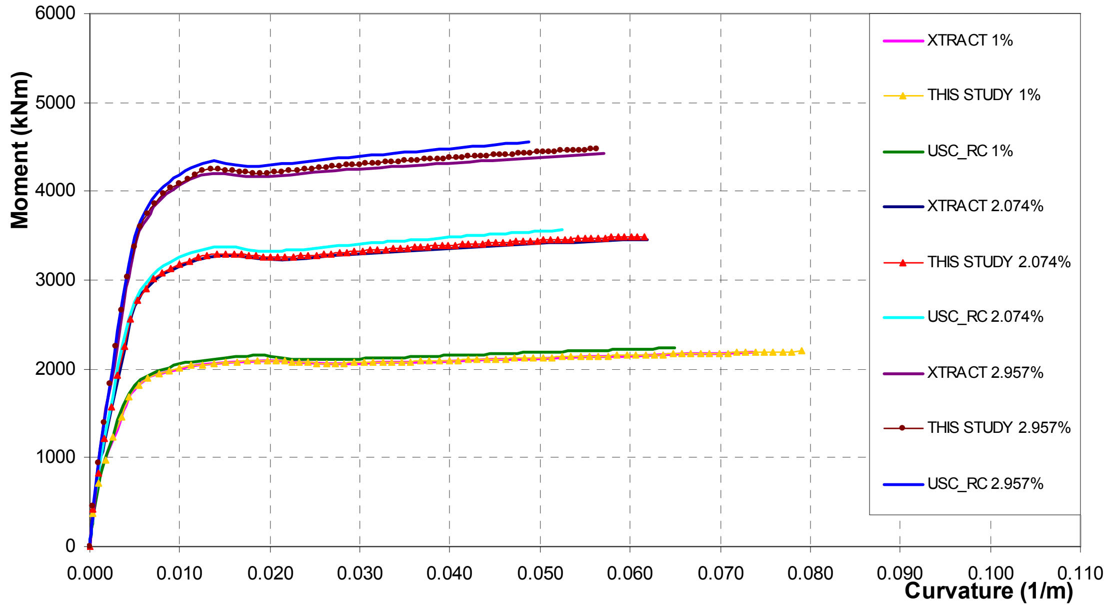

(b)

Figure 3.18 Comparison of Moment Curvature Diagrams, (a) P_d=1 kN, (b) P_d=2000 kN, (c) P_d=4000 kN, (d) P_d=6000 kN, (e) P_d=8000 kN

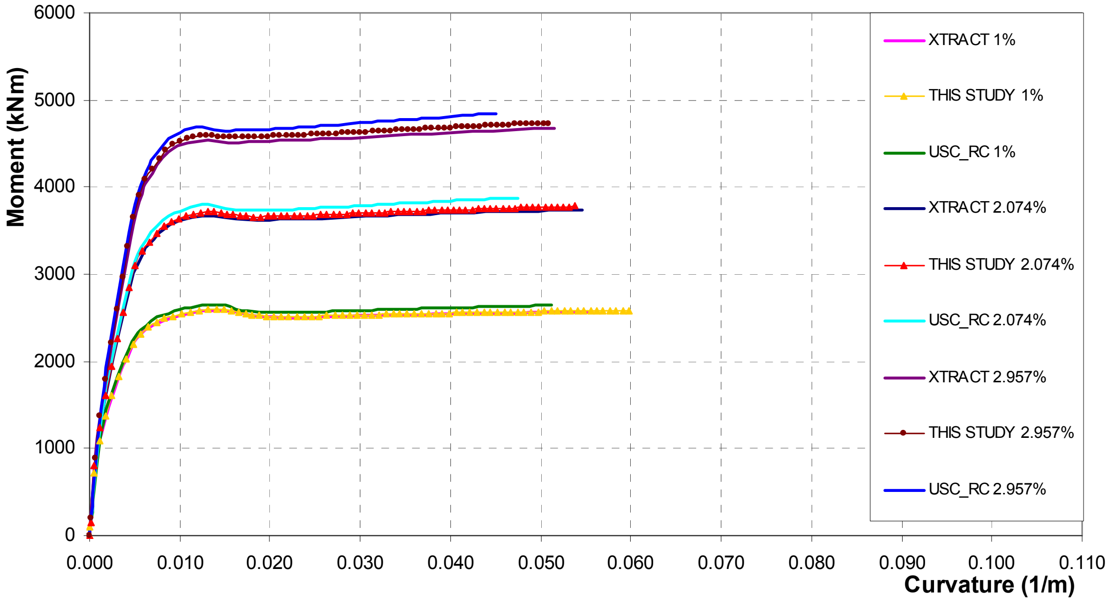

(c)

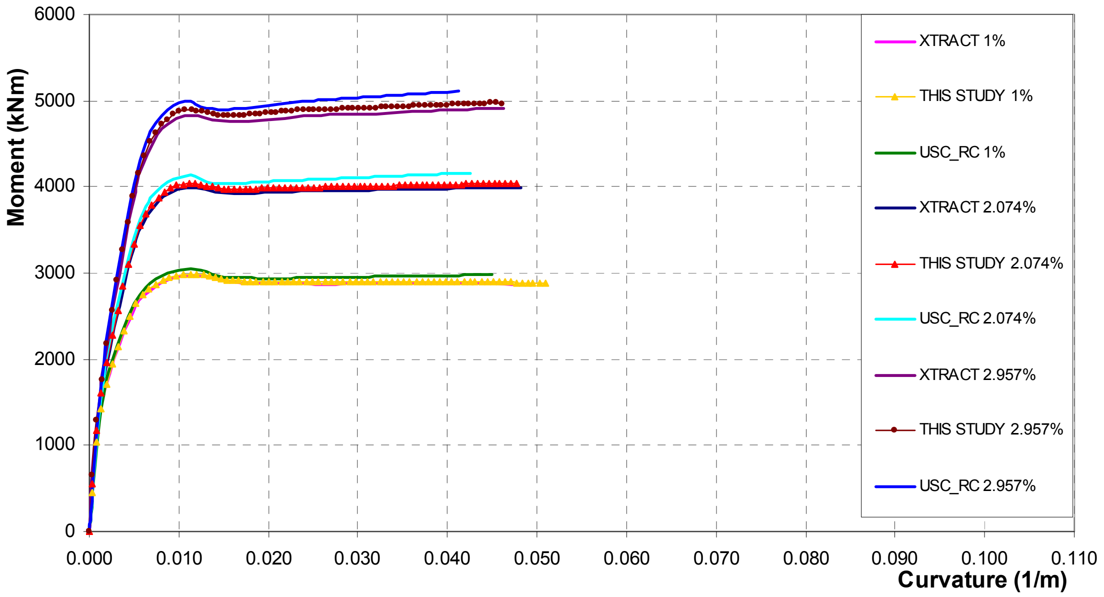

(d)

Figure 3.18 Comparison of Moment Curvature Diagrams, (a) P_d=1 kN, (b) P_d=2000 kN, (c) P_d=4000 kN, (d) P_d=6000 kN, (e) P_d=8000 kN (Continued)

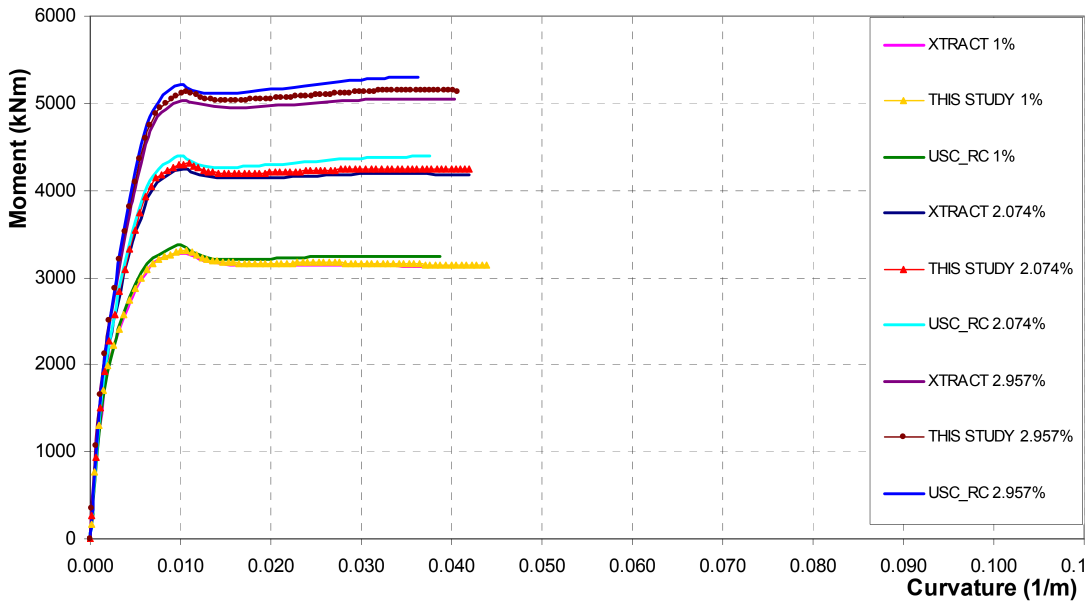

(e)

Figure 3.18 Comparison of Moment Curvature Diagrams, (a) P_d=1 kN, (b) P_d=2000 kN, (c) P_d=4000 kN, (d) P_d=6000 kN, (e) P_d=8000 kN (Continued)

3.8. Pushover Analysis

Assumptions used in developing force-displacement response of cantilever bridge column are given below;

- Anchorage deformation (strain-penetration) is taken into account. Strain-penetration is described as ability of tension reinforcement to develop additional strains up to a depth equal to the true development length of the reinforcement. In other words, the curvature that contributes to deformation capacity of the member does not drop to zero immediately below the column base. By defining a constant curvature over the strain-penetration length below the column base, this drawback is compensated [3].
- Flexural deformations are assumed to dominate force-displacement response. Although this assumption is thought to be reasonable owing to specified minimum requirements of shear and confinement reinforcements, further validation is required for the reliability of the lateral response. For this

purpose, column classifications proposed by Setzler and Sezen [53] are utilized.

These classifications developed for modeling the behavior of reinforced concrete columns subjected to lateral loads are given in Table 3.13.

Table 3.13 Column Classifications for Modeling Lateral Behavior [53]

Category I: $V_n < V_y$ The shear strength is less than the lateral load causing yielding in the tension steel. The column fails in shear while the flexural behavior remains elastic.
Category II: $V_y \le V_n < 0.95V_p$ The shear strength is greater than the yield strength, but less than the flexural strength of the column. The column fails in shear, but inelastic flexural deformation occurring prior to shear failure affects the post-peak behavior.
Category III: $0.95V_p \le V_n \le 1.05V_p$ The shear and flexural strengths are essentially identical. Due to the inherent variability in the models used to predict the strengths, it is not possible to predict conclusively which mechanism will govern the peak response. Shear and flexural failure are assumed to occur "simultaneously," and both mechanisms contribute to the post-peak behavior.
Category IV: $1.05V_p < V_n \le 1.4V_p$ The shear strength is greater than the flexural strength of the column. The column experiences large flexural deformations potentially leading to a flexural failure. Inelastic shear deformations affect the post-peak behavior, and shear failure may occur as displacements increase.
Category V: $V_n > 1.4V_p$ The shear strength is much greater than the flexural strength of the column. The column fails in flexure while the shear behavior remains elastic.

Where;

V_n: Shear strength calculated from the equation proposed by Sezen and Moehle [54]

$$V_n = V_s + V_c = k\frac{A_v f_y d}{s} + k\left(\frac{0.5\sqrt{f_c}}{a/d}\sqrt{1+\frac{P}{0.5\sqrt{f_c}A_g}}\right)0.8A_g \qquad (3.54)$$

a : Distance from maximum moment section to the point of inflection, taken as L

d : Distance from the extreme compression fiber to centroid of tension reinforcement, taken as d_e (Eq.(3.29))

k : Ductility-related strength degradation factor. It is defined to be equal to 1.0 for displacement ductility less than 2, to be equal to 0.7 for displacement ductility exceeding 6, and vary linearly for intermediate displacement ductilities. k is taken as 1.0 in the proposed model for classification purposes.

A_v : Total area of transverse reinforcement within a distance, s (Eq.(3.37))

A_g : Gross area of section

P : Compressive axial load, taken as P_u

V_y : Yield strength defined as the lateral load corresponding to first yielding of the tension bars in the column during the flexural analysis. (M'_y shown in Figure 3.16)

V_p : Flexural strength defined as the lateral load corresponding to maximum moment sustainable by the column cross section. (M_u shown in Figure 3.16)

Table 3.14 Part of Excelsheet Corresponding to Model for Lateral Behavior of RC Columns

MODEL FOR LATERAL BEHAVIOR OF RC COLUMNS				
	(kN)	(kN)	(kN)	
k	**V_n**	**V_y**	**V_p**	**Condition**
-	-	-	-	-
0.70	2128.54	1377.67	2003.02	Category IV
0.70	1990.47	1006.51	1446.19	Category IV
0.70	1689.34	785.31	1087.98	Category V
0.70	1689.34	647.73	876.38	Category V
0.70	1689.34	647.73	876.38	Category V
0.70	1689.34	647.73	876.38	Category V
0.70	1689.34	647.73	876.38	Category V
0.70	1689.34	647.73	876.38	Category V

Calculation steps and classification condition are shown in Table 3.14. According to Setzler and Sezen [53], category IV and V specimens are those that are expected to fail in flexure. For both cases, shear deformation does not constitute crucial portion of deformation response of the column up to peak strength. There are 201 analyses out of 17594 that columns are classified as category II and III. These cases are observed in analyses with low R-factors (R ≤ 1.5) and low aspect ratios (L/D ≤ 3.0). Inconsiderable amount of analyses signify that shear strength estimation and minimum design requirements for transverse reinforcement and confinement specified in AASHTO LRFD [5] provide columns to behave in flexure-dominant manner.

Table 3.15 Part of Excelsheet Corresponding to Pushover Analysis

PUSHOVER ANALYSIS								
(mm)	(m)		(m)	(m)	(m)	(%)		
d_b	**L_{SP}**	**k**	**L_p**	**Δ_y**	**Δ_u**	**Slope of postyield, α**	μ_Δ	**R_μ**
-	-	-	-	-	-	-	-	-
45.29	0.47	0.076	0.95	0.018	0.166	1.37	9.42	0.86
36.17	0.38	0.076	0.76	0.016	0.143	1.43	9.18	1.19
29.77	0.31	0.076	0.62	0.014	0.117	1.27	8.22	1.55
25.00	0.26	0.076	0.52	0.013	0.110	1.13	8.38	1.91
25.00	0.26	0.076	0.52	0.013	0.110	1.13	8.38	1.91
25.00	0.26	0.076	0.52	0.013	0.110	1.13	8.38	1.91
25.00	0.26	0.076	0.52	0.013	0.110	1.13	8.38	1.91
25.00	0.26	0.076	0.52	0.013	0.110	1.13	8.38	1.91

Although it is possible to calculate top displacement by integrating actual curvature distribution through the column height in Figure 3.19, it is observed that this process does not produce force-displacement predictions that agree well with experimental results [3]. Bilinear approximation of moment-curvature response in addition to simplified approach based on the concept of a “plastic hinge length” in Figure 3.19 is incorporated to obtain force-displacement relationship. These approximations are tend to compensate for the increase in displacement resulting from tension shift that is the influence of shear force by inclining the flexural cracks from the horizontal orientation appropriate for pure flexure [3]. Anchorage deformations (strain-penetration) can also be taken into account by defining additional length to the plastic hinge length as shown in Figure 3.19 [3]. Calculations and definitions used in Table 3.15 are explained below;

d_b : Diameter of the longitudinal reinforcement, (mm)

L_{SP} : The strain penetration length, (m) (Figure 3.19)

$$L_{SP} = 0.022 f_y d_b \tag{3.55}$$

k : Given in Eq.(3.56)

$$k = 0.2\left(\frac{f_u}{f_y} - 1\right) \leq 0.08 \tag{3.56}$$

f_y : Yield strength of longitudinal reinforcement given in Figure 3.13. (Mpa)

f_u : Ultimate strength of longitudinal reinforcement given as f_{su} in Figure 3.13, (Mpa)

L_p : Plastic hinge length, (m) (Figure 3.19)

$$L_p = kL + L_{SP} \geq 2L_{SP} \tag{3.57}$$

L : Length from the critical section to the point of contraflexure in the member, (m) (Figure 3.19)

Δ_y : Yield displacement of the member, (m)

$$\Delta_y = \phi_y \left(L + L_{SP}\right)^2 / 3 \tag{3.58}$$

Δ_u : Ultimate displacement capacity of the member, (m)

$$\Delta_u = \Delta_y + \Delta_p = \Delta_y + \phi_p L_p L = \Delta_y + \left(\phi_u - \phi_y\right) L_p L \tag{3.59}$$

μ_Δ : Displacement ductility, (Figure 2.2)

$$\mu_\Delta = \Delta_u / \Delta_y \tag{3.60}$$

R_μ : Ductility reduction factor, (Figure 2.2)

$$R_\mu = M_e / M_y \tag{3.61}$$

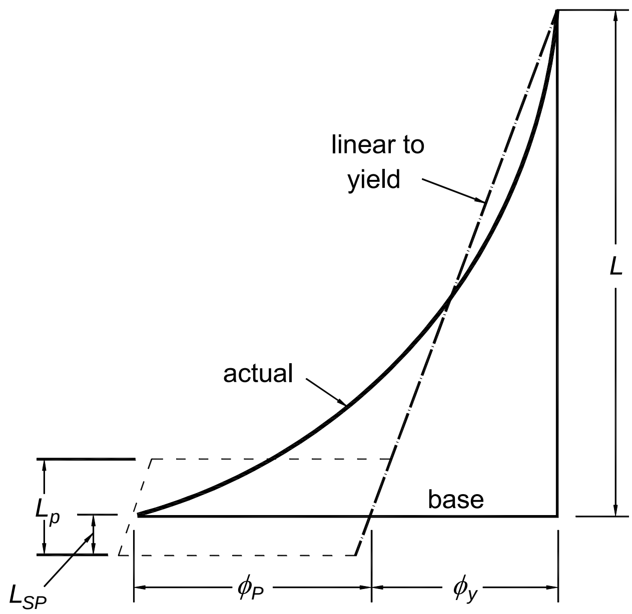

Figure 3.19 Idealization of Curvature Distribution [3]

3.9. Performance and Inelastic Demand Drifts

Performance drift calculations are given in Table 3.16. Corresponding formulations were explained in details in section 2.4.1. For the sake of completeness, they are presented once again.

- The drift limit corresponding to *Fully Functional limit state* is estimated as 1.5 times the effective yield displacement, Δ'_y, calculated according to Eq.(3.62)

$$\Delta'_y = \phi'_y L^2 / 3 \tag{3.62}$$

- The mean drift limit corresponding to *The Operational limit state* is estimated based on Eq.(3.63)

$$\frac{\Delta_{spall\_calc}}{L}(\%) = 1.6\left(1-\frac{P}{A_g f_c^{'}}\right)\left(1+\frac{L}{10D}\right) \tag{3.63}$$

- The mean drift limit corresponding to *The Delayed Operational limit state* is estimated based on Eq.(3.64) with a 20% reduction.

$$\frac{\Delta_{bb\_calc}}{L}(\%) = 0.8\left[3.25\left(1+k_e\rho_{eff}\frac{d_b}{D}\right)\left(1-\frac{P}{A_g f_c^{'}}\right)\left(1+\frac{L}{10D}\right)\right] \tag{3.64}$$

Table 3.16 Part of Excelsheet Corresponding to Calculations of Performance Drifts

PERFORMANCE DRIFTS		
(%)	(%)	(%)
FULLY FUNCTIONAL PERFORMANCE LEVEL	**OPERATIONAL PERFORMANCE LEVEL**	**DELAYED OPERATIONAL PERFORMANCE LEVEL**
-	-	-
0.57	1.80	5.89
0.55	1.80	5.07
0.53	1.80	4.29
0.52	1.80	4.07
0.52	1.80	4.07
0.52	1.80	4.07
0.52	1.80	4.07
0.52	1.80	4.07

Table 3.17 Part of Excelsheet Corresponding to Calculations of Inelastic Demand Drifts

	FIRM SITES (Soil Type I, II and III)				SOFT SITE (Soil Type IV)			
	INELASTIC DEMAND DRIFTS							
(m)			(m)	(%)		(m)	(%)	
$\Delta_{elastic}$	L_{μ}	C_{μ}	$\Delta_{inelastic}$	Demand Drift	C_{μ}	$\Delta_{inelastic}$	Demand Drift	PERFORMANCE LEVEL
-	-	-	-	-	-	-	-	-
0.011	8.45	2.18	0.024	0.94	1.84	0.020	0.80	OPERATIONAL
0.014	8.22	1.96	0.028	1.11	1.66	0.024	0.94	OPERATIONAL
0.017	7.53	1.77	0.030	1.22	1.49	0.026	1.03	OPERATIONAL
0.020	7.73	1.68	0.034	1.38	1.21	0.025	0.99	OPERATIONAL
0.020	7.73	1.68	0.034	1.38	1.21	0.025	0.99	OPERATIONAL
0.020	7.73	1.68	0.034	1.38	1.21	0.025	0.99	OPERATIONAL
0.020	7.73	1.68	0.034	1.38	1.21	0.025	0.99	OPERATIONAL
0.020	7.73	1.68	0.034	1.38	1.21	0.025	0.99	OPERATIONAL

Inelastic demand drift calculations and performance level classifications are given in Table 3.17.Corresponding inelastic displacement ratios were explained in details in section 2.5.4. Additionally;

$\Delta_{elastic}$: Elastic displacement demand of the member, (m)

$$\Delta_{elastic} = \frac{V_e}{k_{eff}} \tag{3.65}$$

C_{μ} : Inelastic displacement ratio defined separately for firm and soft sites

For Soil Type I, II and III, Eq. (3.66) proposed by Chopra and Chintanapakdee [37] is used.

$$C_{\mu} = 1 + \left[\left(L_{\mu} - 1 \right)^{-1} + \left(\frac{a}{\mu^{b}} + c \right) \left(\frac{T_n}{T_c} \right)^{d} \right]^{-1} \tag{3.66}$$

For Soil Type IV, Eq.(3.67) proposed by Garcia and Miranda [39] is used.

$$C_{\mu} = 1 + (\mu - 1)\left[\theta_1 + \theta_2\left(\frac{T}{T_g} + 1.8\right)^{-4.2}\right] + \theta_3(\mu - 1)^{0.5}\left(\frac{T_g}{T}\right)$$
$$\exp\left[\left(2.3 - \frac{32}{\mu}\right)\left(\ln\left\{\frac{T}{T_g}\right\} - 0.1\right)^2\right] - 0.08(\mu - 1) \tag{3.67}$$
$$\left(\frac{T_g}{T}\right)\exp\left[-70\left(\ln\left(\frac{T}{T_g} + 0.67\right)\right)^2\right]$$

$\Delta_{inelastic}$: Inelastic displacement demand of the member, (m)

$$\Delta_{inelastic} = \Delta_{elastic} C_{\mu} \tag{3.68}$$

If demand drift related to given soil type is less than performance drift of Fully Functional Limit State, its performance level is considered as to be *FULLY FUNCTIONAL*. If demand drift is higher than performance drift of Fully Functional Limit State and less than Operational Limit State, its performance level is considered as to be *OPERATIONAL*. Additionally, if demand drift is higher than performance drift of Operational Limit State and less than Delayed Operational Limit State, its performance level is considered as to be *DELAYED OPERATIONAL*. Lastly, if demand drift is higher than performance drift of Delayed Operational Limit State, it is entitled as *OUT OF PERFORMANCE*. In Figure 3.20, regions related to selected performance levels are hatched.

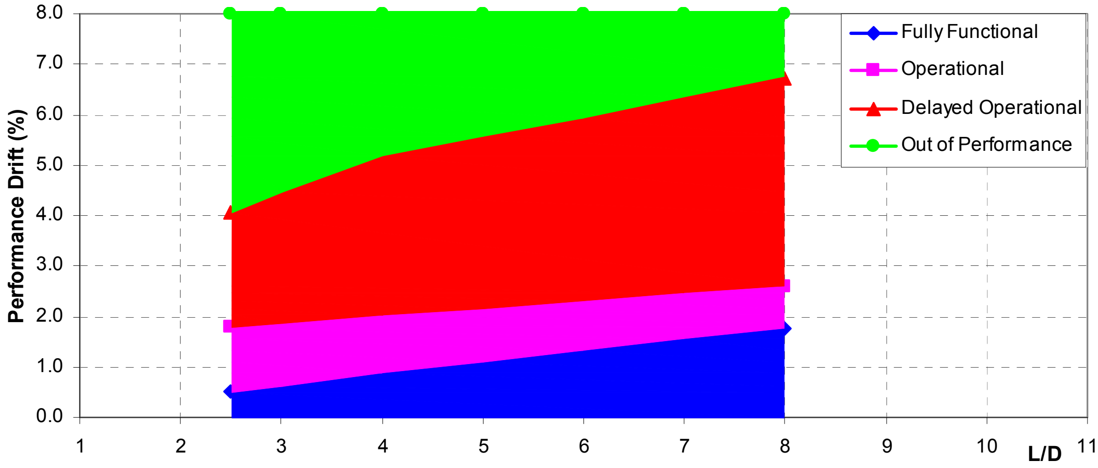

Figure 3.20 Performance Drifts of Assumed Performance Levels for D=1m, P_u/A_gf_c=0.1 and R=3.0

$\left(\frac{\Delta_c}{\Delta_d}\right)_e$: Ratio of ultimate displacement capacity, Δ_u in Eq.(3.59), to elastic displacement demand, $\Delta_{elastic}$ in Table 3.17

$\left(\frac{\Delta_c}{\Delta_d}\right)_{in}$: Ratio of ultimate displacement capacity, Δ_u in Eq.(3.59), to inelastic displacement demand, $\Delta_{inelastic}$ in Table 3.17

μ_D : Displacement ductility demand given in Eq.(3.69)

$$\mu_D = \frac{\Delta_{inelastic}}{\Delta_y} \tag{3.69}$$

$\left(\frac{\Delta_e}{L}\right)_D$: Elastic demand drift (%)

$\left(\frac{\Delta_{in}}{L}\right)_D$: Inelastic demand drift (%)

$\frac{\Delta_u}{L}$: Capacity drift (%)

$\dfrac{\Delta_u}{\Delta_{FF,O,DO}}$: Capacity over performance displacement corresponding to presumed performance levels

Ω : Overstrength factor given in Eq.(3.70)

$$\Omega = \frac{M_y}{M_d} \tag{3.70}$$

3.10. Modifications of the Analysis Tool for Finding R-Factor Corresponding to Performance Level

As stated previously, the analysis tool is modified such that inelastic demand drift is within a given margin of performance drift of Fully Functional and Operational performance levels separately. To achieve this, two boundary values of R-factor are required to be set for binary search algorithm mentioned in Section 3.5. In this part of the study, sought value of R-factor is iterated between minimum and maximum boundaries of 1 and 11, respectively. Flowchart presented in Figure 3.1 is valid with an inclusion of additional loop for searching R-factor embracing the outermost loop of stiffness modification factor, α_{gross}.

In order to minimize convergence problem during R-factor iterations, a physical reasoning behind the problem that should always hold true is necessitated. The basic criterion lying behind iterations is the relationship between R-factor and inelastic demand drift as shown in Figure 3.21. These graphs are obtained from results of first part of this study. Accordingly, as R-factor increases for a given soil type, acceleration coefficient and column aspect ratio, inelastic demand drift increases almost linearly. For an assumed R-factor ranging between 1 and 11, seismic design is conducted as the same of first part of the study.

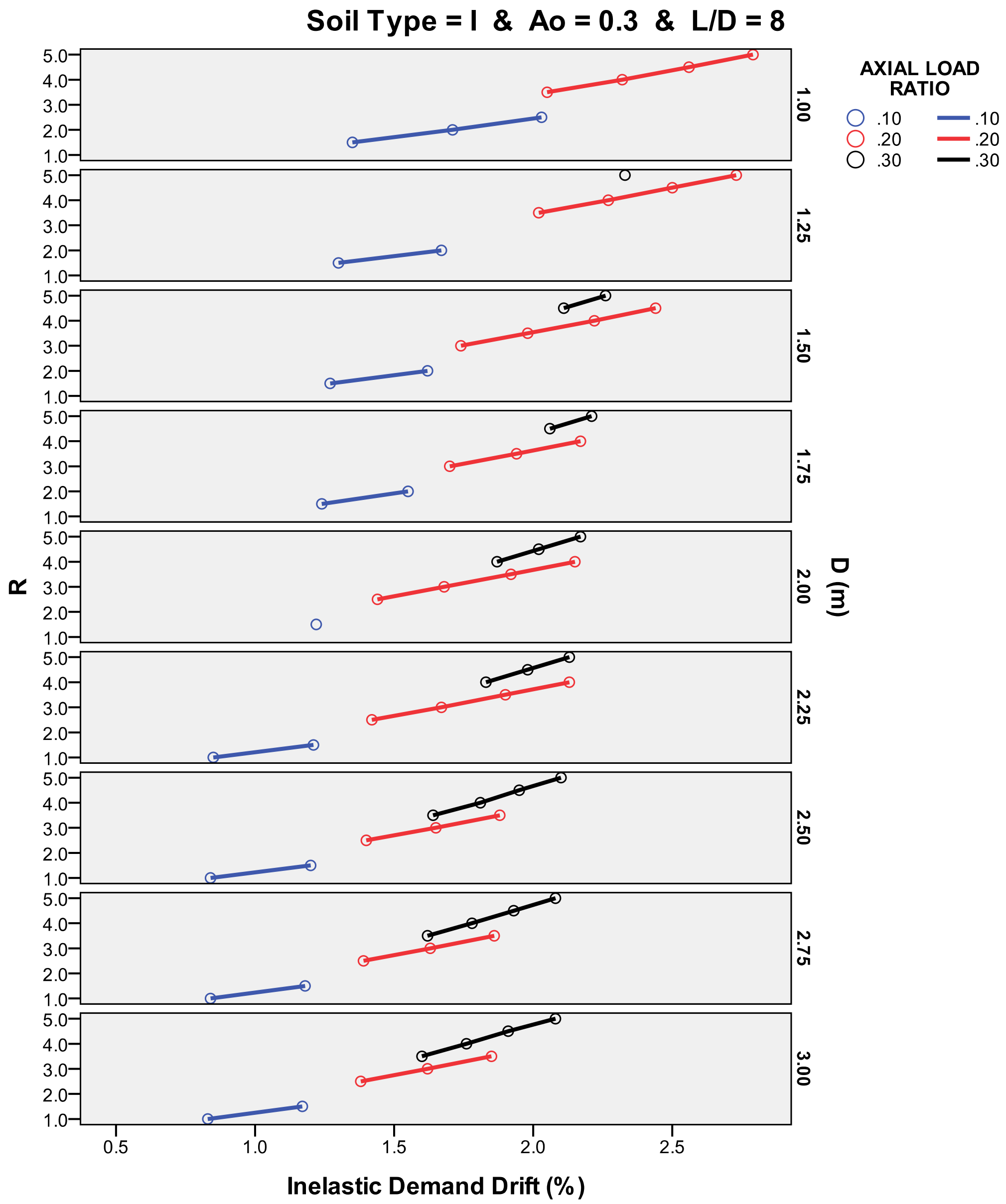

Figure 3.21 Relation Between R-Factor and Inelastic Displacement Demand Excluding Sections Requiring Minimum Longitudinal Reinforcement Ratio

Convergence criteria are given below;

$$\varepsilon \geq \left| \frac{(\Delta_{FF}/L) - (\Delta_{inelastic}/L)}{(\Delta_{inelastic}/L)} \right|$$
$$\varepsilon \geq \left| \frac{(\Delta_{O}/L) - (\Delta_{inelastic}/L)}{(\Delta_{inelastic}/L)} \right| \quad (3.71)$$

Δ_{FF}/L and Δ_O/L correspond to performance drifts of Fully Functional and Operational performance level summarized in Section 3.9. Error tolerance is chosen as 0.02 (2%). If unsatisfied relative error calculated according to Eq.(3.71) is positive, previously assumed R-factor should be increased so that inelastic demand drift increases satisfying the relative error. Similarly, if unsatisfied relative error calculated according to Eq.(3.71) is negative, previously assumed R-factor should be decreased so that inelastic demand drift decreases satisfying the relative error. At the beginning of the iteration of R-factor corresponding to performance level, boundary conditions are tried firstly so that number of iterations would be decreased. In Table 3.18, some of the errors encountered during analyses are explained in terms of occurring conditions.

ERROR 1, 2, 4 and 11 are the most common errors encountered during the analyses Undoubtedly, lower force demands caused by low acceleration coefficients (0.1 and 0.2) lead minimum reinforcement ratio even for elastic design (R=1) ending up with ERROR 1 and 2. In addition, even the lowest value of R-factor cannot be able to satisfy performance drift within a tolerable limit ending up with ERROR 4 in some cases. Finally, in cases where R-factor should be decreased, reinforcement obtained in each iteration is constrained by maximum allowable reinforcement limit. This situation causes the number of iteration to be exceeded resulting with ERROR 11. Therefore, these cases are exempted from statistical studies that will be mentioned in depth.

Table 3.18 Most Common Errors Encountered During Analyses

R-FACTOR	REINF. CONDITION	RELATIVE ERROR	CORRESPONDING ACTION	EXPLANATION
$R_1 = R = 1$	Minimum	$\lvert \varepsilon \rvert > 0.02$ & $\varepsilon > 0$	R ↑	Since R=1 is the lowest value in the boundary, any other R-factor also yields minimum reinforcement. **ERROR 1**
$R_1 = R = 1$	Minimum	$\lvert \varepsilon \rvert > 0.02$ & $\varepsilon < 0$	R ↓	There is no R-factor less than unity. **ERROR 2**
$R_1 = R = 1$	Maximum	$\lvert \varepsilon \rvert > 0.02$ & $\varepsilon < 0$	R ↓	There is no R-factor less than unity. **ERROR 3**
$R_2 = R = 11$	Minimum	$\lvert \varepsilon \rvert > 0.02$ & $\varepsilon > 0$	R ↑	There is no R-factor higher than maximum value of 11. **ERROR 4**
$R_2 = R = 11$	Maximum	$\lvert \varepsilon \rvert > 0.02$ & $\varepsilon > 0$	R ↑	There is no R-factor higher than maximum value of 11. **ERROR 5**
$R_2 = R = 11$	Maximum	$\lvert \varepsilon \rvert > 0.02$ & $\varepsilon < 0$	R ↓	Since R=11 is the highest value in the boundary, any other R-factor also yields maximum reinforcement. **ERROR 6**
$R = (R_1 + R_2) / 2$	-	$\lvert \varepsilon \rvert > 0.02$	-	Maximum number of iteration(20) is reached. **ERROR 11**

CHAPTER 4

ANALYSIS RESULTS AND FINDINGS

4.1. Introduction

As mentioned before, analytical investigations were conducted to assess performance of the single bent circular bridge columns designed according to presumed ranges of R-factor and to compute corresponding R-factor for presumed performance levels. The results of parametric studies are treated separately and presented in Section 4.2 and Section 4.3, respectively.

4.2. Performance Assessment of Bridge Columns Designed According to Presumed Ranges of R-Factor

27216 analyses are employed totally. Wide range of R-factor incorporating proposed values of AASHTO LRFD [5] for different importance categories is included in parametric study. 9622 of overall analyses yield inadequate flexural strength exceeding maximum reinforcement ratio of 4%. 11746 of overall analyses yield more than adequate flexural strength even for minimum reinforcement ratio of 1%. Remaining 5848 analyses can be designed optimally in terms of flexural strength. Number of analyses corresponding to performance state, acceleration coefficient, R-factor and soil site are summarized in Table 4.1. “ND” refers to “Not Designable” in which reinforcement ratio is constrained by maximum limit. In that case, design procedure cannot go further for performance assessment. Although cases satisfying Fully Functional performance level also satisfy Operational and Delayed Operational performance levels, data processing are not performed based on cumulative categorization.

Table 4.1 Number of Analyses Corresponding to Performance Level, Acceleration Coefficient, R-Factor and Soil Site

		SOIL SITE I				SOIL SITE II				SOIL SITE III				SOIL SITE IV			
		A_o = 0.1	A_o = 0.2	A_o = 0.3	A_o = 0.4	A_o = 0.1	A_o = 0.2	A_o = 0.3	A_o = 0.4	A_o = 0.1	A_o = 0.2	A_o = 0.3	A_o = 0.4	A_o = 0.1	A_o = 0.2	A_o = 0.3	A_o = 0.4
R = 1	FF	189	63	33	-	187	54	9	-	175	38	13	4	112	5	-	-
	O	-	-	-	-	-	-	1	-	-	3	5	3	24	20	18	7
	DO	-	-	-	-	-	-	-	-	-	-	-	-	-	-	-	-
	ND	-	126	156	189	2	135	179	189	14	148	171	182	53	164	171	182
R = 1.5	FF	189	85	55	37	189	54	40	14	186	43	26	5	159	31	9	-
	O	-	3	8	9	-	9	14	14	3	20	20	18	24	24	25	23
	DO	-	-	-	-	-	-	-	-	-	-	-	-	-	-	-	-
	ND	-	101	126	143	-	126	135	161	-	126	143	166	6	134	155	166
R = 2	FF	189	119	27	4	189	86	2	1	183	26	2	-	128	29	26	5
	O	-	3	40	59	-	19	61	53	6	54	65	46	59	48	35	28
	DO	-	-	-	-	-	-	-	-	-	-	-	-	-	-	-	-
	ND	-	67	122	126	-	84	126	135	-	109	122	143	2	112	128	156
R = 3	FF	189	160	42	8	189	103	11	-	181	30	-	-	123	29	21	20
	O	-	20	80	80	-	63	94	62	8	101	82	68	53	79	55	39
	DO	-	-	-	-	-	-	-	-	-	-	-	-	-	-	-	-
	ND	-	9	67	101	-	23	84	127	-	58	107	121	13	81	113	130
R = 4	FF	189	138	21	-	189	69	-	-	181	14	-	-	123	34	23	12
	O	-	51	149	119	-	118	145	93	8	160	120	58	53	84	60	40
	DO	-	-	1	3	-	-	2	12	-	1	9	25	13	23	26	29
	ND	-	-	18	67	-	2	42	84	-	14	60	106	-	48	80	108
R = 5	FF	189	134	21	-	189	58	-	-	181	14	-	-	123	39	23	12
	O	-	50	138	121	-	120	136	89	8	144	107	68	53	83	61	42
	DO	-	5	28	43	-	11	39	42	-	29	50	52	13	50	49	46
	ND	-	-	2	25	-	-	14	58	-	2	32	69	-	17	56	89

NOTATION : FF: Fully Functional Performance Level. O: Operational Performance Level. DO: Delayed Operational Performance Level. ND: Not Designable.
R: Response modification factor. A_o: Acceleration coefficient (g).

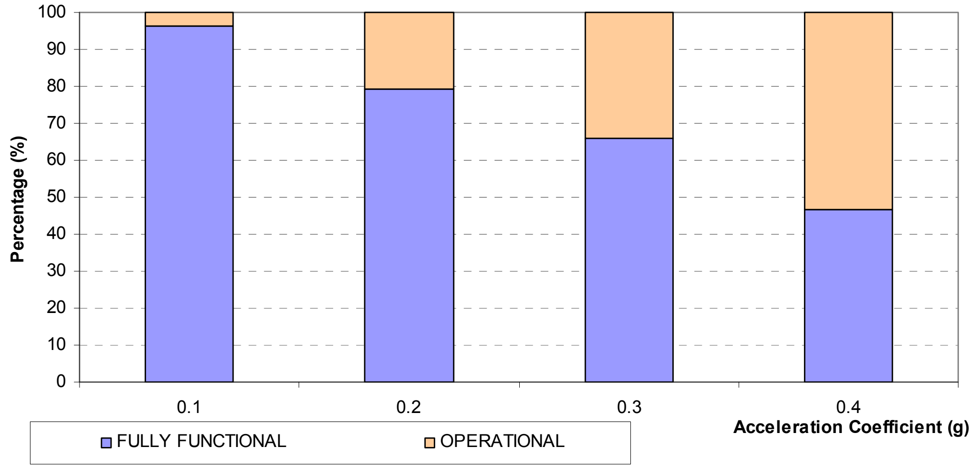

(a)

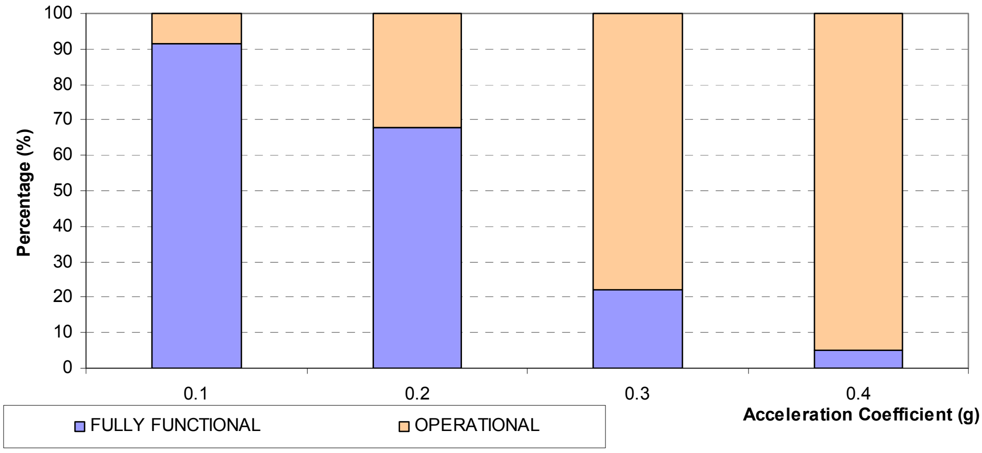

(b)

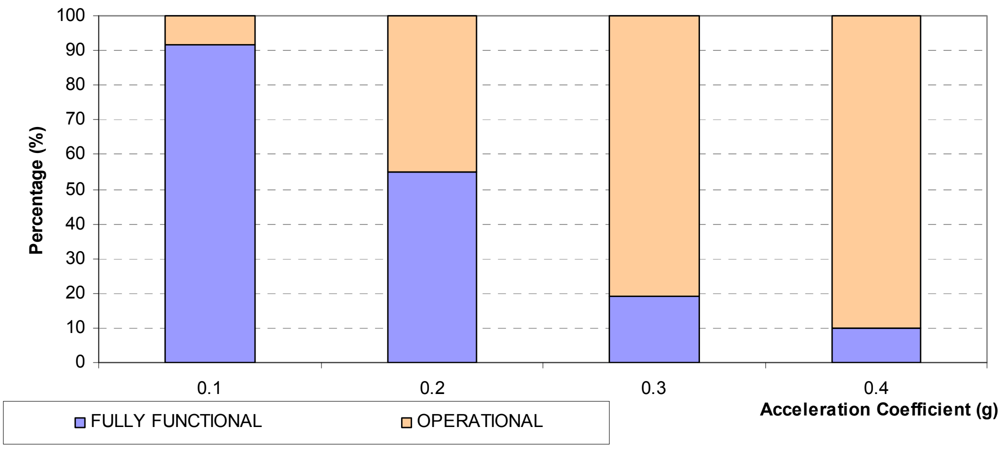

(c)

Figure 4.1 Distribution of Performance Levels for, (a) R=1.5 (# of data=1336), (b) R=2.0 (# of data=1592), (c) R=3.0 (# of data=1990)

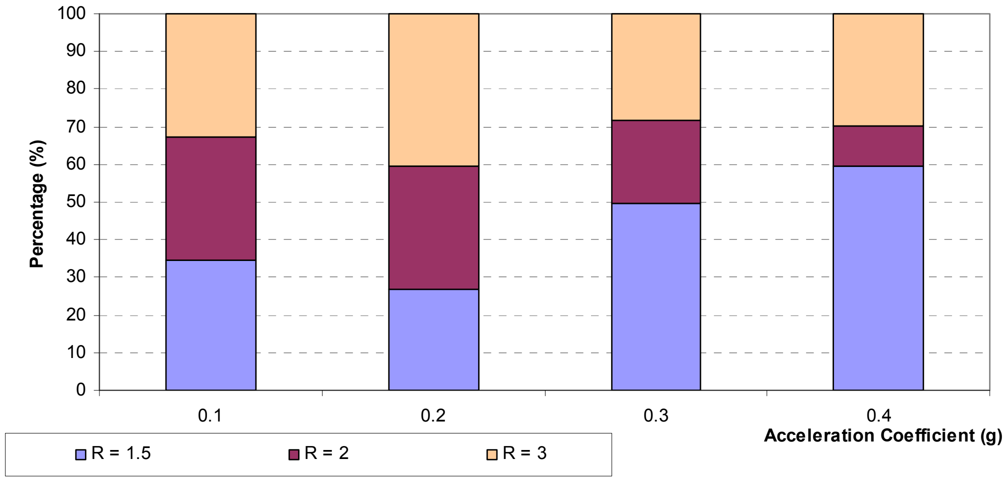

(a)

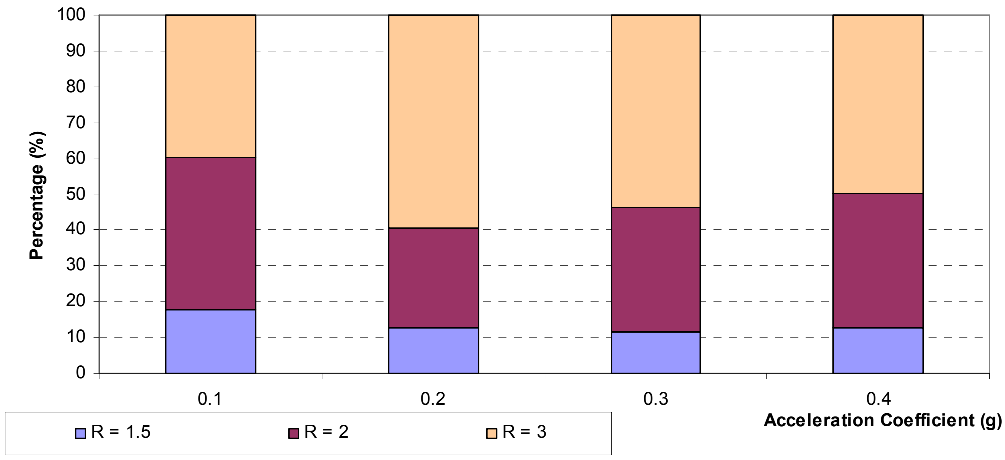

(b)

Figure 4.2 Distribution of Response Modification Factors for, (a) Fully Functional Performance Level (# of data=3244), (b) Operational Performance Level (# of data=1674)

Distribution of performance levels for given R-factors and distribution of R-factors for given performance levels are depicted in Figure 4.1 and Figure 4.2, respectively. Each performance category is investigated separately from each other. Only three R-factors of 1.5, 2.0 and 3.0 are examined that corresponds to critical, essential and other bridge importance categories. While constructing these graphs, Not Designable (ND) cases are not included since they do not have a physical meaning for the scope of this study. Nevertheless, these cases could be eliminated by increasing maximum longitudinal reinforcement ratio limit, using higher strength concrete or reinforcing steel. Cases ending up with minimum reinforcement are counted in calculation of percentages.

- None of the cases designed according to R=1.5, 2.0 and 3.0 eventuate with Delayed Operational performance level that inelastic demand drift exceeds the mean drift ratio at the onset of cover spalling. Furthermore, none of the cases designed for ranges of R-factor used in this study (from 1 to 5) eventuate with Out of Performance that inelastic demand drift exceeds the mean drift ratio at the onset of the bar buckling.
- For $R \geq 3.5$, percentage of Delayed Operational performance level begins to increase, becomes significant for R=5 and Soil Site=IV.
- For A_o=0.1 g, probability of having a column design solely satisfying Fully Functional performance level is at least 90 % for all bridge importance categories. For A_o=0.4 g, having a column solely satisfying Fully Functional performance level declines nearly to 45 % designed according to importance category of Critical bridge. This probability decreases to 10 % for Essential and Other bridge importance categories.
- As the acceleration coefficient increases, probability of having a column solely satisfying Fully Functional performance level decreases since demand drift has a tendency to increase. On the contrary, number of cases solely satisfying Operational performance level increases.
- As R-factor used in seismic design increases, number of cases solely satisfying Operational performance limit state increases for given sectional properties. This is mainly due to having a section with less effective flexural stiffness.

4.2.1. Stiffness Modification Factor

One of the most important advancements superimposed in the analysis tool was iteration for stiffness modification factor, α_{gross} defined in Eq.(3.1), to be utilized in elastic dynamic analysis, slenderness effect in P-Δ analysis and determination of elastic displacement demand. The significance of stiffness modification factor stems from the necessity of moment-curvature analysis in each successive iteration until relative error is satisfied. Instead of proceeding with taskwork routine to use in elastic dynamic analysis that is mostly employed in current seismic design practice, simpler tools as relation or chart for stiffness modification factor are proposed by Caltrans-SDC [18] and Priestley et al. [3]. In Eq. (4.1), a linear correlation obtained using results of 17594 analyses are given;

$$\alpha_{gross} = 0.167 + 0.562\left(P_u / A_g f_c\right) + 0.147\rho_l \tag{4.1}$$

The R^2, coefficient of determination, is calculated as 0.971. It is a statistical measure of how well the regression line shown in Figure 4.3 colored in yellow approximates the real data points. As R^2 becomes closer to unity, regression line perfectly fits the data. Applicability range of Eq.(4.1) is limited with the range of analysis dataset. In addition to yellow colored regression line, lower and upper trendlines of stiffness modification factor for a given axial load ratio are shown in Figure 4.3. Black and red colored lines correspond to upper and lower boundaries, respectively. Stiffness modification factor can be linearly interpolated between axial load ratios.

For $P_u/A_g f_c=0.1$;

$$\begin{aligned} \alpha_{gross\_upper} &= 0.228 + 0.165\rho_l \\ \alpha_{gross\_lower} &= 0.205 + 0.130\rho_l \end{aligned} \tag{4.2}$$

For $P_u/A_g f_c=0.2$;

$$\begin{aligned} \alpha_{gross\_upper} &= 0.299 + 0.157\rho_l \\ \alpha_{gross\_lower} &= 0.261 + 0.124\rho_l \end{aligned} \tag{4.3}$$

For $P_u/A_g f_c=0.3$;

$$\alpha_{gross\_upper} = 0.344 + 0.159\rho_l$$
$$\alpha_{gross\_lower} = 0.335 + 0.133\rho_l \quad (4.4)$$

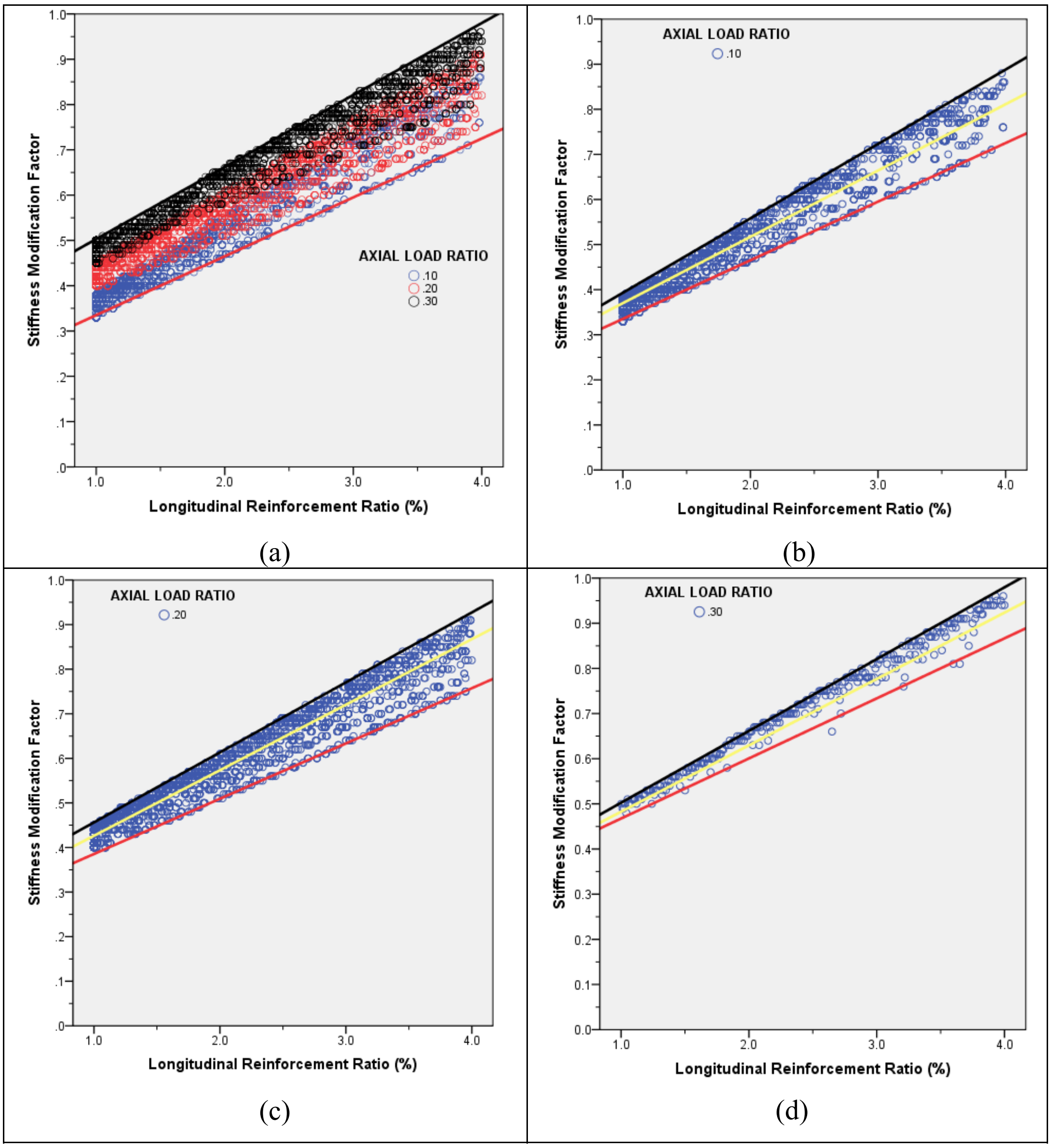

Figure 4.3 Trendline Boundaries of Stiffness Modification Factor for Axial Load Ratio of, (a) P_u/A_gf_c= All, (b) P_u/A_gf_c=0.1, (c) P_u/A_gf_c=0.2, (d) P_u/A_gf_c=0.3

For the sake of completeness, Eq.(4.1) is compared with Caltrans-SDC [18] and Priestley et al. [3] for presumed longitudinal reinforcement ratio in Figure 4.4. Caltrans-SDC [18] can be thought as lower bound estimate of stiffness modification factor regardless of reinforcement and axial load ratio. Eq.(4.1) can be thought as upper bound estimate of stiffness modification factor except for 1% reinforcement ratio and axial load ratio greater than 0.25. Difference between the estimates of stiffness modification factor originates mainly from assumed bilinearization rule of moment curvature curve.

Graphs point out the fact that there is a strong dependence of effective flexural stiffness on axial load ratio and reinforcement ratio. Therefore, the use of constant member stiffness independent of flexural strength that is generally assumed in force based design approach is improper [3].

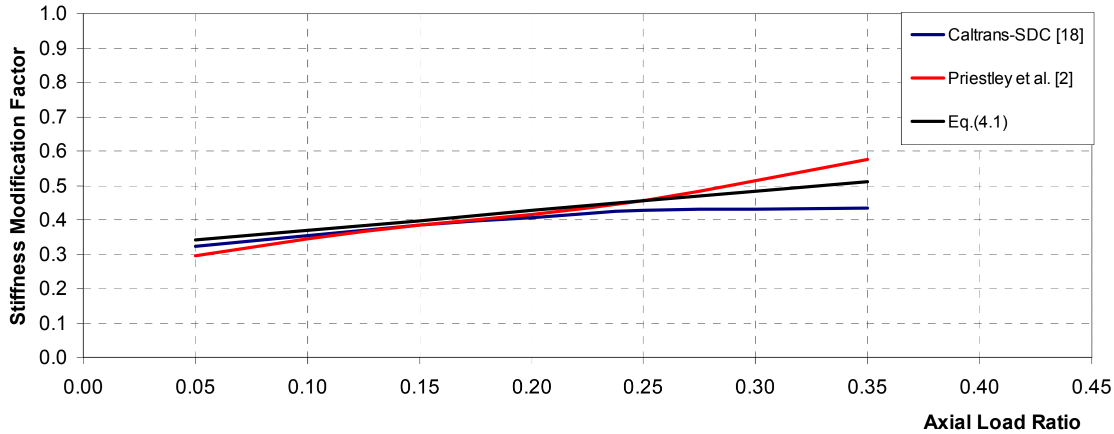

(a)

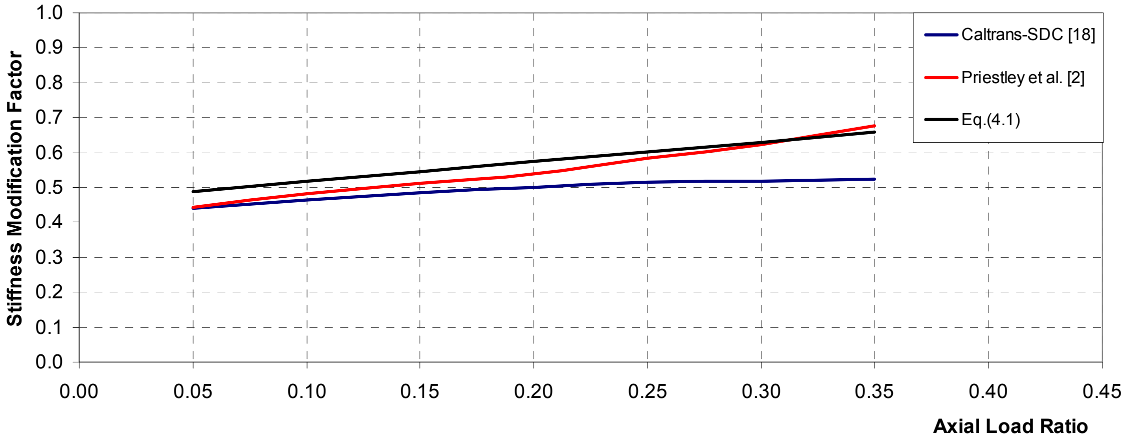

(b)

Figure 4.4 Comparison of Stiffness Modification Factors for Longitudinal Reinforcement Ratio of, (a) ρ_l=1 %, (b) ρ_l=2 %, (c) ρ_l=3 %, (d) ρ_l=4 %

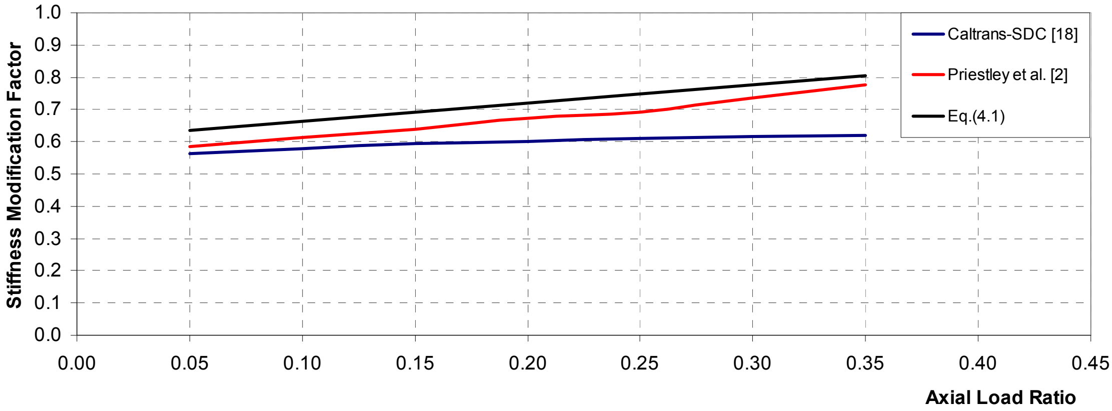

(c)

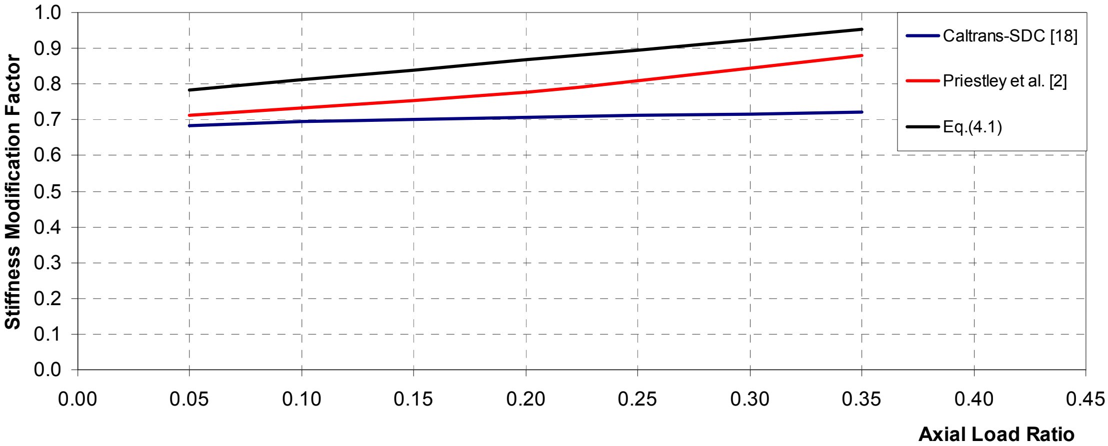

(d)

Figure 4.4 Comparison of Stiffness Modification Factors for Longitudinal Reinforcement Ratio of, (a) ρ_l=1 %, (b) ρ_l=2 %, (c) ρ_l=3 %, (d) ρ_l=4 % (Continued)

4.2.2. Yield Curvature

Estimation of yield curvature is necessitated for two purposes. First, it is required for calculation of limit displacement given in Eq.(3.58) and Eq.(3.59). Second, it is required for calculation of inelastic displacement coefficient by means of the displacement ductility. Therefore, a linear regression analysis for yield curvature of circular concrete column is conducted using the results of 17594 cases. Although the data were generated from specific material strengths, dimensionless results to be used for other material strengths could be obtained by normalizing constant multiplier by expected yield strain of reinforcing steel. Best fit curve of the yield curvature is given in Eq.(4.5);

$$\phi_y = 2.27\frac{\varepsilon_y}{D} \tag{4.5}$$

Coefficient of determination (R^2) is estimated as 0.975. Lower and upper bound trendline of yield curvature are shown in Figure 4.5. Black and red colored lines constitute upper and lower boundaries, respectively. Yellow colored line represents Eq.(4.5). Correlations for boundary trendlines are given in Eq.(4.6);

$$\begin{aligned} \phi_{y\_lower} &= 2.12\frac{\varepsilon_y}{D} \\ \phi_{y\_upper} &= 2.57\frac{\varepsilon_y}{D} \end{aligned} \tag{4.6}$$

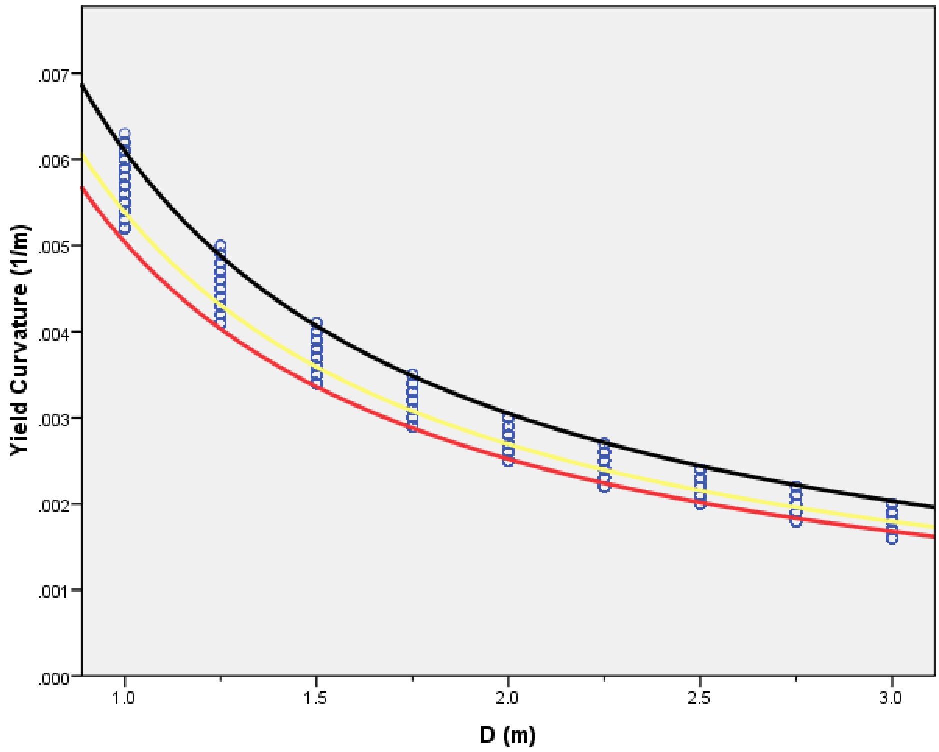

Figure 4.5 Trendline Boundaries of Yield Curvature

Although Priestley et al. [3] has used different bilinear representation of moment curvature graph, constant multiplier in Eq.(4.5) is proposed as 2.25 within a ± 10% margin from the average. It should be noted that yield curvature is independent of reinforcement content and axial load ratio. For a given diameter of circular column and yield strain of reinforcing steel, yield curvature does not change according to flexural strength provided to the column. This is the reason why effective flexural stiffness increases when flexural strength increases.

4.2.3. Moment Magnification Factor

Accompanied with stiffness modification factor, second advancement in the analysis tool is the inclusion of more refined approach for slenderness effect in P-Δ analysis. In AASHTO LRFD [5], moment magnification factor based on constant effective flexural stiffness of 0.3 with the use of stiffness reduction factor is assumed in second order analysis. In Figure 4.6 (a), percent frequency distribution of stiffness modification factor is shown. Minimum of the dataset is 0.33 with a mean value of 0.48. Effective flexural stiffness embedded in Eq.(3.10) and Eq.(3.11) is less than even the minimum of the dataset. Therefore, it is highly probable to conclude higher moment magnification factor that increases moment demand. To compare results of moment magnification factor computed from AASHTO LRFD [5] approximate procedure and solution procedure discussed in Section 3.4, histogram of ratio of $\delta_{LRFD}/\delta_{THEORY}$ is drawn in Figure 4.6 (b). AASHTO LRFD [5] may produce up to 50 % higher moment demand for high axial load ratios and column aspect ratios. Mean value of $\delta_{LRFD}/\delta_{THEORY}$ is estimated as 1.07 with a standard deviation of 0.08.

In Figure 4.7, variation of one standard deviation above/below mean of $\delta_{LRFD}/\delta_{THEORY}$ with respect to axial load ratio and column aspect ratio is illustrated. With reference to Figure 4.7, AASHTO LRFD [5] approximate procedure could be used for axial load ratios equal or less than 0.1. As the slenderness of the column for constant axial load ratio increases, ratio of $\delta_{LRFD}/\delta_{THEORY}$ grows exponentially. In addition, dispersion of $\delta_{LRFD}/\delta_{THEORY}$ increases significantly at high axial load ratios.

In Figure 4.6 (c), frequency distribution of $\delta_{LRFD\_mod}/\delta_{THEORY}$ is plotted. δ_{LRFD_mod} corresponds to moment magnification factor calculated according to AASHTO LRFD [5] approximate procedure that utilizes the same stiffness modification factor as in the calculation of δ_{THEORY}. Apparently, $\delta_{LRFD\_mod}/\delta_{THEORY}$ approaches to unity. AASHTO LRFD [5] approximate procedure results using an appropriate stiffness modification factor are consistent with the more refined solutions as the one proposed for this thesis. Author of this thesis recommends to use AASHTO LRFD [5] procedure with stiffness modification factor estimated from Eq.(4.1) to Eq.(4.4) excluding stiffness reduction factor, ϕ_K.

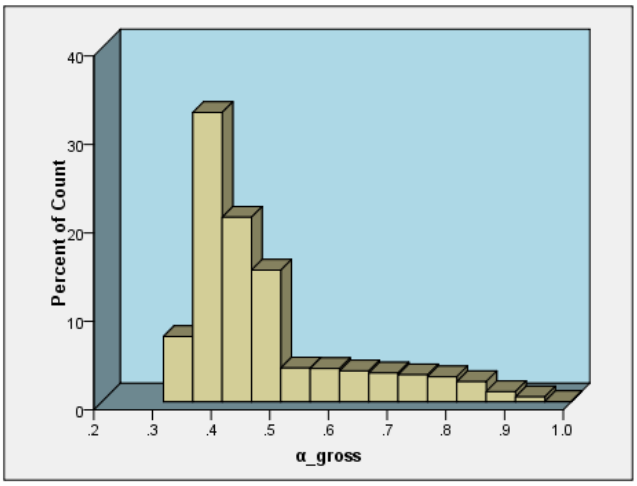

(a)

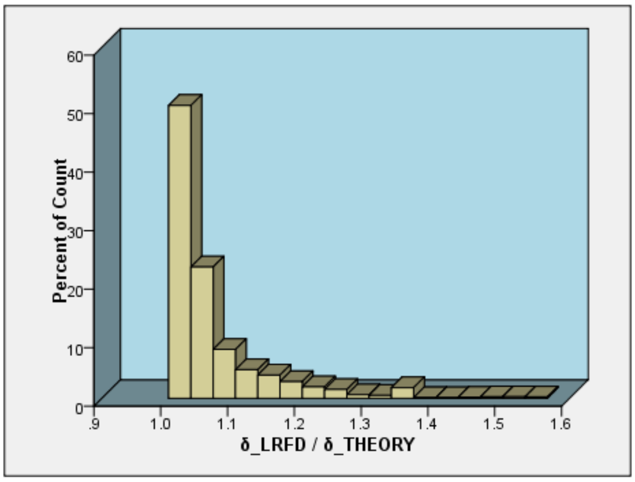

(b)

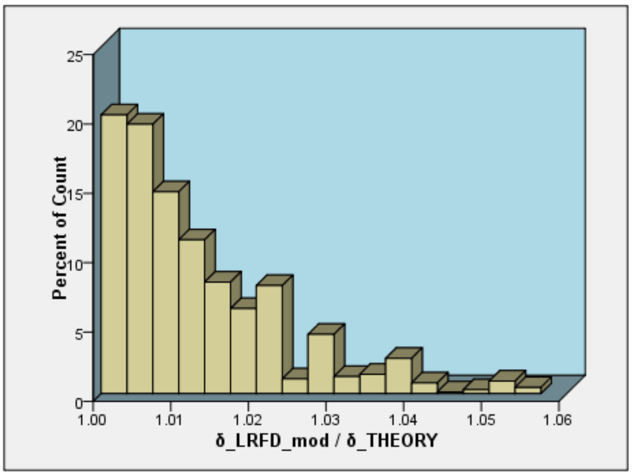

(c)

Figure 4.6 Percentage Histograms of, (a) α_{gross}, (b) $\delta_{LRFD}/\delta_{THEORY}$, (c) $\delta_{LRFD\ mod}/\delta_{THEORY}$

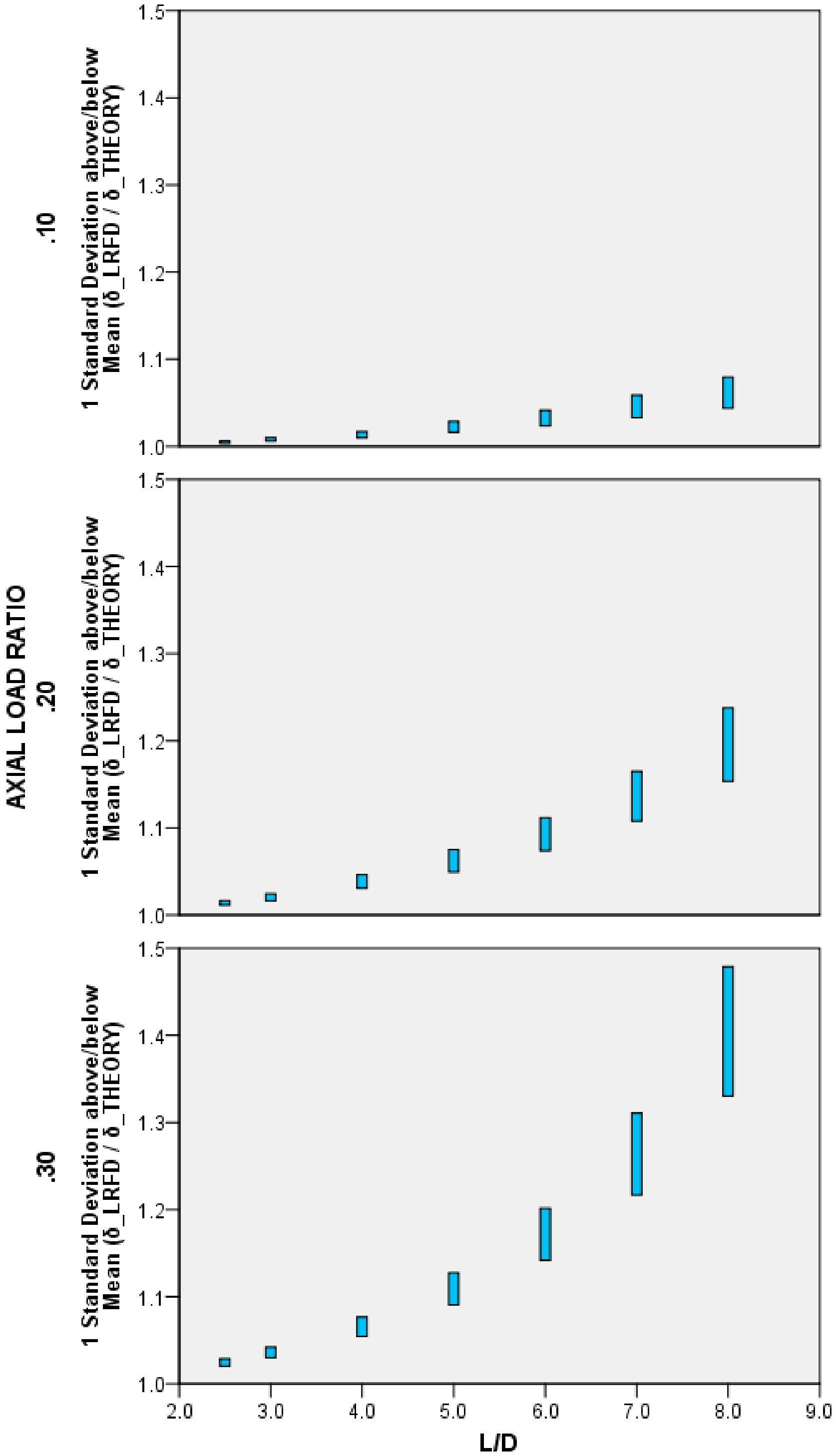

Figure 4.7 Plots of One Standard Deviation Above/Below Mean of $\delta_{LRFD}/\delta_{THEORY}$

4.2.4. Histograms and Statistical Results of Response Measures

Although cases ending up with minimum reinforcement ratio are acceptable for design routine, they have a potential to insert bias into the statistical results. Therefore, statistical studies presented in this section are performed based on analysis results excluding cases ending up with minimum reinforcement ratio. In Table 4.2, mean and standard deviation of response measures categorized solely for performance levels are given. Histograms categorized solely for performance levels are plotted in Figure 4.8. In Table 4.3, mean and standard deviation of response measures categorized solely for acceleration coefficients and performance levels are given. Additionally, statistical results of response measures categorized solely for soil site and performance levels are given in Table 4.4.

Table 4.2 Statistical Results of Response Measures Categorized Solely for Performance Levels

		A_o= 0.1, 0.2, 0.3 & 0.4								
		FULLY FUNCTIONAL PERFORMANCE LEVEL								
		R	μ_ϕ	μ_Δ	μ_D	$(\Delta_c/\Delta_d)_e$	$(\Delta_c/\Delta_d)_{in}$	$(\Delta_e/L)_D$	$(\Delta_{in}/L)_D$	Δ_u/Δ_{FF}
SOIL SITE I, II, III & IV	Mean	2.06	9.94	4.20	0.95	5.52	4.97	0.98	0.87	3.60
	Std. Dev.	1.02	1.84	0.83	0.40	2.42	1.80	0.47	0.36	1.31
	# of Case	1879								
		OPERATIONAL PERFORMANCE LEVEL								
		R	μ_ϕ	μ_Δ	μ_D	$(\Delta_c/\Delta_d)_e$	$(\Delta_c/\Delta_d)_{in}$	$(\Delta_e/L)_D$	$(\Delta_{in}/L)_D$	Δ_u / Δ_O
	Mean	3.36	10.71	4.99	1.48	4.54	3.52	1.15	1.30	2.31
	Std. Dev.	1.08	1.98	1.38	0.36	2.45	1.16	0.55	0.43	0.55
	# of Case	3267								
		DELAYED OPERATIONAL PERFORMANCE LEVEL								
		R	μ_ϕ	μ_Δ	μ_D	$(\Delta_c/\Delta_d)_e$	$(\Delta_c/\Delta_d)_{in}$	$(\Delta_e/L)_D$	$(\Delta_{in}/L)_D$	Δ_u / Δ_{DO}
	Mean	4.50	10.19	4.33	1.87	2.79	2.33	2.13	2.40	1.12
	Std. Dev.	0.61	2.09	1.23	0.46	1.22	0.39	0.70	0.53	0.11
	# of Case	702								

NOTATION : A_o: Acceleration coefficient (g). R: Response modification factor. μ_ϕ: Curvature ductility. μ_Δ: Displacement ductility. μ_D: Displacement ductility demand. $(\Delta_c/\Delta_d)_e$: Capacity over elastic demand displacement. $(\Delta_c/\Delta_d)_{in}$: Capacity over inelastic demand displacement. $(\Delta_e/L)_D$: Elastic demand drift (%). $(\Delta_{in}/L)_D$: Inelastic demand drift (%). Δ_u/Δ_{FF}: Capacity over performance displacement corresponding to *Fully Functional* performance level. Δ_u/Δ_O: Capacity over performance displacement corresponding to *Operational* performance level. Δ_u/Δ_{DO}: Capacity over performance displacement corresponding to *Delayed Operational* performance level.

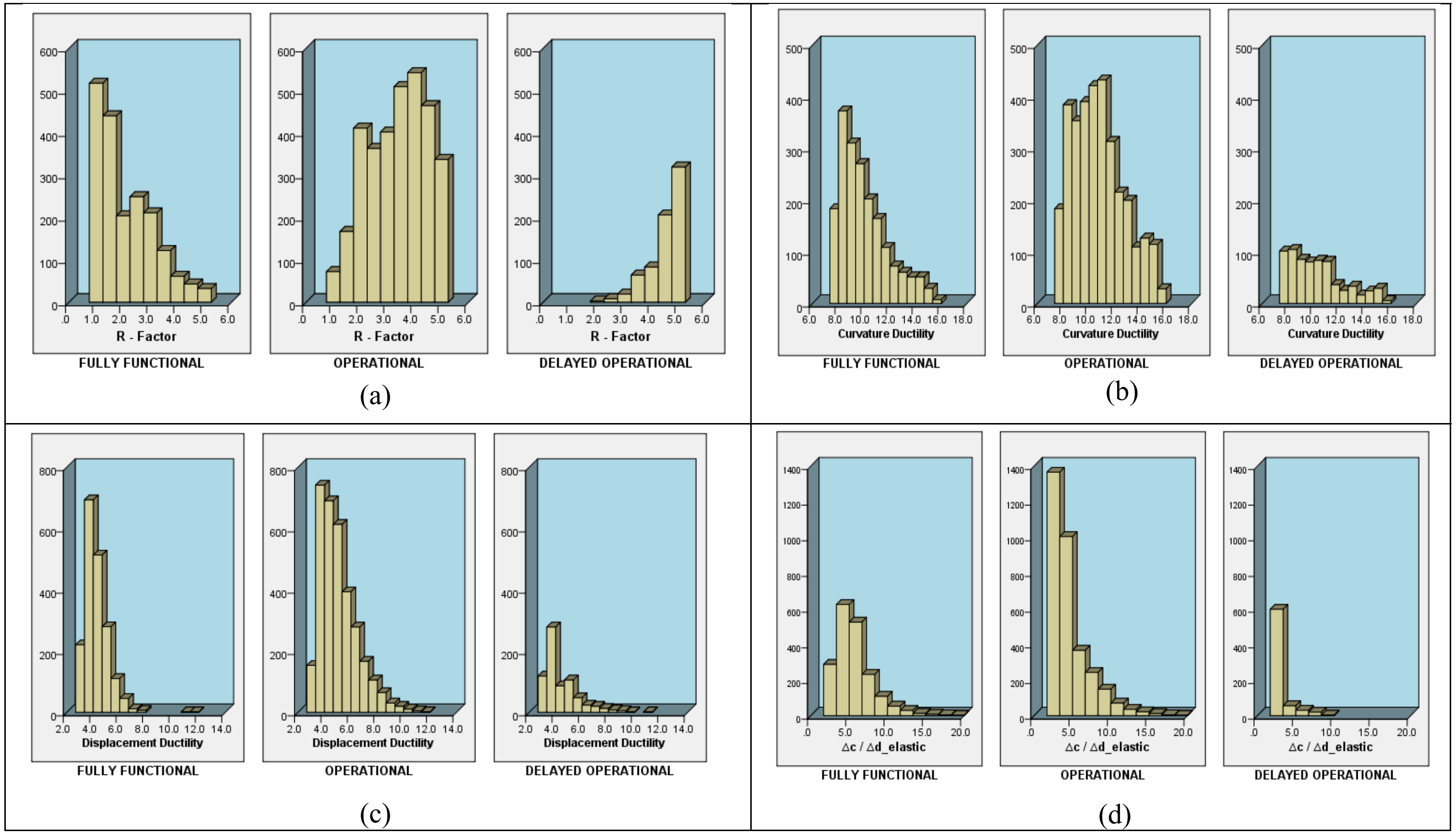

Figure 4.8 Histograms of Response Measures, (a) R-factor, (b) μ_ϕ, (c) μ_Δ, (d) $(\Delta_c/\Delta_d)_e$, (e) $(\Delta_c/\Delta_d)_{in}$, (f) A_o, (g) Soil site, (h) $(\Delta_e/L)_D$, (i) $(\Delta_{in}/L)_D$, (j) ϕ_u, (k) α_{gross}, (l) ρ_l, (m) R_μ, (n) Ώ, (p) μ_D, (r) T, (s) Δ_u/L, (t) Δ_u/Δ_{FF}, Δ_u/Δ_O, Δ_u/Δ_{DO}

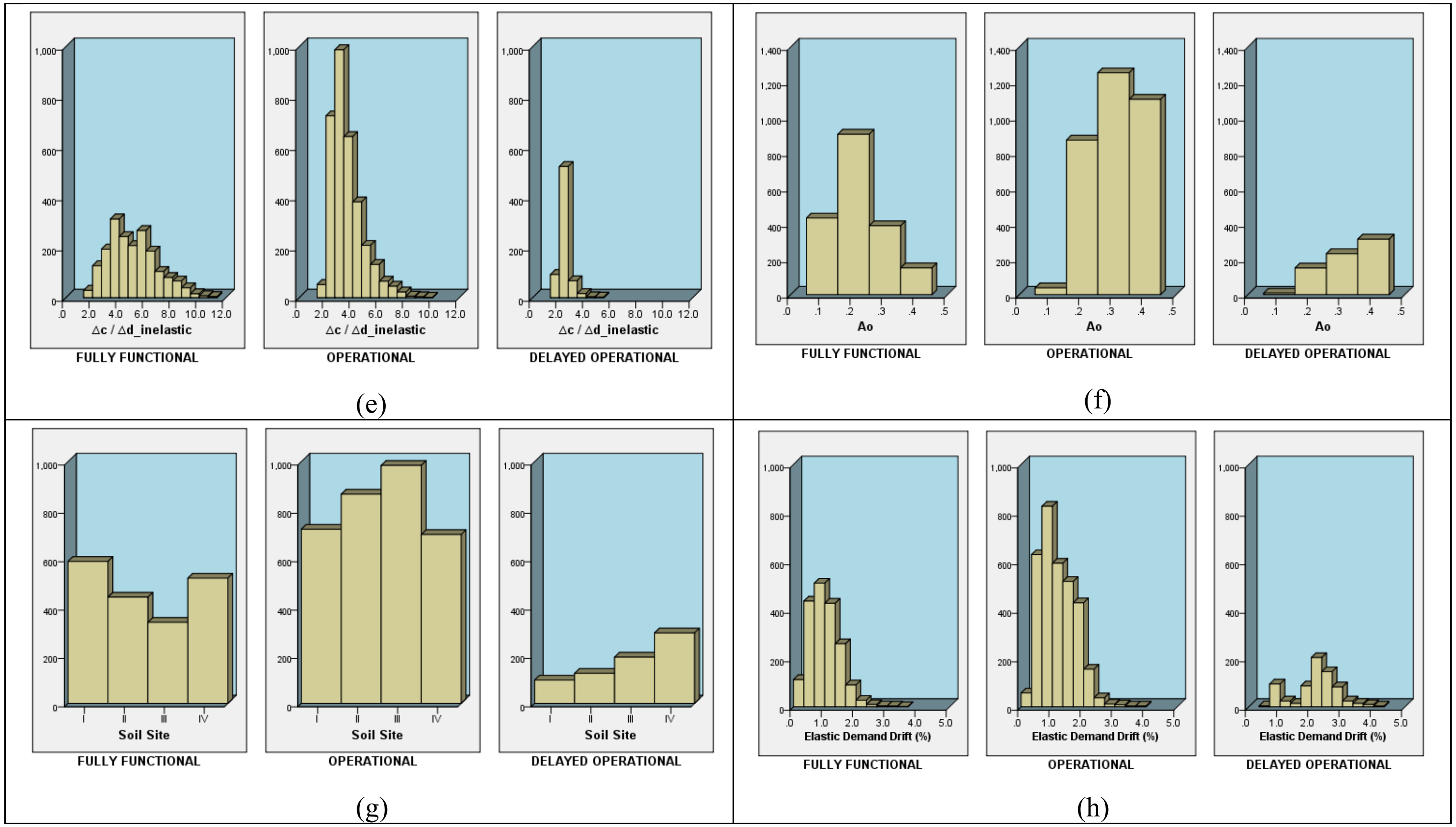

Figure 4.8 Histograms of Response Measures, (a) R-factor, (b) μ_ϕ, (c) μ_Δ, (d) $(\Delta_c/\Delta_d)_e$, (e) $(\Delta_c/\Delta_d)_{in}$, (f) A_o, (g) Soil site, (h) $(\Delta_e/L)_D$, (i) $(\Delta_{in}/L)_D$, (j) ϕ_u, (k) α_{gross}, (l) ρ_l, (m) R_μ, (n) Ω, (p) μ_D, (r) T, (s) Δ_u/L, (t) Δ_u/Δ_{FF}, Δ_u/Δ_O, Δ_u/Δ_{DO} (Continued)

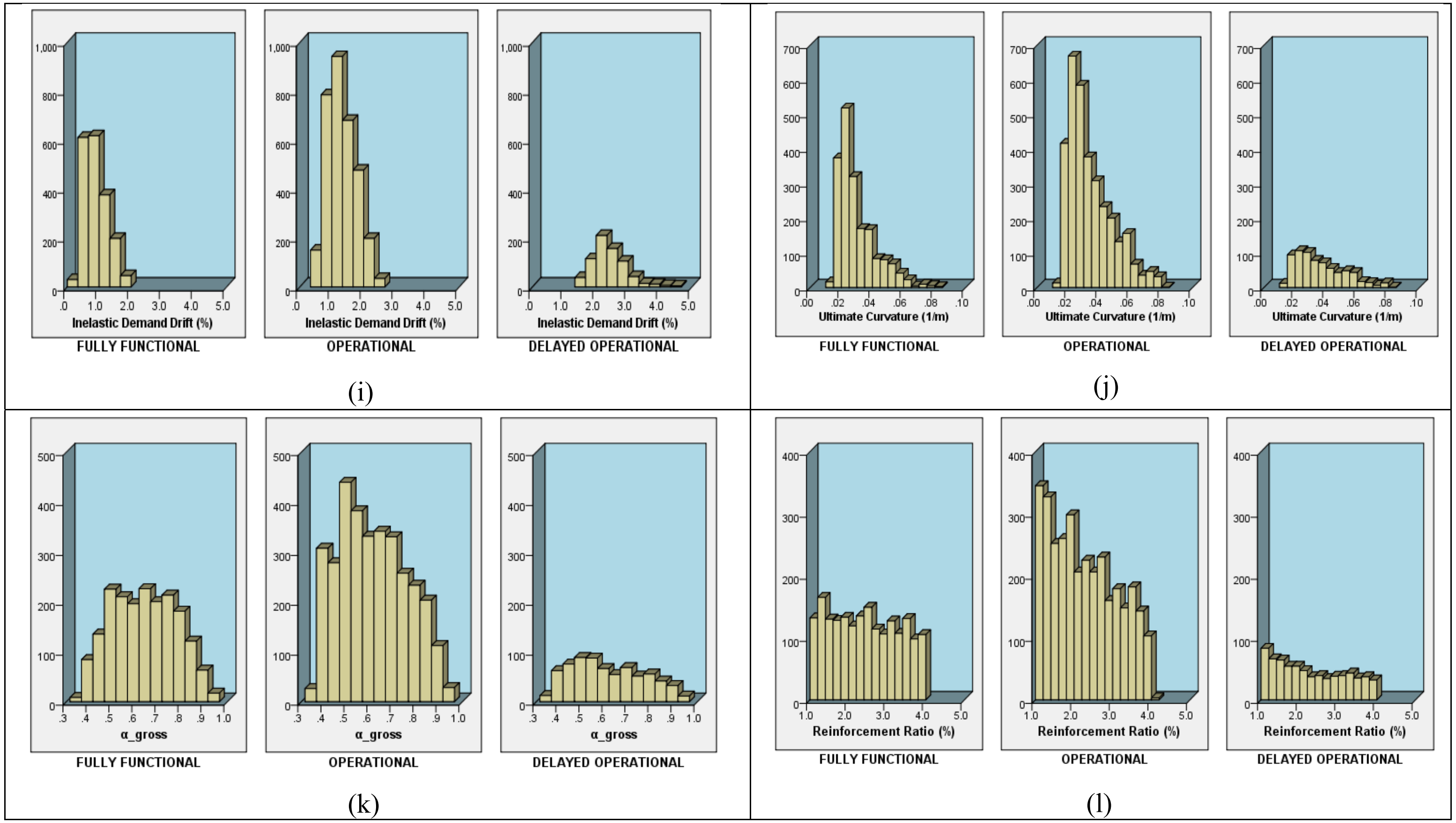

Figure 4.8 Histograms of Response Measures, (a) R-factor, (b) μ_ϕ, (c) μ_Δ, (d) $(\Delta_c/\Delta_d)_e$, (e) $(\Delta_c/\Delta_d)_{in}$, (f) A_o, (g) Soil site, (h) $(\Delta_e/L)_D$, (i) $(\Delta_{in}/L)_D$, (j) ϕ_u, (k) α_{gross}, (l) ρ_l, (m) R_μ, (n) Ω, (p) μ_D, (r) T, (s) Δ_u/L, (t) Δ_u/Δ_{FF}, Δ_u/Δ_O, Δ_u/Δ_{DO} (Continued)

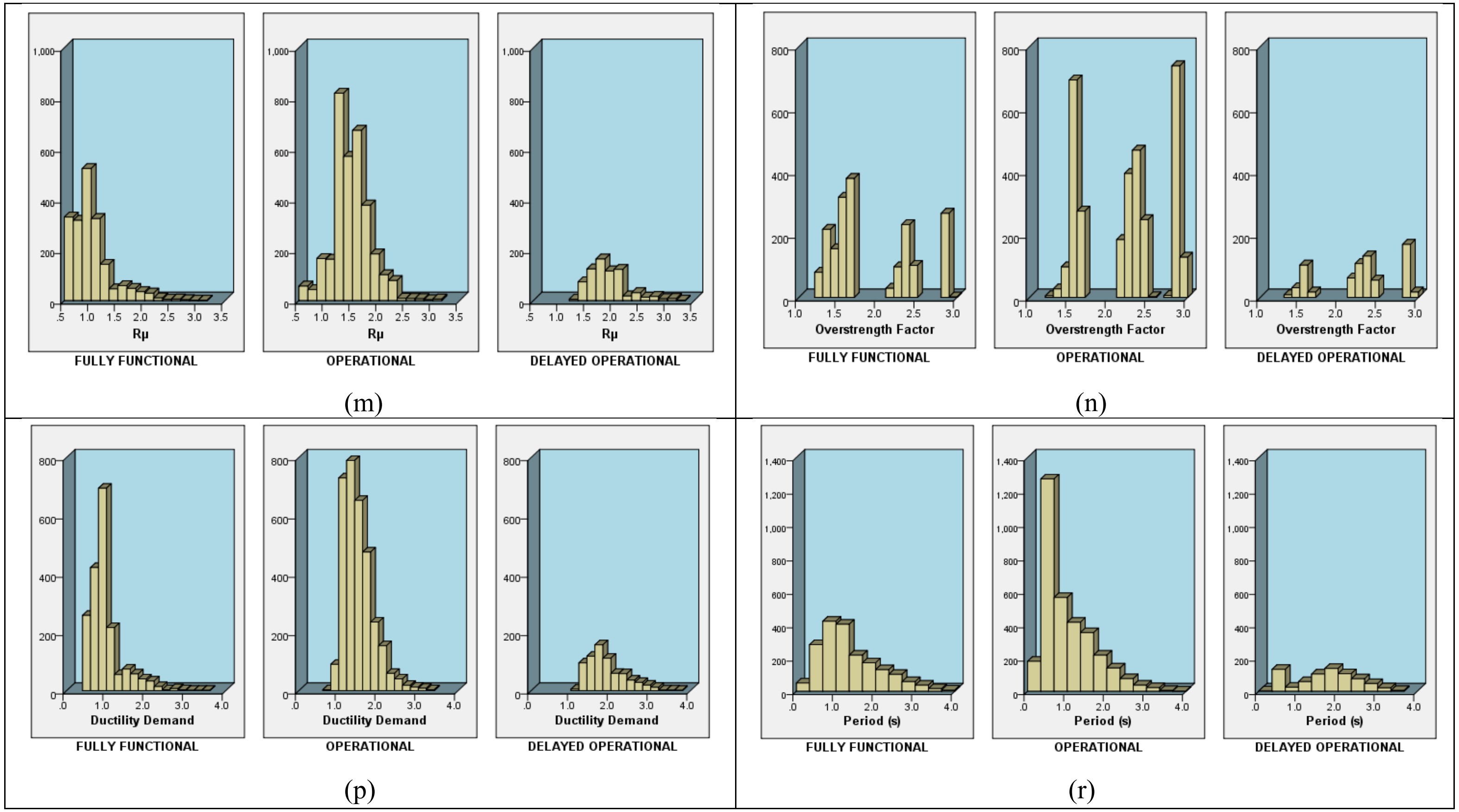

Figure 4.8 Histograms of Response Measures, (a) R-factor, (b) μ_ϕ, (c) μ_Δ, (d) $(\Delta_c/\Delta_d)_e$, (e) $(\Delta_c/\Delta_d)_{in}$, (f) A_o, (g) Soil site, (h) $(\Delta_e/L)_D$, (i) $(\Delta_{in}/L)_D$, (j) ϕ_u, (k) α_{gross}, (l) ρ_l, (m) R_μ, (n) Ω, (p) μ_D, (r) T, (s) Δ_u/L, (t) Δ_u/Δ_{FF}, Δ_u/Δ_O, Δ_u/Δ_{DO} (Continued)

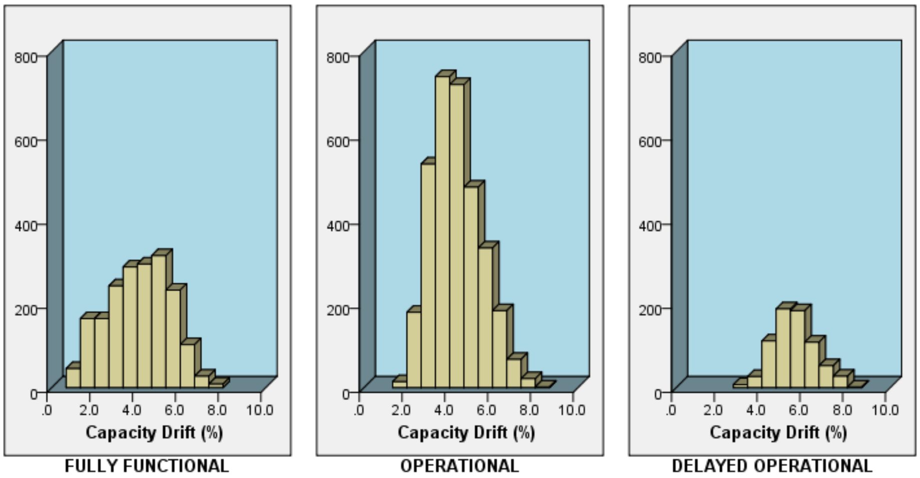

(s)

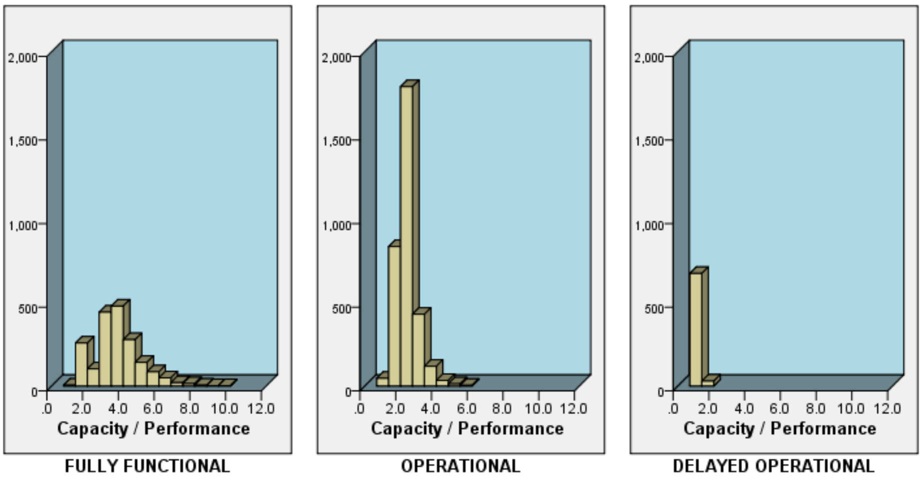

(t)

Figure 4.8 Histograms of Response Measures, (a) R-factor, (b) μ_ϕ, (c) μ_Δ, (d) $(\Delta_c/\Delta_d)_e$, (e) $(\Delta_c/\Delta_d)_{in}$, (f) A_o, (g) Soil site, (h) $(\Delta_e/L)_D$, (i) $(\Delta_{in}/L)_D$, (j) ϕ_u, (k) α_{gross}, (l) ρ_l, (m) R_μ, (n) Ω, (p) μ_D, (r) T, (s) Δ_u/L, (t) Δ_u/Δ_{FF}, Δ_u/Δ_O, Δ_u/Δ_{DO} (Continued)

Table 4.3 Statistical Results of Response Measures Categorized Solely for Acceleration Coefficients and Performance Levels

		SOIL SITE I, II, III & IV																										
		FULLY FUNCTIONAL PERFORMANCE LEVEL									OPERATIONAL PERFORMANCE LEVEL									DELAYED OPERATIONAL PERFORMANCE LEVEL								
	A_o	R	μ_ϕ	μ_Δ	μ_D	$(\Delta_c/\Delta_d)_e$	$(\Delta_c/\Delta_d)_{in}$	$(\Delta_e/L)_D$	$(\Delta_{in}/L)_D$	Δ_u/Δ_{FF}	R	μ_ϕ	μ_Δ	μ_D	$(\Delta_c/\Delta_d)_e$	$(\Delta_c/\Delta_d)_{in}$	$(\Delta_e/L)_D$	$(\Delta_{in}/L)_D$	Δ_u / Δ_O	R	μ_ϕ	μ_Δ	μ_D	$(\Delta_c/\Delta_d)_e$	$(\Delta_c/\Delta_d)_{in}$	$(\Delta_e/L)_D$	$(\Delta_{in}/L)_D$	Δ_u / Δ_{DO}
Mean	0.1g	1.18	9.30	3.93	0.74	5.99	5.50	0.80	0.78	3.43	1.55	8.89	4.38	1.08	5.97	4.21	0.95	1.22	2.70	2.44	8.61	3.45	1.30	2.77	2.69	2.00	2.29	1.29
Std. Dev.		0.28	1.60	0.66	0.18	1.65	1.27	0.31	0.34	1.03	0.49	0.94	0.93	0.16	3.11	1.27	0.59	0.52	0.39	0.32	0.45	0.12	0.16	0.33	0.31	0.19	0.22	0.05
# of Case		433									38									8								
Mean	0.2g	2.34	9.92	4.19	0.91	5.58	5.06	0.95	0.89	3.74	3.52	9.93	4.72	1.33	4.70	3.65	1.07	1.22	2.38	4.64	9.21	3.95	1.61	2.86	2.44	1.95	2.24	1.16
Std. Dev.		1.00	1.92	0.85	0.30	2.51	1.90	0.41	0.36	1.26	1.00	1.73	1.34	0.25	2.58	1.21	0.50	0.42	0.56	0.43	1.35	1.05	0.31	1.15	0.33	0.56	0.41	0.09
# of Case		906									873									150								
Mean	0.3g	2.19	10.45	4.42	1.08	5.36	4.67	1.08	0.90	3.67	3.40	10.72	5.01	1.45	4.58	3.57	1.14	1.28	2.33	4.61	9.86	4.20	1.78	2.77	2.36	2.12	2.33	1.11
Std. Dev.		1.01	1.78	0.79	0.43	2.79	1.88	0.50	0.35	1.53	1.07	1.98	1.39	0.32	2.49	1.17	0.53	0.43	0.55	0.52	1.96	1.19	0.36	1.20	0.39	0.63	0.45	0.11
# of Case		389									1253									231								
Mean	0.4g	2.53	10.59	4.46	1.45	4.26	3.65	1.42	0.95	3.02	3.25	11.37	5.21	1.63	4.30	3.34	1.24	1.38	2.23	4.41	10.94	4.63	2.08	2.77	2.24	2.22	2.52	1.10
Std. Dev.		1.08	1.51	1.00	0.67	2.25	1.52	0.68	0.32	1.43	1.10	1.92	1.37	0.42	2.24	1.08	0.58	0.43	0.53	0.64	2.23	1.27	0.49	1.28	0.41	0.80	0.61	0.12
# of Case		151									1103									313								

NOTATION : A_o: Acceleration coefficient (g). R: Response modification factor. μ_ϕ: Curvature ductility. μ_Δ: Displacement ductility. μ_D: Displacement ductility demand. $(\Delta_c/\Delta_d)_e$: Capacity over elastic demand displacement. $(\Delta_c/\Delta_d)_{in}$: Capacity over inelastic demand displacement. $(\Delta_e/L)_D$: Elastic demand drift (%). $(\Delta_{in}/L)_D$: Inelastic demand drift (%). Δ_u/Δ_{FF}: Capacity over performance displacement corresponding to *Fully Functional* performance level. Δ_u/Δ_O: Capacity over performance displacement corresponding to *Operational* performance level. Δ_u/Δ_{DO}: Capacity over performance displacement corresponding to *Delayed Operational* performance level.

Table 4.4 Statistical Results of Response Measures Categorized Solely for Soil Site and Performance Levels

		A_o= 0.1, 0.2, 0.3 & 0.4																													
		FULLY FUNCTIONAL PERFORMANCE LEVEL										OPERATIONAL PERFORMANCE LEVEL										DELAYED OPERATIONAL PERFORMANCE LEVEL									
	SOIL SITE	R	μ_ϕ	μ_Δ	μ_D	$(\Delta_c/\Delta_d)_e$	$(\Delta_c/\Delta_d)_{in}$	$(\Delta_e/L)_D$	$(\Delta_{in}/L)_D$	Δ_u/Δ_{FF}	A_o	R	μ_ϕ	μ_Δ	μ_D	$(\Delta_c/\Delta_d)_e$	$(\Delta_c/\Delta_d)_{in}$	$(\Delta_e/L)_D$	$(\Delta_{in}/L)_D$	Δ_u / Δ_O	A_o	R	μ_ϕ	μ_Δ	μ_D	$(\Delta_c/\Delta_d)_e$	$(\Delta_c/\Delta_d)_{in}$	$(\Delta_e/L)_D$	$(\Delta_{in}/L)_D$	Δ_u / Δ_{DO}	A_o
Mean	–	2.08	9.80	4.19	0.79	6.00	5.62	0.87	0.90	4.08	0.24	3.62	10.34	4.82	1.32	4.17	3.74	1.20	1.26	2.39	0.33	4.80	9.07	3.59	1.53	2.37	2.36	2.24	2.25	1.09	0.36
Std. Dev.		0.88	1.83	0.90	0.17	2.48	1.87	0.38	0.37	1.14	0.07	0.97	1.98	1.49	0.23	2.00	1.32	0.46	0.43	0.54	0.07	0.30	1.41	0.39	0.20	0.18	0.17	0.27	0.27	0.07	0.06
# of Case		587										720										96									
Mean	=	1.95	9.70	4.13	0.80	5.92	5.40	0.88	0.92	4.01	0.20	3.48	10.68	4.96	1.41	4.28	3.62	1.19	1.30	2.36	0.31	4.70	9.52	3.77	1.63	2.36	2.32	2.30	2.34	1.08	0.34
Std. Dev.		0.91	1.67	0.86	0.17	2.48	1.64	0.39	0.37	1.08	0.07	1.02	2.06	1.46	0.29	2.14	1.18	0.49	0.43	0.54	0.08	0.44	1.85	0.67	0.25	0.34	0.23	0.31	0.31	0.08	0.07
# of Case		439										865										124									
Mean	≡	1.48	9.80	4.22	0.79	6.40	5.52	0.81	0.87	4.14	0.18	3.35	10.75	4.98	1.48	4.46	3.46	1.14	1.32	2.31	0.29	4.52	10.33	4.25	1.84	2.55	2.31	2.31	2.44	1.08	0.33
Std. Dev.		0.64	1.69	0.80	0.14	2.35	1.26	0.37	0.34	1.01	0.08	1.05	1.92	1.31	0.32	2.37	1.05	0.50	0.44	0.52	0.08	0.59	2.31	1.20	0.37	1.04	0.43	0.52	0.46	0.09	0.08
# of Case		335										984										191									
Mean	≥	2.50	10.39	4.24	1.36	4.08	3.52	1.29	0.81	2.34	0.22	2.96	11.07	5.23	1.71	5.34	3.27	1.08	1.31	2.19	0.28	4.31	10.75	4.86	2.11	3.26	2.33	1.90	2.44	1.16	0.30
Std. Dev.		1.24	2.01	0.71	0.52	1.61	1.26	0.52	0.34	0.93	0.11	1.18	1.86	1.23	0.49	3.09	1.06	0.72	0.44	0.59	0.09	0.69	2.02	1.36	0.51	1.56	0.47	0.93	0.69	0.13	0.09
# of Case		518										698										291									

NOTATION : A_o: Acceleration coefficient (g). R: Response modification factor. μ_ϕ: Curvature ductility. μ_Δ: Displacement ductility. μ_D: Displacement ductility demand. $(\Delta_c/\Delta_d)_e$: Capacity over elastic demand displacement. $(\Delta_c/\Delta_d)_{in}$: Capacity over inelastic demand displacement. $(\Delta_e/L)_D$: Elastic demand drift (%). $(\Delta_{in}/L)_D$: Inelastic demand drift (%). Δ_u/Δ_{FF}: Capacity over performance displacement corresponding to *Fully Functional* performance level. Δ_u/Δ_O: Capacity over performance displacement corresponding to *Operational* performance level. Δ_u/Δ_{DO}: Capacity over performance displacement corresponding to *Delayed Operational* performance level.

When the statistical results presented in Table 4.2, Table 4.3 and Table 4.4 are analyzed, following conclusions can be drawn;

- R-factor has a tendency to increase from Fully Functional to Delayed Operational performance level for a given acceleration coefficient regardless of soil site classification (Table 4.3). This is due to the fact that as R-factor increases for a particular soil type, acceleration coefficient and column aspect ratio, inelastic demand drift increases almost linearly. Besides, R-factor decreases slightly from soil site I to soil site IV for a presumed performance level regardless of acceleration coefficient (Table 4.4).
- For design purposes, *R=1.0-1.5* for Fully Functional performance level, *R=2.2-2.8* for Operational performance level and *R=3.8-4.2* for Delayed Operational performance level can be set regardless of soil condition and acceleration coefficient (Table 4.2). These ranges are assumed to be within half and one standard deviation below mean of R-factor. Coefficient of variation (standard deviation/mean) of R-factor obtained for Delayed Operational performance level is significantly less than the ones obtained for other performance levels.
- Curvature ductility, μ_{ϕ}, follows a similar trend for all performance levels. It is in the range of *9-11* with a coefficient of variation 0.2. It can be concluded that columns designed and detailed according to specifications of AASHTO LRFD [5] provide at least that much curvature ductility (Table 4.2).
- Increase in acceleration coefficient for a given performance level cause increase in displacement ductility, μ_{Δ}, regardless of soil site (Table 4.3). This increase is much more apparent in Operational and Delayed Operational performance levels. Similarly, same trend holds true for change in soil site from I to IV regardless of acceleration coefficient (Table 4.4).
- Displacement ductility demand, μ_D, is higher for Delayed Operational performance level than for Fully Functional performance level. Poor soil site condition consistently increases the ductility demand since it produces higher inelastic displacement demand. Similarly, higher hazard levels at a specific

site condition necessitate higher ductility demand for presumed performance level. Furthermore, ductility demand shows less scatter (coefficient of variation close to 0.2-0.3) compared with the other response measures (Table 4.2).

- For a given soil condition, higher capacity over elastic demand displacement, $(\Delta_c/\Delta_d)_e$, is expected for Fully Functional performance level. It is unsurprisingly the same trend observed in capacity over inelastic demand displacement, $(\Delta_c/\Delta_d)_{in}$ (Table 4.4). It can be concluded that site condition except soil site IV and acceleration coefficient have no notable effect on the trend of $(\Delta_c/\Delta_d)_e$ and $(\Delta_c/\Delta_d)_{in}$. In addition, $(\Delta_c/\Delta_d)_{in}$ is less scattered than $(\Delta_c/\Delta_d)_e$.
- For a given soil condition, higher elastic demand drift, $(\Delta_e/L)_D$, is expected for Delayed Operational performance level. Soil condition except soil site IV has no notable effect on elastic demand drift for a particular performance level (Table 4.4). For any site condition and particular performance level, seismic hazard level increases the elastic demand drift. Same trends can be observed for inelastic demand drift, $(\Delta_{in}/L)_D$.

4.2.5. Response Modification Factor

Although AASHTO LRFD [5] does not state anticipated performance level of bridges designed according to presumed bridge importance category, several considerations related to serviceability and seismic hazard level regarding to importance of the bridge are described roughly. Accordingly, *Critical Bridges* are supposed to be open to all traffic immediately after the design earthquake, i.e., a 475-year return period event. Additionally, it should stay usable by emergency vehicles and for security/defense purposes immediately after a large earthquake, e.g., a 2500-year return period event. This definition may correspond to a damage state where residual cracks are small enough that no repair is required for design earthquake defined in AASHTO LRFD [5]. Therefore, *Critical Bridge* importance category can be matched with Fully Functional performance level whose performance definition and demand parameter is explained in Section 2.4.1 in depth. When it comes to the *Essential Bridges*, they are supposed to be open to emergency vehicles and for security/defense purposes immediately after the design earthquake. Not all traffic is allowed to use bridge in the days or weeks following the earthquake. Closure of the bridge may be required until an inspection is completed, and partial lane closures to be only used by emergency vehicles may be required to repair damage. All traffic could be open to access after repairs are completed in the days and weeks following the earthquake. This category can be paired with Operational performance level. Finally, there is no definition related to importance category of *Other Bridges* in terms of serviceability and seismic hazard level. However, it is obvious that minimum requirement related to any category is to prevent collapse of bridges following with life safety. Other bridge category can correspond to damage state of Delayed Operational performance level that is characterized by severe damage to structural components. Complete replacement of the bridge is not anticipated, but repair and replacement of components requires closures to all but emergency traffic. As previously mentioned, bridges merged in different importance categories are to be designed with different R-factors summarized in Table 1.1.

Assuming that Fully Functional performance level is represented by $R=1.5$ corresponding to Critical bridges, Operational performance level represented by $R=2.0$ corresponding to Essential bridges and Delayed Operational performance level represented by $R=3.0$ corresponding to Other bridges, correlations between R-factor, axial load ratio, column aspect ratio, acceleration coefficient and soil site are investigated throughout Figure 4.9 to Figure 4.12. To compare results of R-factor with the ones assumed for bridges importance categories of AASHTO LRFD [5], red lines passing through R=1.5, 2.0 and 3.0 are shown in the relevant figures. Statistical studies presented in this section are performed based on analysis results excluding cases ending up with minimum reinforcement ratio. Following conclusions can be made;

- For Fully Functional performance level, R=1.5 seems to be satisfactory lower bound value except for axial load ratio of 0.1 and column aspect ratio equal and less than 4.0 according to Figure 4.9. For Operational performance level, R=2.0 seems to be highly satisfactory except for axial load ratio of 0.1 and column aspect ratio equal and less than 4.0 according to Figure 4.9. R=3.0 and R=3.5 can be used for axial load ratios of 0.2 and 0.3 to ensure Operational performance level respectively. Nevertheless, R=2.0 can be thought as a guaranteed limit value for Operational performance level regardless of axial load ratio.

- R=4.0 can be used for normalized axial load levels of 0.2 and 0.3 to ensure Delayed Operational performance level. R=3.5 can be a conservative limit value to anticipate Delayed Operational performance level regardless of axial load ratio (Figure 4.9). In other saying, columns designed according to requirements of Other bridge importance category (R=3.0) probably perform better than Delayed Operational performance level.
- Increase in acceleration coefficient for presumed performance and axial load ratio causes increase in R-factor due to higher force demand. Stipulated R-factor for Critical bridges mostly satisfy Fully Functional performance level except for acceleration coefficient of 0.1 (Figure 4.10). Likewise, bridges designed according to Important bridge category mostly satisfy Operational performance level except for acceleration coefficient of 0.1 and axial load ratios of 0.2 and 0.3. Other bridges designed according to R=3.0 will highly assure Delayed Operational performance level. Alternatively, these columns probably demonstrate better performance level than Delayed Operational (Figure 4.10).
- R=1.5 may be thought as a reliable lower bound for seismic design of Critical bridge importance category that assures Fully Functional performance level except for normalized axial load level of 0.1 according to Figure 4.11. As axial load ratio increases for a given performance level, mean of R-factor has a tendency to increase. It could be expected that increase in axial load ratio decreases performance drift according to Eq.(3.63) and Eq.(3.64) resulting with a lower inelastic displacement demand in turn with a lower response modification factor. However, higher axial load ratios advances force demand

for section design. In that case, higher R-factors are cumulated at higher axial load ratios. Soil site IV has a greater dispersion in terms of R-factor according to Figure 4.11. The reason comes to light from Figure 2.14. In the range of 0.75–1.4 seconds of normalized periods of vibration, T/T_g, inelastic drift demand becomes less than elastic drift demand. Therefore, to increase inelastic drift to fall into a given performance category, R-factor should be increased to compensate this drawback. From Figure 4.11, R=3.5 can readily be used for Delayed Operational performance level regardless of axial load ratio.

- From Figure 4.12, it can be observed that mean of R-factor becomes nearly uniform for particular performance levels categorized according to normalized axial load level except soil site IV. Column aspect ratios less than 4 have a tendency to produce smaller R-factor than the uniform trendline. R=*1.0–1.5* for Fully Functional, R=*2.0–2.5* for Operational, R=*3.5–4.0* for Delayed Operational performance level can be suggested for seismic design according to AASHTO LRFD [5]. Bridges located in soil site IV should be treated separately in terms of seismic design since its inelastic demand displacement highly dependent on normalized period of vibration.

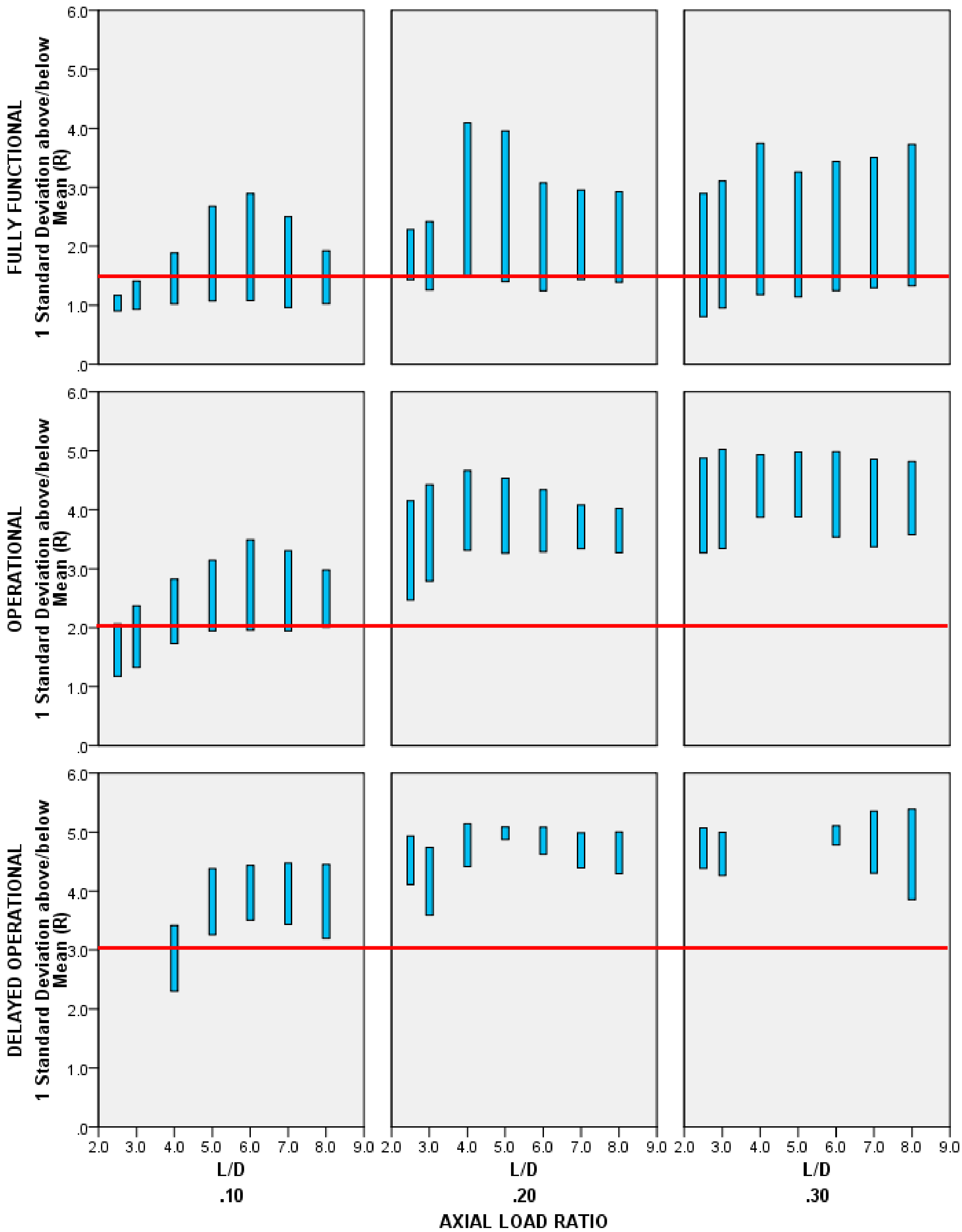

Figure 4.9 Plots of One Standard Deviation Above/Below Mean of R-Factor with respect to Column Aspect Ratio Categorized for Axial Load Ratio and Performance Level

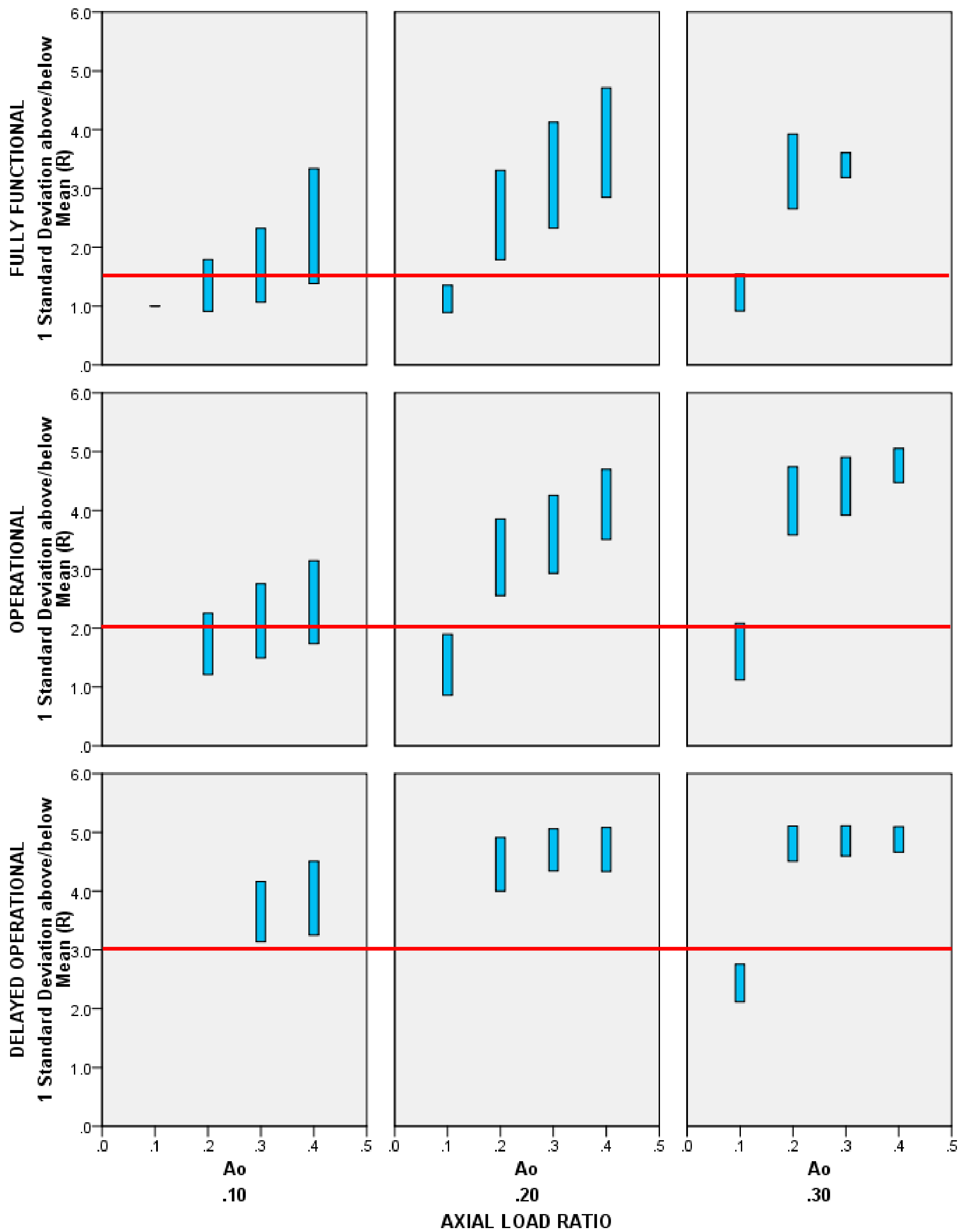

Figure 4.10 Plots of One Standard Deviation Above/Below Mean of R-Factor with respect to Acceleration Coefficient Categorized for Axial Load Ratio and Performance Level

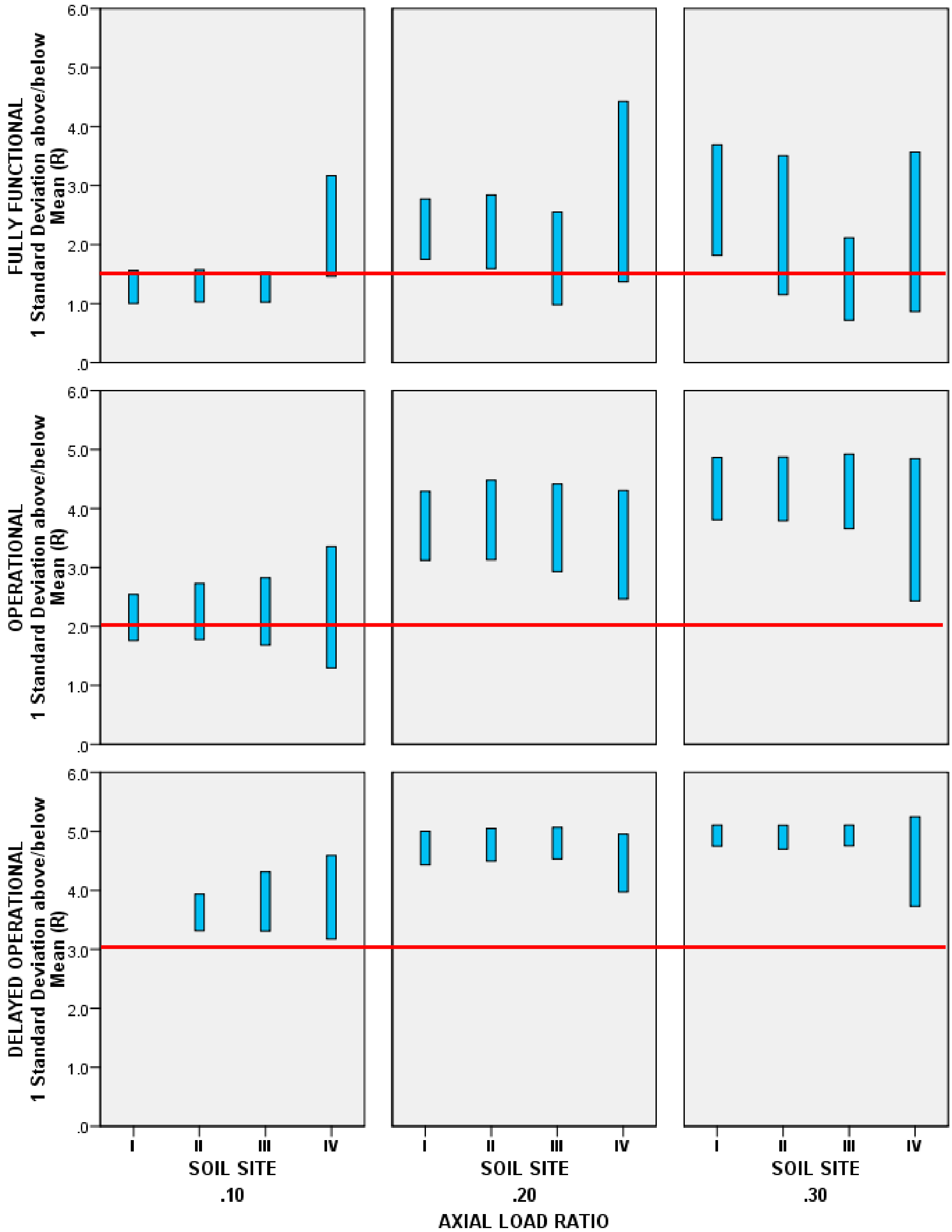

Figure 4.11 Plots of One Standard Deviation Above/Below Mean of R-Factor with respect to Soil Site Categorized for Axial Load Ratio and Performance Level

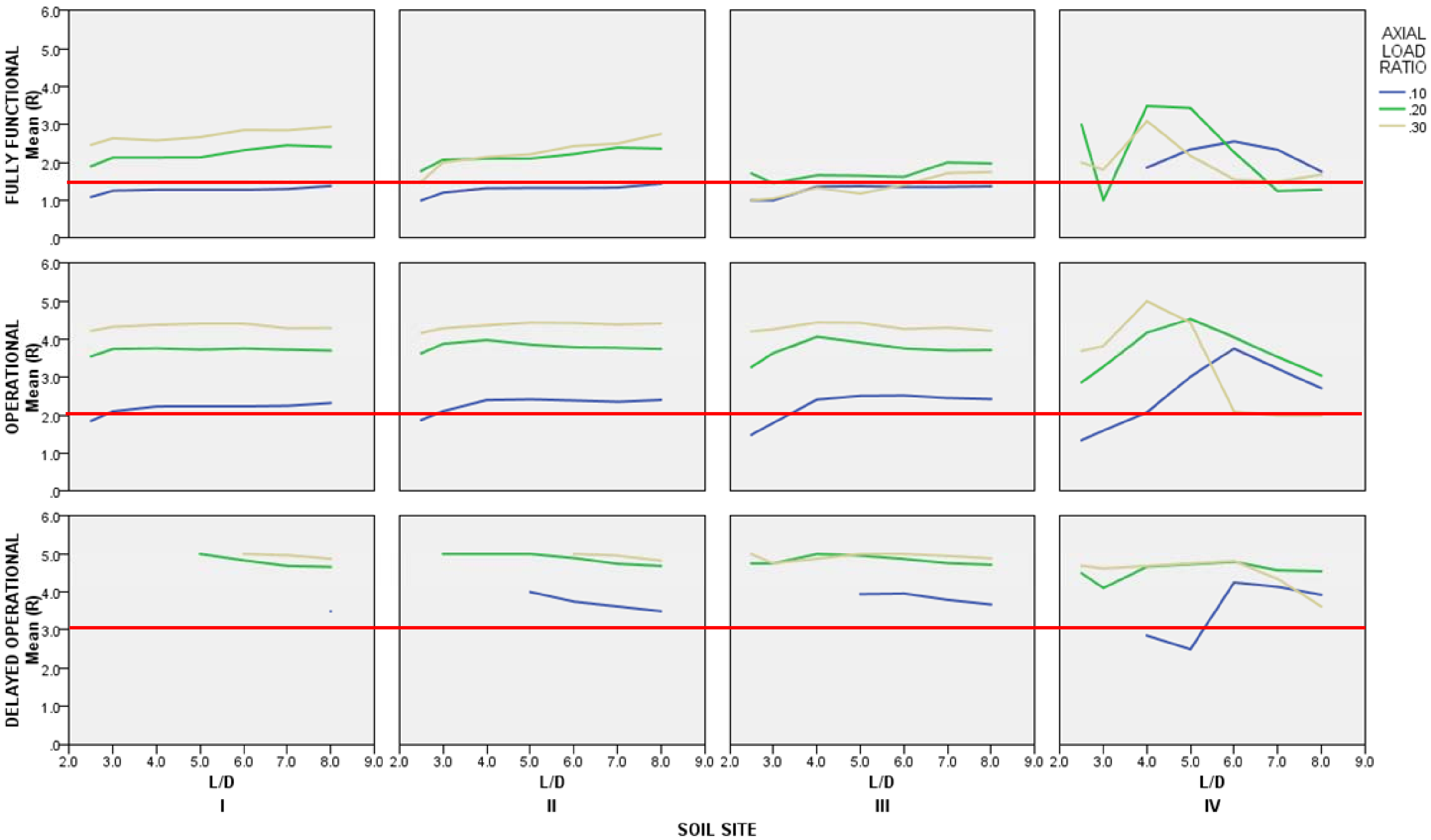

Figure 4.12 Plots of Mean of R-Factor with respect to Column Aspect Ratio Categorized for Axial Load Ratio, Soil Site and Performance Level

4.2.6. Displacement Ductility

In ATC 32-1 [55], force reduction factor, Z, is expressed in terms of displacement ductility by the following relationship.

$$Z = 1 + 0.67(\mu - 1)\frac{T}{T_0} \le \mu \tag{4.7}$$

Where T_o is the peak elastic spectral response, T is the first-mode period and μ is the ductility level given in Figure 4.13 with red line proposed for *cantilever columns*. It is stated that columns designed to these ductility levels are expected to repairable after the design level of shaking [55]. In addition, No differential of Z factors has been proposed between Ordinary and Important bridge classification. These bridge categories defined in ATC 32 [16] are given in Section 2.3 accordingly. As a further advancement for displacement ductility, two different allowable displacement ductility limits presented in Figure 4.13 are proposed for *Normal (Ordinary)* and *Important bridge* categories. Eventually, corresponding ductility limit is used in Eq.(4.8) to calculate force reduction factor.

$$Z = 1 + (\mu - 1)\frac{T}{T_g} \le \mu \tag{4.8}$$

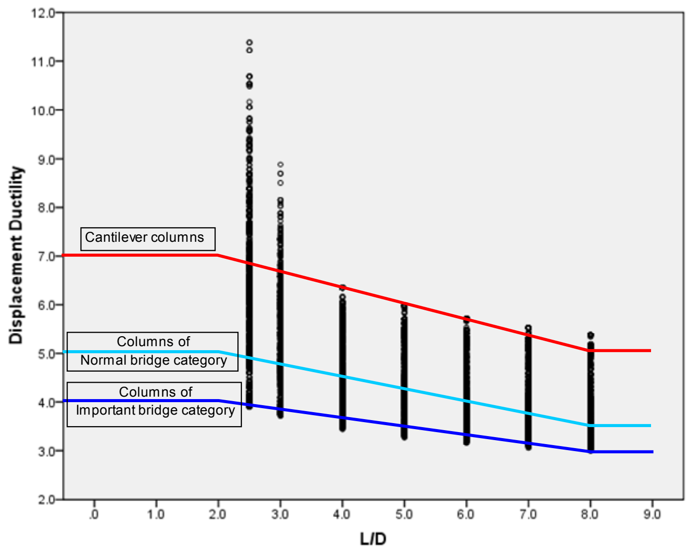

Figure 4.13 Proposed Design Ductility Levels of ATC 32-1 [55]

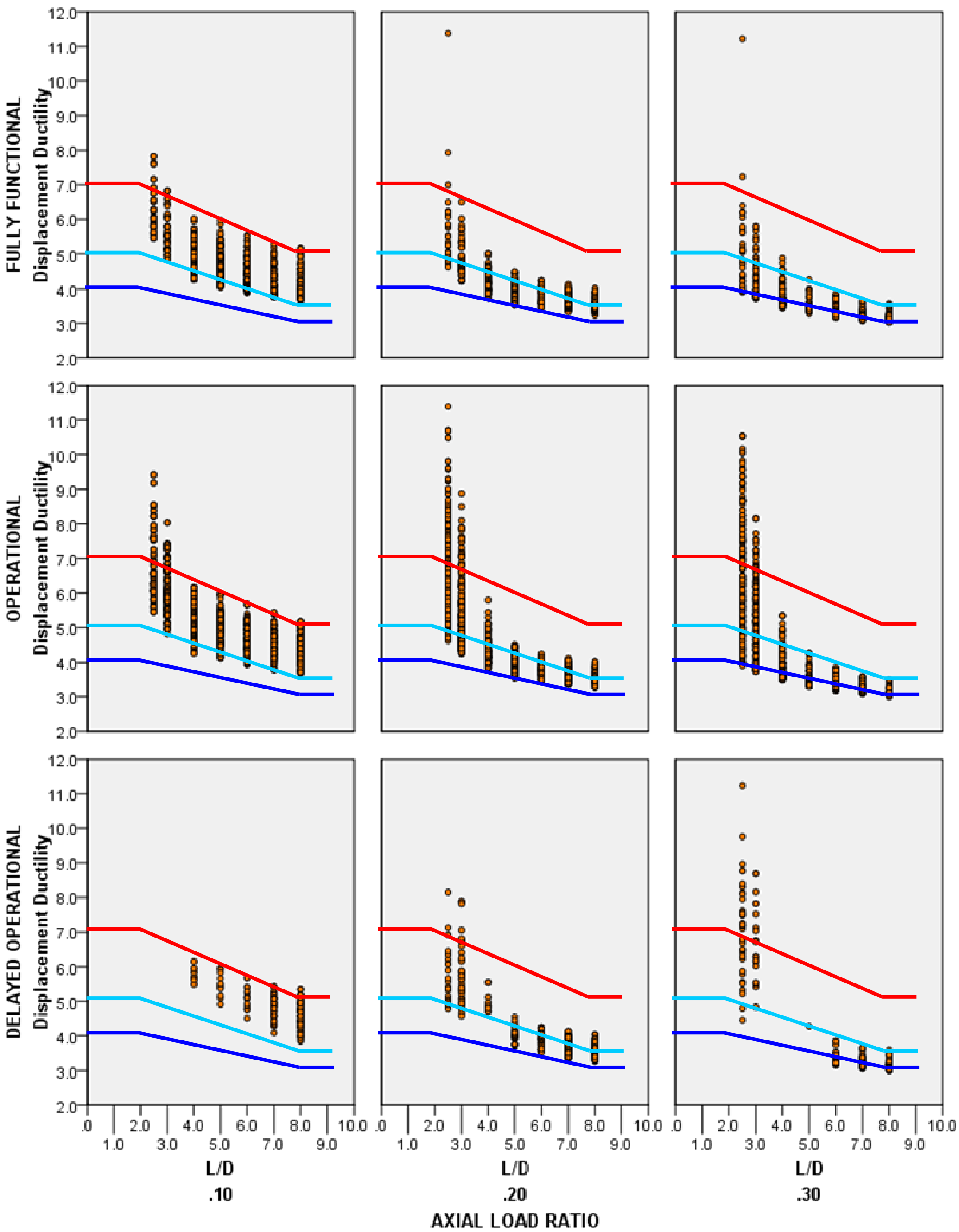

Figure 4.14 Comparison of Proposed Design Ductility Levels of ATC 32-1 [55] with Analysis Results Categorized for Axial load Ratio and Performance Level

In Figure 4.13 and Figure 4.14, displacement ductility versus column aspect ratio obtained from analyses are plotted. Allowable ductility levels proposed for cantilever column and important bridge category constitute upper and lower boundary of analysis results. Column aspect ratio less than 4 produces very high displacement ductility values up to 11. This is mainly due to supplying required transverse reinforcement instead of minimum amount for confinement as explained in Section 3.6. For axial load ratio of 0.1, analysis results are confined between cantilever column and column of normal bridge category limits. Besides, axial load ratio greater than 0.1 yields displacement ductility results confined between column of normal and important bridge category limits except column aspect ratio less than 4.

4.3. Estimation of R-Factors Corresponding to Performance Levels

Utilizing seven different column aspect ratio, nine different column diameter, three different design axial load ratio, four different acceleration coefficient ,four different soil type, and two different performance levels, 7x9x3x4x4x2=6048 analyses are performed. Due to the drawbacks discussed in Section 3.10, 1536 analysis results could be obtained. 101 analyses out of total end up with more than adequate flexural strength even for minimum longitudinal reinforcement ratio of 1%. Number of analyses corresponding to performance level and soil site is shown in Table 4.5.

Table 4.5 Number of Analyses Corresponding to Performance Level and Soil Site Excluding Minimum Reinforcement Ratio

	SOIL SITE I	SOIL SITE II	SOIL SITE III	SOIL SITE IV
FULLY FUNCTIONAL	233	235	212	186
OPERATIONAL	102	130	159	178

It is decided to separate soil site IV from the rest of the results due to following reason. R-factors categorized for soil site IV show higher dispersion among others as demonstrated in Figure 4.11 and Figure 4.12 due to deamplification effect in inelastic displacement demand for a specific range of normalized periods of vibration.

Therefore, results of soil site IV are not included in subsequent sections and remaining soil site classifications are considered together during data processing. R-factor estimations for Delayed Operational performance level are not studied. It is thought that designing a bridge according to R-factor just satisfying Delayed Operational performance levels does seem to be reasonable. During generic studies attempting to find R-factor corresponding to that performance level produced very high values even exceeding R=11 that is the upper bound. Moreover, most of them ended up with minimum longitudinal reinforcement ratio due to low flexural strength demand during design process.

4.3.1. Response Modification Factor

As assumed in Section 4.2.5, estimated R-factors corresponding to Fully Functional performance level are paired with Critical bridge category of AASHTO LRFD [5]. With the same analogy, estimated R-factors corresponding to Operational performance level are matched with Essential bridge category of AASHTO LRFD [5]. When the plots demonstrated in Figure 4.15, Figure 4.16 and Figure 4.17, following conclusions can be drawn;

- In Figure 4.15, as column aspect ratio increases, R-factor satisfying Fully Functional performance level increases. This trend holds true even for various axial load ratios. This tendency can be explained in that way. The drift limit of Fully Functional performance level is calculated with (ϕ'_y L)/2 where effective yield curvature, ϕ'_y, is inversely proportional with diameter of the section that is parallel to yield curvature estimation, ϕ_y, in Eq.(4.5). Eventually, demand performance drift simplifies to a function of column aspect ratio, L/D. Analogously, increase in column aspect ratio causes an increase in inelastic displacement drift demand. As previously discussed in Section 3.10, it requires R-factor to be increased to satisfy relative error of drift. Below, R-factor estimations for lower bound of Fully Functional performance level are given for various axial load ratios. Additionally, trendlines represented by Eq.(4.9), Eq.(4.10) and Eq.(4.11) are demonstrated with red colored lines in mentioned figures.

For $P_u/A_g f_c$=0.1;

$$R = 1 + 0.164\left(L/D - 2.5\right) \tag{4.9}$$

For $P_u/A_g f_c$=0.2;

$$R = 1.7 + 0.255\left(L/D - 2.5\right) \tag{4.10}$$

For $P_u/A_g f_c$=0.3;

$$R = 2.5 + 0.218\left(L/D - 2.5\right) \tag{4.11}$$

- In Figure 4.15, as column aspect ratio increases, R-factor satisfying Operational performance level tends to decrease. This observation is much more prominent for axial load ratios greater than 0.1. Although it is expected that lower column aspect ratio ends up with lower normalized periods of vibration, T/T_g, resulting with higher inelastic displacement coefficient, C_μ, elastic displacement grows faster than inelastic displacement coefficient for a given force demand. In other words, decrease in column aspect ratio influences elastic displacement demand roughly proportional with L^3/D^4. Therefore, at low column aspect ratios, inelastic displacement demand should be increased by increasing R-factor so that target performance drift is satisfied within a given tolerance margin. Instead of proposing an equation that decreases with respect to column aspect ratio, a constant R-factor is preferred for various axial load ratios to embrace wide dispersion at low aspect ratios. Accordingly, *R=3.0* is proposed for *$P_u/A_g f_c$=0.1, R=4.0* for *$P_u/A_g f_c$=0.2,* and *R=4.5* for *$P_u/A_g f_c$=0.3*. The reason of higher response modification factor at high axial load ratio can be explained by requirement of higher force demand. Base shear is a function of ($m^{2/3}$, $k^{1/3}$) in which *m* is the lumped mass of superstructure used in dynamic analysis, *k* is the flexural stiffness of the generic column. Although higher force demand probably increases the elastic displacement demand and decreases inelastic displacement coefficient, it brings about cases where lower R-factors result in maximum reinforcement ratio to be exceeded. Therefore, higher R-factors providing sections designed optimally is observed at high axial load ratios. Dispersion existing in low aspect ratio for Operational performance level can be observed easily in Figure 4.16. This dispersion even increases at high axial load ratios. If same figure is interpreted further, recommended R-factors to be used in seismic design of Essential bridges according to AASHTO LRFD [5] are highly conservative for column aspect ratios less than 7.

- In Figure 4.17, period dependency of R-factor is demonstrated. It is obvious that period is directly proportional with column aspect ratio. Instead of using constantly increasing R-factor relation for Fully Functional performance level as given in Eq.(4.9), Eq.(4.10) and Eq.(4.11), two-staged response modification factor is proposed since it is more explicitly distinguished in scatter plot. Equations for various axial load ratios shown in Figure 4.17 with blue colored lines are given below;

For $P_u/A_g f_c$=0.1;

$$\begin{aligned} R &= 1.7 && \text{for } 2.3 \geq \mathrm{T} \geq 0.8 \\ R &= 1 + 1.4(T - 0.3) && \text{for } 0.8 > \mathrm{T} \geq 0.3 \end{aligned} \tag{4.12}$$

For $P_u/A_g f_c$=0.2;

$$\begin{aligned} R &= 2.7 && \text{for } 3.1 \geq \mathrm{T} \geq 1.0 \\ R &= 1.7 + 1.43(T - 0.3) && \text{for } 1.0 > \mathrm{T} \geq 0.3 \end{aligned} \tag{4.13}$$

For $P_u/A_g f_c$=0.3;

$$
\begin{aligned}
R &= 3.4 && \text{for } 3.9 \geq \mathrm{T} \geq 1.2 \\
R &= 2.5 + 1.2(T - 0.45) && \text{for } 1.2 > \mathrm{T} \geq 0.45
\end{aligned} \tag{4.14}
$$

- Similar dispersion of R-factor for Operational performance level observed in Figure 4.15 in terms of column aspect ratio holds true in Figure 4.17 in terms of period of vibration. Therefore, $R=3.0$ for $P_u/A_g f_c=0.1$, $R=4.0$ for $P_u/A_g f_c=0.2$, and $R=4.5$ for $P_u/A_g f_c=0.3$ could be recommended.

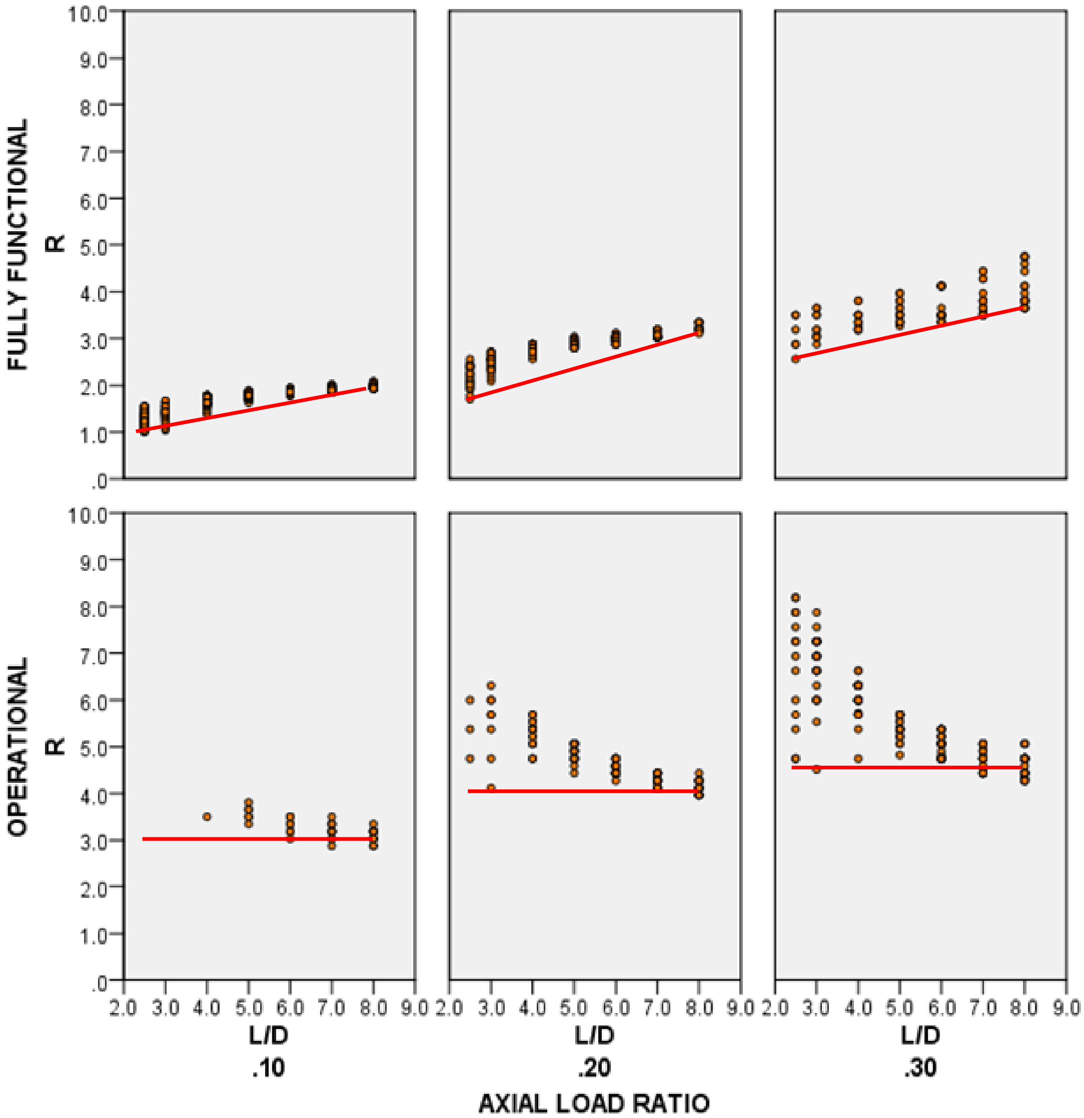

Figure 4.15 Scatter Plots of R-Factor with respect to Column Aspect Ratio Categorized for Axial Load Ratio and Performance Level

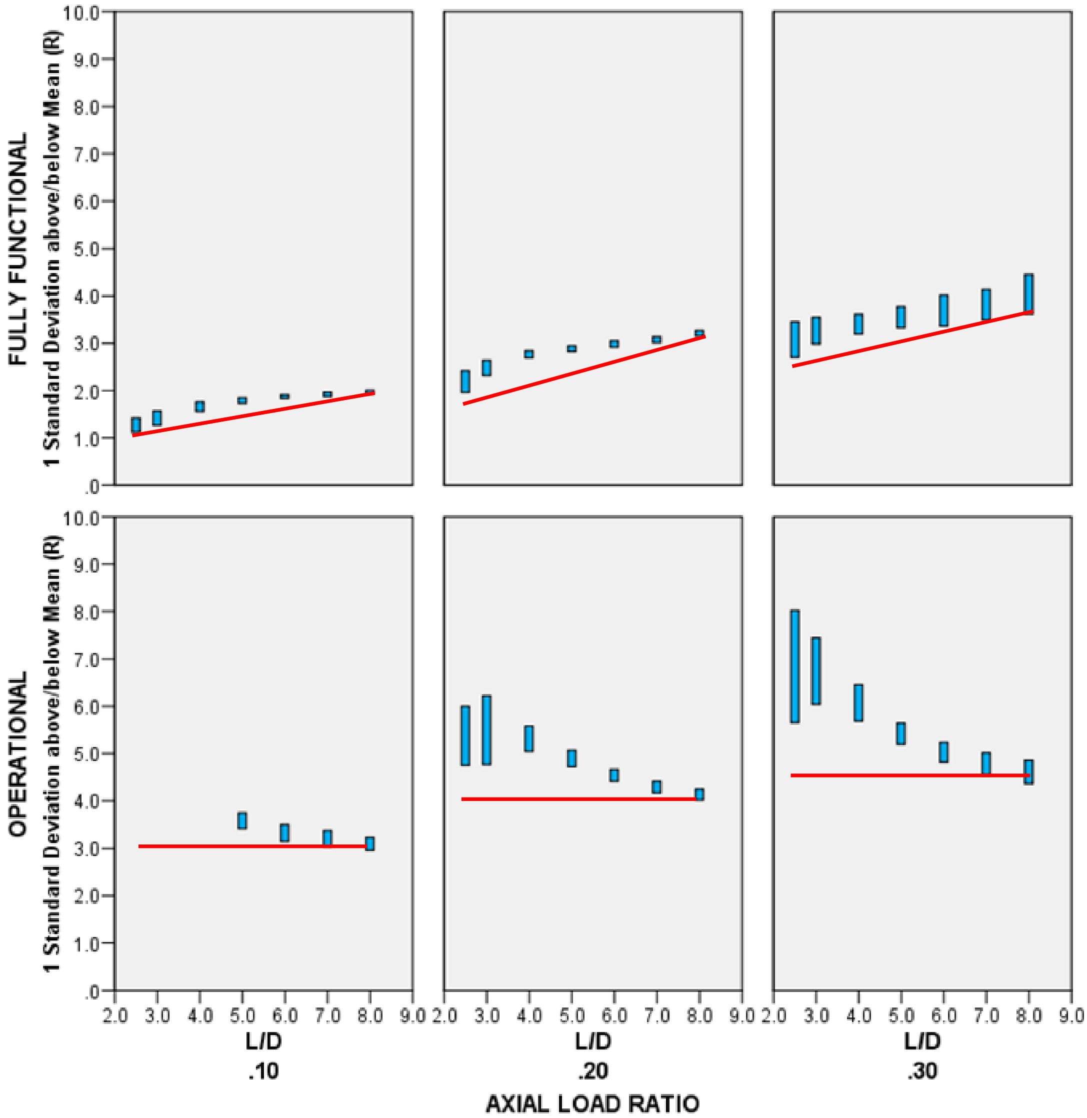

Figure 4.16 Plots of One Standard Deviation Above/Below Mean of R-Factor with respect to Column Aspect Ratio Categorized According to Axial Load Ratio and Performance Level

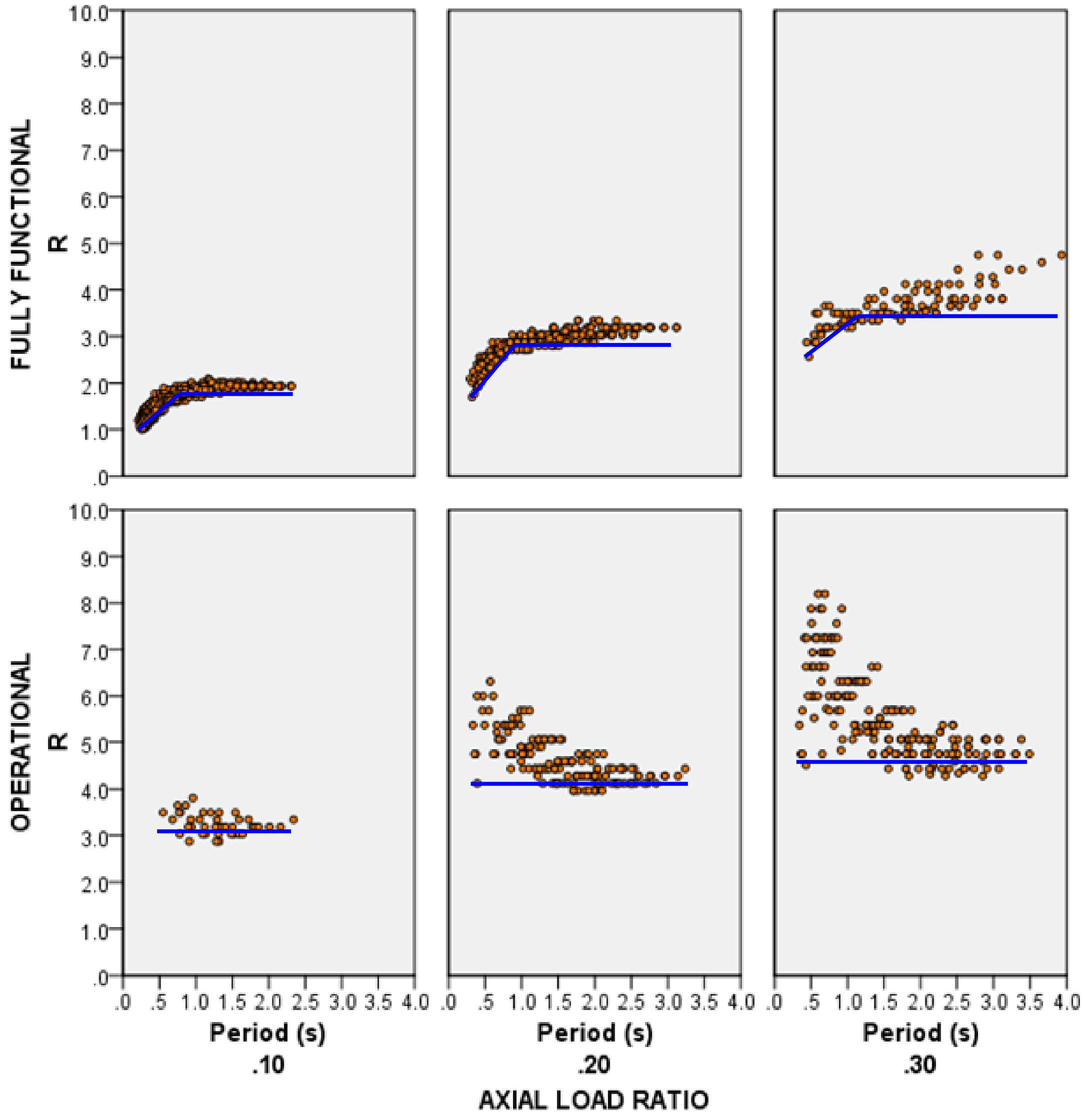

Figure 4.17 Scatter Plots of R-Factor with respect to Period of Vibration Categorized According to Axial Load Ratio and Performance Level

4.3.2. Capacity over Elastic and Inelastic Demand Displacement

Since $(\Delta_c/\Delta_d)_e$ and $(\Delta_c/\Delta_d)_{in}$ are directly related to capacity and demand displacements, they can be thought to be logical and reliable response measures for limiting the performance levels. In Figure 4.18 and Figure 4.19, comparison of capacity over elastic and inelastic demand displacements in terms of column aspect ratio and period of vibration are given. Following conclusions can be drawn;

- According to Figure 4.18, $(\Delta_c/\Delta_d)_{in}$ seems to be less scattered than $(\Delta_c/\Delta_d)_e$ especially for column aspect ratio less than 4 with respect to Fully Functional performance level. Capacity over elastic and inelastic demand displacements are very sensitive to column aspect ratios smaller than 4. Similar scatter observation can be made for column aspect ratios less than 4 and axial load ratio of 0.3 in terms of Operational performance level. Use of column aspect ratio less than 4 should be avoided during design process. Upper bound trendlines of $(\Delta_c/\Delta_d)_{in}$ for Fully Functional performance level represented by Eq.(4.15) and Eq.(4.16) are demonstrated with red colored lines in mentioned figure.

  For $P_u/A_g f_c$=0.1;

$$\begin{aligned} \left(\Delta_c/\Delta_d\right)_{in} &= 9.3-2.2\left(L/D-2.5\right) \qquad \text{for } 4 \geq \left(L/D\right) \geq 2.5 \\ \left(\Delta_c/\Delta_d\right)_{in} &= 6-0.3\left(L/D-4\right) \qquad \text{for } 8 \geq \left(L/D\right) > 4 \end{aligned} \tag{4.15}$$

  For $P_u/A_g f_c$=0.2 & 0.3;

$$\begin{aligned} \left(\Delta_c/\Delta_d\right)_{in} &= 8-2.33\left(L/D-2.5\right) \qquad \text{for } 4 \geq \left(L/D\right) \geq 2.5 \\ \left(\Delta_c/\Delta_d\right)_{in} &= 4.5-0.25\left(L/D-4\right) \qquad \text{for } 8 \geq \left(L/D\right) > 4 \end{aligned} \tag{4.16}$$

  Compared to decreasing trend of $(\Delta_c/\Delta_d)_{in}$ for Fully Functional performance level, there is virtually a constant trend in terms of Operational performance level regardless of axial load ratio. Accordingly, Capacity over elastic and inelastic demand displacements can be taken as *3.0* and *2.7* respectively to be used for further design check.

- According to Figure 4.19, $(\Delta_c/\Delta_d)_{in}$ seems to be less scattered than $(\Delta_c/\Delta_d)_e$ in terms of Fully Functional performance level. Capacity over elastic and inelastic demand displacements are very sensitive to period of vibration smaller than corner periods marked with blue circle. These corner periods corresponding to increasing axial load ratio are 0.6, 0.85 and 1.0 seconds in terms of Fully Functional performance level. Upper bound trendlines of $(\Delta_c/\Delta_d)_{in}$ for Fully Functional performance level represented by Eq.(4.17), Eq.(4.18) and Eq.(4.19) are demonstrated with red colored lines in mentioned figure.

For $P_u/A_g f_c$=0.1;

$$\begin{aligned} (\Delta_c/\Delta_d)_{in} &= 9.5 - 11.43(T-0.25) \quad \text{for } 0.6 \geq \mathrm{T} \geq 0.25 \\ (\Delta_c/\Delta_d)_{in} &= 5.5 - 0.57(T-0.6) \quad \text{for } 2.35 \geq \mathrm{T} > 0.6 \end{aligned} \tag{4.17}$$

For $P_u/A_g f_c$=0.2;

$$\begin{aligned} (\Delta_c/\Delta_d)_{in} &= 8 - 8(T-0.35) \quad \text{for } 0.85 \geq \mathrm{T} \geq 0.35 \\ (\Delta_c/\Delta_d)_{in} &= 4 - 0.31(T-0.85) \quad \text{for } 3.1 \geq \mathrm{T} > 0.85 \end{aligned} \tag{4.18}$$

For $P_u/A_g f_c$=0.3;

$$\begin{aligned} (\Delta_c/\Delta_d)_{in} &= 7.9 - 7.8(T-0.5) \quad \text{for } 1 \geq \mathrm{T} \geq 0.5 \\ (\Delta_c/\Delta_d)_{in} &= 4 - 0.48(T-1) \quad \text{for } 3.9 \geq \mathrm{T} > 1 \end{aligned} \tag{4.19}$$

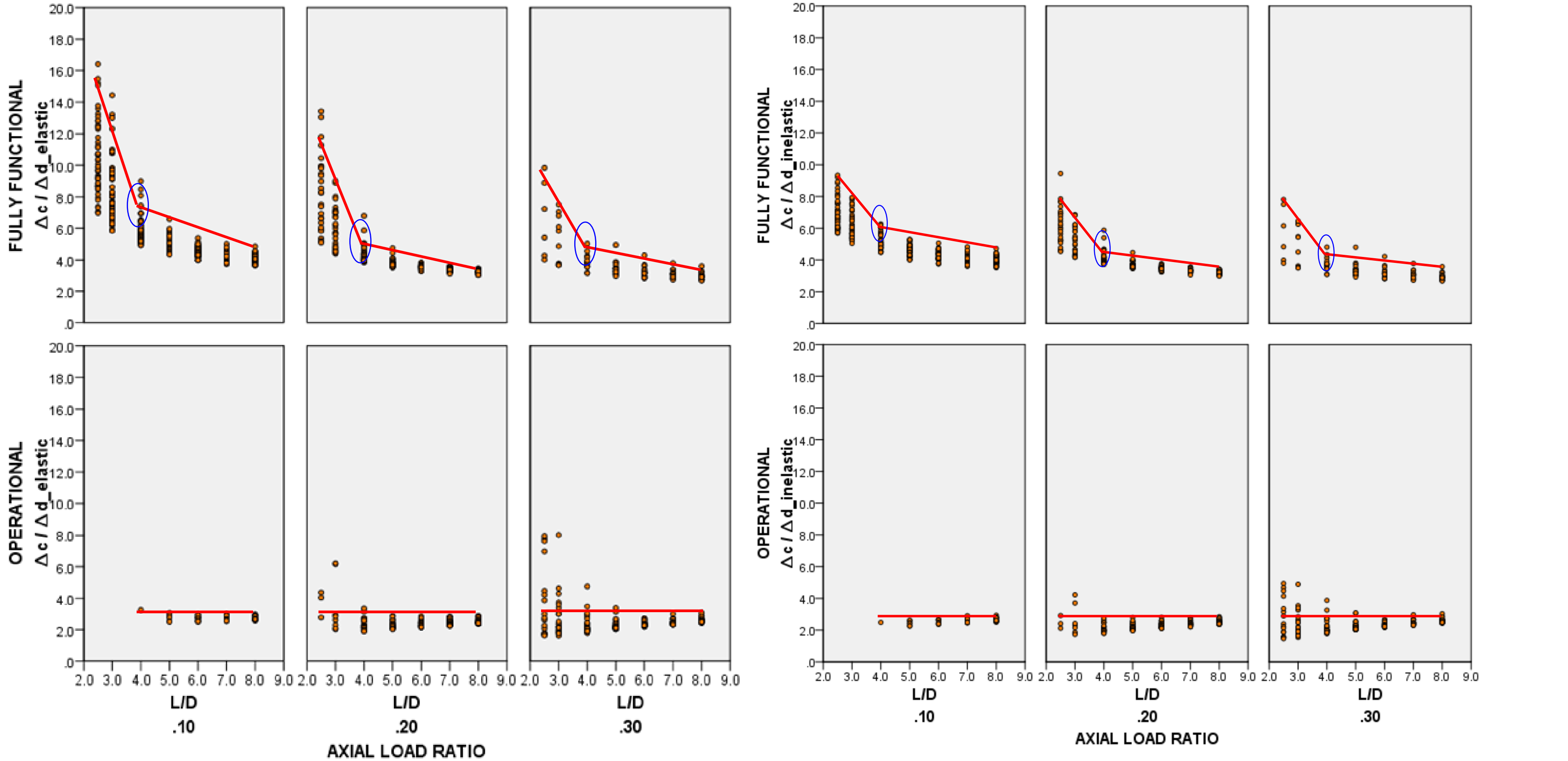

Figure 4.18 Scatter Plots of $(\Delta_c/\Delta_d)_e$ and $(\Delta_c/\Delta_d)_{in}$ with respect to Column Aspect Ratio Categorized for Axial Load Ratio and Performance Level

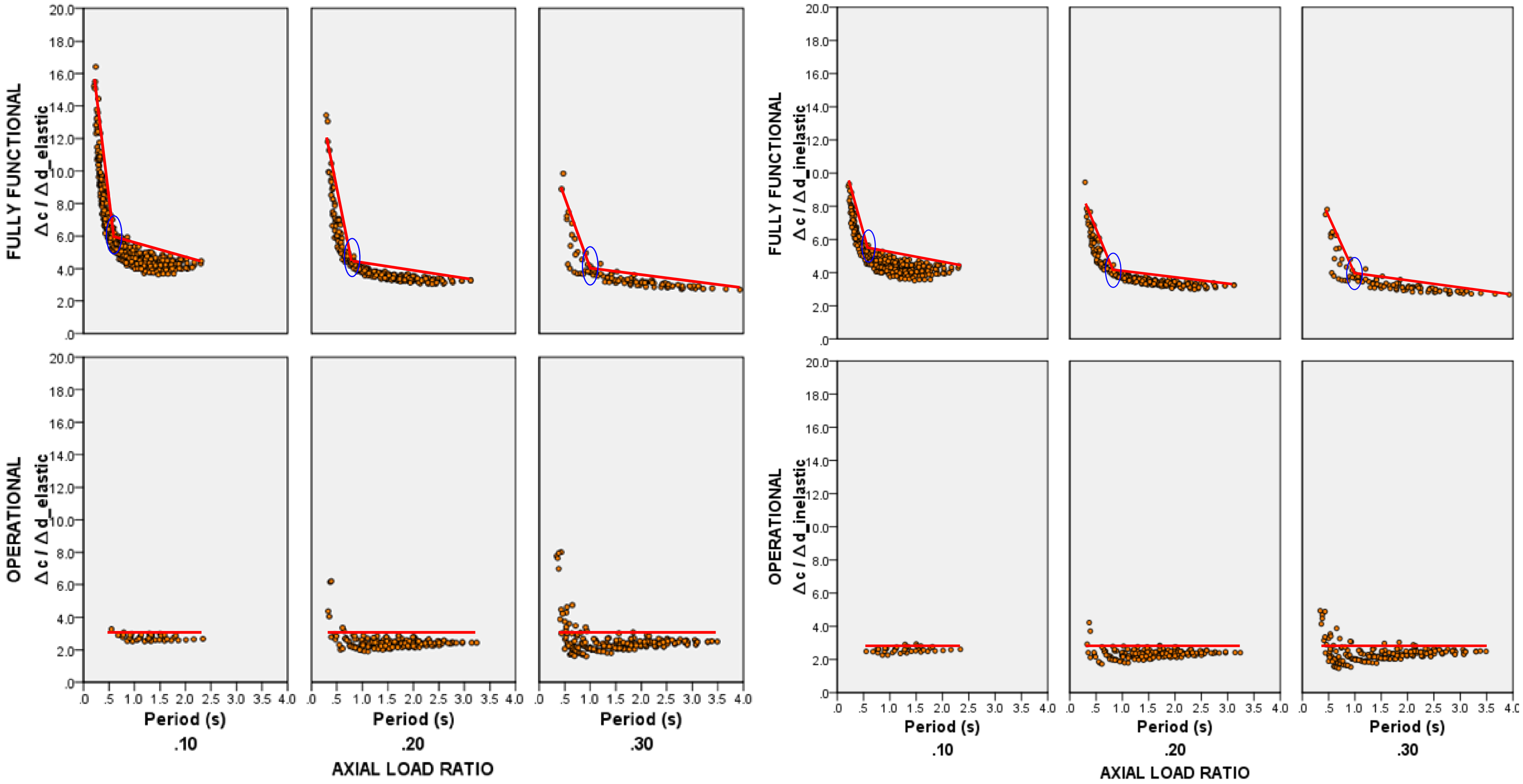

Figure 4.19 Scatter Plots of $(\Delta_c/\Delta_d)_e$ and $(\Delta_c/\Delta_d)_{in}$ with respect to Period of Vibration Categorized for Axial Load Ratio and Performance Level

4.3.3. Elastic Demand Drift

Although R-factor given in Section 4.3.1 can be used for seismic design of single bent circular bridge column to satisfy anticipated performance level, additional engineering measures to limit the applicability of R-factor to be used for a preferred column aspect ratio are necessitated. Elastic demand drift can be thought as an appropriate response measure since it can be directly estimated from elastic dynamic analysis. It is worth to state that elastic demand measures are calculated by using cracked section properties to reflect realistic behavior during ground shaking. As previously discussed, cracked section stiffness is proportional to amount of reinforcement supplied to the column. Nevertheless, it is possible to end up with a converging estimate of elastic demand drift with an appropriate prediction of stiffness modification factor presented in Section 4.2.1. In Figure 4.20, upper and lower bounds of elastic drift demand are demonstrated with blue and red trendlines for Fully Functional and Operational performance levels respectively. Corresponding relations of elastic demand drift are given in Eq.(4.20) and Eq.(4.21).

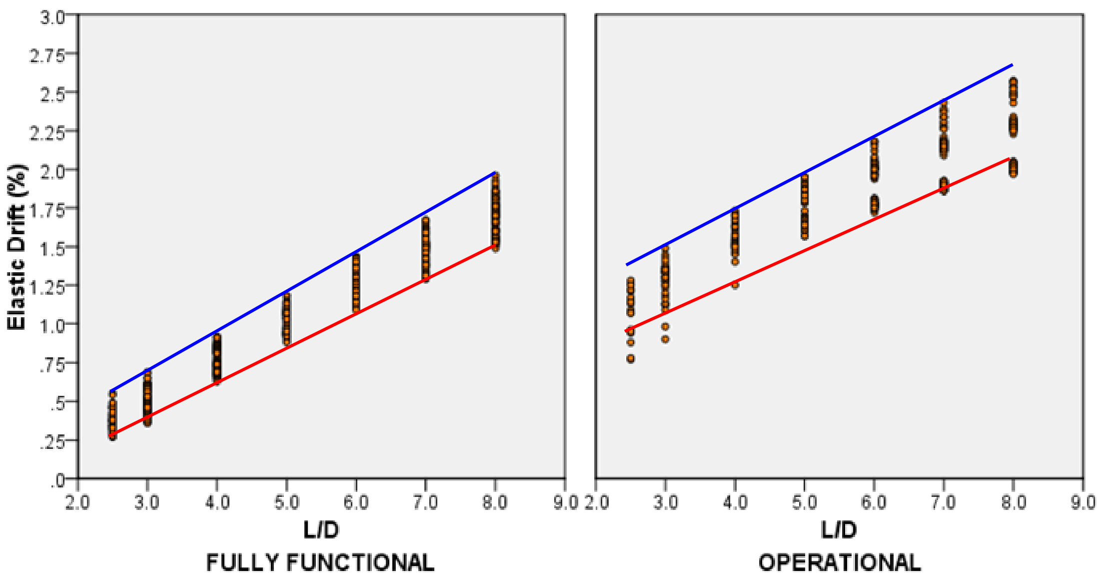

Figure 4.20 Scatter Plot of Elastic Demand Drift, (Δ_e/L) with respect to Column Aspect Ratio Categorized for Performance Level

For Fully Functional performance level;

$$\begin{aligned}(\Delta_e/L)_{upper} &= 0.55 + 0.255(L/D - 2.5)\\(\Delta_e/L)_{lower} &= 0.25 + 0.227(L/D - 2.5)\end{aligned} \tag{4.20}$$

For Operational performance level;

$$\begin{aligned}(\Delta_e/L)_{upper} &= 1.38 + 0.235(L/D - 2.5)\\(\Delta_e/L)_{lower} &= 0.95 + 0.2(L/D - 2.5)\end{aligned} \tag{4.21}$$

It can be concluded that columns producing higher elastic demand drift than upper bound trendline proposed for a particular performance level cannot achieve corresponding performance criterion. Therefore, further progression of seismic design may become waste of time. It is required to select another column aspect ratio to be within the given range of elastic demand drift. On the contrary, elastic demand drifts producing less than lower bound trendline proposed for presumed performance level assures corresponding performance criterion. However, designer may wish to revise column aspect ratio to come up with an optimum solution.

CHAPTER 5

LIMITATIONS AND CONCLUSIONS OF THE STUDY

5.1. General

Analytical investigation of response modification factor (R-factor) and seismic performance levels of circular bridge columns complying with the requirements of AASHTO LRFD [5] were presented in this study. The aim of the study was to investigate R-factor of AASHTO LRFD [5] corresponding to critical, essential and other bridge importance categories. Considering the inadequacy of comprehensive performance definition of importance categories, reliable limit values were striven for R-factors to be used in seismic design for a presumed performance levels.

Two groups of analyses have been undertaken in the scope of thesis. Firstly, single bridge columns seismically designed with respect to predefined range of R-factor were statistically studied. By taking advantage of large amount of response outcomes, several conclusions for stiffness modification factor, yield curvature, moment magnification factor, capacity over elastic and inelastic displacement and response modification factor were drawn and expressions were derived. Secondly, modifying the analysis tool developed for the first part of study, boundary value of R-factor was estimated for presumed performance level. In addition to R-factor, capacity over elastic and inelastic displacement was studied in terms of column aspect ratio and period of vibration. Additionally, upper and lower limits of elastic demand drift were derived in terms of column aspect ratio.

5.2. Limitations of the Study

Soil-structure interaction (SSI) is not considered due to voluminous number of analyses and parameters. It is stated in Caltrans-SDC [18] that "columns or piers with flexible foundations will naturally have low displacement ductility demands because of the foundation's contribution to yield displacement". Therefore, exclusion of foundation flexibility in soft soils may influence capacity and demand characteristics of bridge piers that might affect performance categorization of the given column in the dataset.

The author notices that acceleration coefficients employed in this study are based on accepted seismic risk corresponding to building type of structures [56]. Gülkan et al. [56] states that acceleration coefficients would be different in terms of engineering purposes that the most distinctive aspect of this fact is the balance between economy and safety. Accordingly, design of high dams, electricity distribution networks or bridges shall necessitate different coefficients than the ones used in this study.

Conclusions derived in this study hold true for analysis models of a lumped mass at the top of the column in which massless frame only provides stiffness to the system. This assumption is employed in ATC 32-1 [55] Appendix E where single-degree-of-freedom oscillators consisting of reinforced concrete columns with a circular cross-section of 2 meter diameter were studied. Moreover, Kowalsky [22] developed dimensionless serviceability and damage control curvature relationships for lumped mass oscillators of circular bridge columns. Validity of the design procedure is based on the single-mode spectral approach that holds true for simple bridge structures with relatively straight alignment, small skewness and well-balanced spans with equally distributed stiffness [5]. Other bridges not obeying the given assumptions cannot utilize the results of the report.

The author recognizes that the results presented in this thesis are only valid for presumed performance levels whose qualitative descriptions of damage states described in ACI Committee 341 [28] are given in terms of column *mean* drift ratio based on statistical study of column test database.

Reliability of the results is parallel to the reliability of the *median* inelastic displacement ratios since inelastic demand drift for a particular case is compared with performance drift. As an observation, R-factor obtained from back calculation for a particular performance level is very sensitive to inelastic demand drift. In addition, force displacement relationship depends on material models used for concrete and reinforcing steel, ultimate concrete crushing strain, axial-shear-flexure interaction, bilinearization rule of moment curvature relationship and analysis assumptions. Bar slip and shear deformation may have important contributions to total displacement capacity which probably affects inelastic displacement demand of the column at the end.

5.3. Conclusions of the Study

The following conclusions can be drawn for this study;

- Expressions are developed to relate stiffness modification factor to axial load ratio and longitudinal reinforcement ratio. Best fit line is given in Eq.(4.1). Upper and lower bound fit lines corresponding to various axial load ratios are given in Eq.(4.2), Eq.(4.3) and Eq.(4.4). Stiffness modification factors of Caltrans-SDC [18] can be thought as lower bound to be used to estimate elastic displacement demand conservatively.
- Expressions are developed to predict yield curvature of the circular column for a given yield strain of reinforcing steel. Best fit curve is given in Eq.(4.5). Upper and lower bound fit curves are given in Eq.(4.6). Yield curvature keeps constant regardless of flexural strength provided to section. In opposition to the assumption of constant member stiffness that is generally proceeded in force-based design approach, flexural strength dependent member stiffness phenomenon holds true and requires iterative procedure to perform an

accurate analysis of either the elastic period of vibration, or of the elastic distribution of required strength.

- In most of the cases, approximate moment magnification factor approach recommended in AASHTO LRFD [5] yields higher values as compared with the solutions based on actual effective flexural stiffness of the column. AASHTO LRFD [5] produce higher flexural strength demand up to 50-60 % compared to software solutions for high axial load ratios and column aspect ratios. Having a flexural design more than needed strength causes plastic hinging forces to be greater than elastic forces in opposition to desired seismic design approach. Subsequently, design of foundation and its components as pile may be overly conservative because of the use of elastic force demand. To overcome this conclusion, it is recommended that approximate approach can be used with lower bound estimates of stiffness modification factor excluding stiffness reduction factor, ϕ_K.
- None of the bridges designed according to R-factor stipulated by bridge importance category of AASHTO LRFD [5] eventuate with *Delayed Operational* performance level that inelastic demand drift exceeds the mean drift ratio at the onset of cover spalling.
- It is concluded that columns designed according to R=1.5 (Critical Bridges) are capable of satisfying *Fully Functional* performance level except for axial load ratio of 0.1 and column aspect ratio less than 4.0.
- It is seen that columns designed according to R=2.0 (Essential Bridges) are capable of satisfying *Operational* performance level except for axial load ratio of 0.1 and column aspect ratio less than 4.0. Axial load ratios higher than 0.1 probably will perform better than *Operational* performance level. More frequent residual crack widths of 0.01 in (0.25 mm) or wider may be expected as a damage state. Concrete cover spalling is not anticipated.
- Columns designed according to R=3.0 (Other Bridges) are capable of satisfying a performance level better than *Delayed Operational* performance level. Increasing height of spalled region around the bottom of the column can be observed as a damage state. However, initiation of bar buckling is

prevented for columns designed according to requirements of other bridge importance category.

- As a preliminary seismic design recommendation, *R=1.0-1.5* for *Fully Functional*, *R=2.2-2.8* for *Operational* and *R=3.8-4.2* for *Delayed Operational* performance level can be used. Column aspect ratios less than 4.0 should be avoided not to encounter with R-factor out of the given range.
- Due to the deamplification nature of displacement demand observed in soft soil sites (Soil Site IV in AASHTO LRFD [5]) within the range of 0.75-1.4 seconds of normalized periods of vibration, T/T_g, R-factors should be revised including foundation flexibility.
- Dependence of R-factor on the column aspect ratio is established for *Fully Functional* performance level. Expressions (Eq.(4.9), Eq.(4.10) and Eq.(4.11)) are developed to predict R-factor for a particular axial load ratio. It should be kept in mind that R-factor estimates given in corresponding equations constitute upper bound values since inelastic displacement demand is very close proximity of corresponding performance drifts within a given margin. For *Operational* performance level, *R=3.0* can be used for $P_u/A_gf_c=0.1$, *R=4.0* for $P_u/A_gf_c=0.2$, and *R=4.5* for $P_u/A_gf_c=0.3$ as an upper bound estimates.
- In addition to column aspect ratio dependent relations of R-factor, expressions (Eq.(4.12), Eq.(4.13) and Eq.(4.14)) are developed to relate R-factor to period of vibration for a particular axial load ratio. For *Fully Functional* performance level, period of vibrations higher than 2.3 seconds for $P_u/A_gf_c=0.1$, 3.1 seconds for $P_u/A_gf_c=0.2$ and 3.9 seconds for $P_u/A_gf_c=0.3$ are not possible to proceed further with seismic design of circular bridge column. Equations dependent on both column aspect ratio and period of vibration yield almost same R-factor.
- The use of R-factor in seismic design of bridges may not clarify the need for additional checks beyond obtaining moments from elastic analysis and having a design by dividing them by R-factor. Therefore, elastic demand drift and

capacity over inelastic demand displacement measures can become a check in the column design process.

- Elastic demand drift limits given in Eq.(4.20) and Eq.(4.21) can be used for deciding whether selected column aspect ratio is acceptable to satisfy anticipated performance level.
- Expressions for *Fully Functional* performance level (Eq.(4.15) and Eq.(4.16)) are developed to estimate capacity over inelastic demand displacement for a particular axial load ratio. Since columns having aspect ratios less than *4.0* produce higher estimates of capacity over inelastic demand displacement, it should be avoided during design procedure.
- Capacity over inelastic demand displacement equations dependent to period of vibration (Eq.(4.17), Eq.(4.18) and Eq.(4.19)) can be utilized for upper bound estimates of *Fully Functional* performance level.
- Constant capacity over elastic and inelastic demand displacement ranging between *2.7* and *3.0* can be utilized for *Operational* performance level.

REFERENCES

1. Borzi, B., Elnashai, A. S., (2000), Refined Force Reduction Factors for Seismic Design. *Engineering Structures*, 22, 1244-1260.

2. Lehman, D., Moehle, J., Mahin, S., Calderone, A., Henry, L. (2004), Experimental Evaluation of the Seismic Performance of Reinforced Concrete Bridge Columns. *ASCE Journal of Structural Engineering*, 130(6), 869-879.

3. Priestley, M. J. N., Calvi, G. M., Kowalsky, M. J. (2007), *Displacement Based Seismic Design of Structures.* Italy: IUSS PRESS.

4. AASHTO, 2002, *Standard Specifications for Highway Bridges*, American Association of State Highway and Transportation Officials, Washington D.C.

5. AASHTO, 2007, *LRFD Bridge Design Specifications*, American Association of State Highway and Transportation Officials, Washington D.C.

6. Floren, A., Mohammadi, J. (2001), Performance-based Design Approach in Seismic Analysis of Bridges. *ASCE Journal of Bridge Engineering*, 6(1), 37-45.

7. Uang, C. M., Tsai, K. C., and Bruneau, M., 2000, *Seismic Design of Steel Bridges*, Chapter of Bridge Engineering Handbook, edited by Chen W.F., Duan L., CRC Press.

8. Elnashai, A. S., Mwafy, A. M. (2002), Overstrength and Force Reduction Factors of Multistorey Reinforced-Concrete Buildings. *The Structural Design of Tall Buildings,* 11, 329-351.

9. Newmark, N.M., Hall, W. J. (1982), Earthquake Spectra and Design. *EERI Monograph Series.* Oakland: EERI.

10. Riddell, R., Hidalgo, P., Cruz, E. (1987), Statistical Analysis of the Response of Nonlinear Systems Subjected to Earthquakes. *Earthquake Engineering and Structural Dynamics,* 15, 91-104.

11. Miranda, E., Bertero, V. V. (1994), Evaluation of Strength Reduction Factors for Earthquake-Resistant Design. *Earthquake Spectra.* 10(2), 357-379.

12. Nassar, A. A., Krawinkler, H. (1991), Seismic Demands for SDOF and MDOF Systems, Report No.95. *The John A. Blume Earthquake Engineering Center,* Stanford University, Stanford, California.

13. Miranda, E. (1993), Site Dependent Strength Reduction Factor. *ASCE Journal of Structural Engineering*, 119(12),3503-3519.

14. SEAOC, 1995, *Performance based Seismic Engineering of Buildings – Volume I.* Structural Engineers Association of California, Sacramento, California.

15. PEER 2003/18, Performance Models for Flexural Damage in Reinforced Concrete Columns. Michael Berry and Marc Eberhard. August 2003.

16. ATC, 1996, *ATC 32, Improved Seismic Design Criteria for Californian Bridges: Provisional Recommendations*, Applied Technology Council, Redwood City, CA.

17. CALTRANS, 1999, *Bridge Memo to Designers 20-1*: *Seismic Design Methodology*, California Department of Transportation.

18. CALTRANS, 2006, *Seismic Design Criteria Version 1.4*, California Department of Transportation.

19. ATC/MCEER, 2001, *Recommended LRFD Guidelines for the Seismic Design of Highway Bridges*, Applied Technology Council/Multidisciplinary Center for Earthquake Engineering Joint Venture for the National Cooperative Highway Research Program (NCHRP), Washington DC.

20. Avşar Ö., 2009, *Fragility Based Seismic Vulnerability Assessment of Ordinary Highway Bridges in Turkey*, PhD Thesis, Department of Civil Engineering, METU, Ankara.

21. Hose, Y., Silva, P. and Seible, F. (2000), Development of a Performance Evaluation Database for Concrete Bridge Components and Systems under Simulated Seismic Loads. *Earthquake Spectra,* 16(2), 413-442.

22. Kowalsky, M.J., (2000), Deformation Limit States for Circular Reinforced Concrete Bridge Columns. *ASCE Journal of Structural Engineering*, 126(8), 869-878.

23. Priestley, M.J.N., Seible, F. and Calvi, G.M., (1996), *Seismic Design and Retrofit of Bridges*, John Wiley & Sons, Inc., New York, NY.

24. Mander, J.B., Priestley, M.J.N. and Park, R., (1988), Theoretical Stress-Strain Model for Confined Concrete, *Journal of the Structural Division, American Society of Civil Engineers*, Vol. 114, No. 8, 1804-1826.

25. PEER 2000/08, Behavior of Reinforced Concrete Bridge Columns Having Varying Aspect Ratios and Varying Lengths of Confinement. Antony J. Calderone, Dawn E. Lehman and Jack P. Moehle . January 2001.

26. Erduran, E. and Yakut, A., (2004), Drift Based Damage Functions for Reinforced Concrete Columns. *Computers and Structures*, Volume 82 pp. 121-130.

27. PEER 1998/01, Seismic Performance of Well-Confined Concrete Bridge Columns. Dawn E. Lehman and Jack P. Moehle. December 2000.

28. ACI Committee 341, Earthquake-Resistant Concrete Bridges, (1990),Bridge Column Report, Revised SLB 3-24-06, *American Concrete Institute*.

29. PEER 2007/07, Performance Modeling Strategies for Modern Reinforced Concrete Bridge Columns. Michael P. Berry and Marc O. Eberhard. April 2008.

30. PEER 2004/01, Structural Performance Database User's Manual (Version 1.0). Michael Berry, Myles Parrish and Marc Eberhard. January 2004.

31. Camarillo, Haili R., Evaluation of Shear Strength Methodologies for Reinforced Concrete Columns, Department of Civil and Environmental Engineering, University of Washington, 2003.

32. Kunnath K. S., El-Bahy, Ashraf., Taylor, W. A. and Stone, C. W., (1997), NISTIR 6075, Cumulative Seismic Damage of Reinforced Concrete Bridge Piers., *Building and Fire Research Laboratory, National Institute of Standards and Technology*, Gaithersburg.

33. European Committee for Standardization, Eurocode 8, (2005), Design of Structures for Earthquake Resistance Part 3: Assessment and Retrofitting of Buildings, *European Standard EN 1998-3:2005*, Brussels.

34. Moehle, J. P. (1992), Displacement-based Design of RC Structures Subjected to Earthquakes. *Earthquake Spectra.* 8(3), 403-428.

35. Miranda, E., (2001), Estimation of Inelastic Deformation Demands of SDOF Systems. *ASCE Journal of Structural Engineering*, 127(9), 1005-1012.

36. Miranda, E., (2000), Inelastic Displacement Ratios for Structures on Firm Sites. *ASCE Journal of Structural Engineering*, 126(10), 1150-1159.

37. Chopra, A. K, and Chintanapakdee, C. (2004), Inelastic Deformation Ratios for Design and Evaluation of Structures: Single-Degree-of-Freedom Bilinear System. *ASCE Journal of Structural Engineering*, 130(9), 1309-1319.

38. Garcia, R. J. and Miranda, E., (2004), Inelastic Displacement Ratios for Design of Structures on Soft Soil Sites. *ASCE Journal of Structural Engineering*, 130(12), 2051-2061.

39. Garcia, R. J. and Miranda, E., (2005), Errata for "Inelastic Displacement Ratios for Design of Structures on Soft Soil Sites". *ASCE Journal of Structural Engineering*, June 2005, 999.

40. Turkstra, C. J. (1970), Theory of structural design decisions. Study no. 2. Ontario, Canada: Solid Mechanics Division, University of Waterloo.

41. General Directorate of Disaster Affairs Earthquake Research Department, Republic of Turkey, *Türkiye Deprem Bölgeleri Haritası*, www.deprem.gov.tr, last visited: 09.04.2010.

42. Galambos, T. V. (1998), *Guide to Stability Design for Metal Structures.* 5th Edition. Structural Stability Research Council. John Wiley and Sons, Inc., New York, NY.

43. White, D. W., and J. F. Hajjar, (1991), Application of Second-Order Elastic Analysis in LRFD: Research to Practice. *AISC Engineering Journal*, American Institute of Steel Construction, Chicago, IL, 28(4), 133-148.

44. McGuire, W., Gallagher, R. H., and Ziemian, R. D. (2000), *Matrix Structural Analysis.* 2nd Edition. John Wiley and Sons, Inc., New York, NY.

45. Wilson, E. L. and Habibullah, A., SAP2000, *Structural Analysis Program*, Computer and Structures Inc., Berkeley, California, USA, 1995.

46. LARSA 4D, 2008, *Structural and Earthquake Engineering Integrated Analysis and Design Software*, LARSA Inc., New York, USA.

47. Cormen, Thomas H.; Leiserson, Charles E.; Rivest, Ronald L.; Stein, Clifford (2001), *Introduction to Algorithms* (2nd ed.). MIT Press and McGraw-Hill.

48. PCACOL, 1999, *Design and Investigation of Reinforced Concrete Column Sections*, Portland Cement Association, Skokie, IL, USA.

49. Priestley, M. J. N., Seible, F., Calvi, G. M.,1996, *Seismic Design and Retrofit of Bridges*, John Wiley & Sons, New York.

50. Turkish Earthquake Code (2007), Ministry of Public Works and Settlement, Government of Republic of Turkey.

51. USC_RC, *Moment-Curvature, Force-Deflection and Axial Force-Bending Moment Interaction Analysis*, University of Southern California, Civil Engineering Department.

52. XTRACT, 2007, *Cross-Section Analysis Program for Structural Engineers*, TRC/Imbsen Software Systems, California, USA.

53. Setzler E. J., and Sezen, H. (2008), Model for the Lateral Behavior of Reinforced Concrete Columns Including Shear Deformations. *Earthquake Spectra*, 24(2), 493-511.

54. Sezen, H., and Moehle, J. P., (2004), Shear Strength Model for Lightly Reinforced Concrete Columns. *ASCE Journal of Structural Engineering*, 130(11), 1692-1703.

55. ATC, 1996, *ATC 32-1, Improved Seismic Design Criteria for California Bridges: Resource Document*, Applied Technology Council, Redwood City, CA.

56. Gülkan, P., Koçyiğit, A., Yücemen, M. S., Doyuran, V., and Başöz, N., (1993), *En Son Verilere Göre Hazırlanan Türkiye Deprem Bölgeleri Haritası.* Deprem Mühendisliği Araştırma Merkezi, Rapor No. 93-01.

APPENDIX A

SOURCE CODE OF THE ANALYSIS TOOL

****
*** **MAIN FUNCTION** ***
****

```
Private Sub CommandButton2_Click()

Dim n, p, t, steeltension, ratiosteel, fi, seismiczone, start As Double
Dim finishh, alfagross, alfagross1, erroralfa, dataset As Double

dataset = Cells(16, 5).Value
startt = Cells(15, 17).Value - 21
finishh = Cells(15, 19).Value - 21
seismiczone = Cells(5, 11).Value

'ITERATION FOR DATASET, (n)
For n = startt To finishh
If n = dataset + 1 Then
Cells(3, 11).Value = 0.2
seismiczone = Cells(5, 11).Value
ElseIf n = 2 * dataset + 1 Then
Cells(3, 11).Value = 0.3
seismiczone = Cells(5, 11).Value
ElseIf n = 3 * dataset + 1 Then
Cells(3, 11).Value = 0.4
```

```
seismiczone = Cells(5, 11).Value
End If
fi = Cells(21 + n, 42).Value
alfagross1 = 0.4
Cells(21 + n, 11).Value = alfagross1

'ITERATION FOR FINDING ALFAGROSS, (t)
For t = 1 To 10000
If seismiczone = 2 Then

'CALL FOR PROCEDURE "steelratio" FOR SECTION DESIGN
ratiosteel = steelratio(n, fi)
Cells(21 + n, 43).Value = ratiosteel
If ratiosteel = "MAX." Then
Cells(21 + n, 44).Value = "-"
Cells(21 + n, 46).Value = "-"
Cells(21 + n, 47).Value = "-"
Cells(21 + n, 82).Value = "-"
Cells(21 + n, 83).Value = "-"
Cells(21 + n, 84).Value = "-"
Cells(21 + n, 85).Value = "-"
Cells(21 + n, 86).Value = "-"
Cells(21 + n, 87).Value = "-"

'EXIT FOR ITERATION FOR FINDING ALFAGROSS, (t)
Exit For
ElseIf ratiosteel <> "MAX." Then

'CALL FOR PROCEDURE "steelstrain" TO CALCULATE EXTREME TENSION STEEL STRAIN
steeltension = -1 * steelstrain(n)
Cells(21 + n, 44).Value = steeltension
```

```
'CALL FOR PROCEDURE "nominalmoment" TO CALCULATE NOMINAL MOMENT CAPACITY
Cells(21 + n, 47).Value = nominalmoment(n, 2) / 1000000
'CALL FOR PROCEDURE "momentcurvature" TO OBTAIN MOMENT CURVATURE RELATIONSHIP
momentcurvature (n)
alfagross = Cells(21 + n, 89).Value
erroralfa = Abs((alfagross1 - alfagross) / alfagross1) * 100
If erroralfa <= 1 Then

'EXIT FOR ITERATION FOR FINDING ALFAGROSS, (t)
Exit For
ElseIf erroralfa > 1 Then
alfagross1 = (alfagross + alfagross1) / 2
Cells(21 + n, 11).Value = alfagross1
End If
End If
ElseIf seismiczone <> 2 Then
ratiosteel = steelratio(n, fi)
Cells(21 + n, 43).Value = ratiosteel
If ratiosteel = "MAX." Then
Cells(21 + n, 44).Value = "-"
Cells(21 + n, 46).Value = "-"
Cells(21 + n, 47).Value = "-"
Cells(21 + n, 82).Value = "-"
Cells(21 + n, 83).Value = "-"
Cells(21 + n, 84).Value = "-"
Cells(21 + n, 85).Value = "-"
Cells(21 + n, 86).Value = "-"
Cells(21 + n, 87).Value = "-"

'EXIT FOR ITERATION FOR FINDING ALFAGROSS, (t)
```

```
Exit For
ElseIf ratiosteel <> "MAX." Then
If Cells(21 + n, 42).Value <> 0.5 Then
steeltension = -1 * steelstrain(n)
Cells(21 + n, 44).Value = steeltension
End If
Cells(21 + n, 47).Value = nominalmoment(n, 2) / 1000000
momentcurvature (n)
alfagross = Cells(21 + n, 89).Value
erroralfa = Abs((alfagross1 - alfagross) / alfagross1) * 100
If erroralfa <= 1 Then

'EXIT FOR ITERATION FOR FINDING ALFAGROSS, (t)
Exit For
ElseIf erroralfa > 1 Then
alfagross1 = (alfagross + alfagross1) / 2
Cells(21 + n, 11).Value = alfagross1
End If
End If
End If

Next t
Next n

End Sub
```

```
**********************************************************************
***             PROCEDURE “steelratio” FOR SECTION DESIGN            ***
**********************************************************************
```

```
Public Function steelratio(n, fi)
Dim fc, fy, ec, ey, elasmod, min, max, limitp, limitm As Double
```

```
Dim spacing, cover, d, pdesign, mdesign As Double
Dim c1, c2, c, ratio1, ratio2, ratio, pi, x As Double
Dim nbar, areasteel, errorp, errorm, k1 As Double
Dim dist, area1, area2, area, alfa, cofgrav, cofgrav1 As Double
Dim forcesteel, momentsteel, forceconcrete, momentconcrete, totalforce As Double
Dim steelx(500), steely(500), strainsteel(500), totalmoment(10000) As Double
Dim i, k, j, m, t

pi = 3.14159265358979
fc = Cells(4, 16).Value
fy = Cells(4, 19).Value
cover = Cells(9, 16).Value
spacing = Cells(11, 19).Value
min = Cells(10, 16).Value
max = Cells(11, 16).Value
limitp = Cells(9, 19).Value
limitm = Cells(10, 19).Value
ec = Cells(7, 16).Value
elasmod = Cells(5, 19).Value
ey = Cells(6, 19).Value
If fc <= 28 Then
k1 = 0.85
ElseIf (0.85 - (fc - 28) * 0.05 / 7) <= 0.65 Then
k1 = 0.65
ElseIf fc > 28 Then
k1 = 0.85 - (fc - 28) * 0.05 / 7
End If
d = 1000 * Cells(21 + n, 2).Value
pdesign = 1000 * Cells(21 + n, 35).Value
mdesign = 1000000 * Cells(21 + n, 39).Value
nbar = Int(pi * (d - 2 * cover) / spacing)
steelx(1) = 0
```

steely(1) = d / 2 – cover

'ITERATION FOR FINDING COORDINATES OF REINFORCING STEEL, (i)

For i = 2 To nbar

steelx(i) = steelx(1) + Sin(2 * pi * (i - 1) / nbar) * steely(1)

steely(i) = Cos(2 * pi * (i - 1) / nbar) * steely(1)

Next i

ratio1 = 1

ratio2 = 1

'ITERATION FOR OPTIMUM REINFORCEMENT RATIO, (m)

For m = 1 To 10000

KONTROL:

ratio = (ratio1 + ratio2) / 2

areasteel = (pi * (d ^ 2) / 4) * (ratio / 100) / nbar

c1 = 0

c2 = 4 * d

'ITERATION FOR FINDING NEUTRAL AXIS DEPTH, (k)

For k = 1 To 10000

c = (c1 + c2) / 2

totalforce = 0

totalmoment(m) = 0

'ITERATION FOR REINFORCING BAR STRESS, (j)

For j = 1 To nbar

If (d / 2) > steely(j) And steely(j) >= (d / 2 - c) Then

strainsteel(j) = ec * (1 - (d / 2 - steely(j)) / c)

If Abs(strainsteel(j)) >= (ey) Then

forcesteel = fy * areasteel

```
momentsteel = forcesteel * steely(j)
ElseIf (ey) > Abs(strainsteel(j)) Then
forcesteel = strainsteel(j) * elasmod * areasteel
momentsteel = forcesteel * steely(j)
End If
ElseIf (d / 2 - c) > steely(j) And steely(j) > (-d / 2) Then
strainsteel(j) = ec * (((c - d / 2) + steely(j)) / c)
If Abs(strainsteel(j)) >= (ey) Then
forcesteel = fy * areasteel * (-1)
momentsteel = forcesteel * steely(j)
ElseIf (ey) > Abs(strainsteel(j)) Then
forcesteel = strainsteel(j) * elasmod * areasteel
momentsteel = forcesteel * steely(j)
End If
End If
totalforce = totalforce + forcesteel
totalmoment(m) = totalmoment(m) + momentsteel

Next j

'RECTANGULAR STRESS BLOCK CALCULATION
If (k1 * c) <= (d / 2) Then
dist = d / 2 - k1 * c
x = 1 - 2 * k1 * c / d
alfa = Atn(-x / Sqr(-x * x + 1)) + 2 * Atn(1)
area1 = (d ^ 2) * alfa / 4
area2 = dist * d * Sin(alfa) / 2
area = area1 - area2
cofgrav = (area1 * d * Sin(alfa) / (3 * alfa) - area2 * 2 * dist / 3) / area
ElseIf d > (k1 * c) And (k1 * c) > (d / 2) Then
dist = k1 * c - d / 2
x = 2 * k1 * c / d - 1
```

```
alfa = Atn(-x / Sqr(-x * x + 1)) + 2 * Atn(1)
area1 = (d ^ 2) * alfa / 4
area2 = dist * d * Sin(alfa) / 2
area = pi * (d ^ 2) / 4 - (area1 - area2)
cofgrav1 = (area1 * d * Sin(alfa) / (3 * alfa) - area2 * 2 * dist / 3) / (area1 - area2)
cofgrav = (area1 - area2) * cofgrav1 / area
ElseIf (k1 * c) >= d Then
area = pi * (d ^ 2) / 4
cofgrav = 0
End If
forceconcrete = 0.85 * fc * area
momentconcrete = forceconcrete * cofgrav
totalforce = totalforce + forceconcrete
totalmoment(m) = totalmoment(m) + momentconcrete
errorp = ((fi * totalforce - pdesign) / pdesign) * 100        '
If limitp >= errorp And errorp >= (-limitp) Then

'EXIT FOR ITERATION FOR FINDING NEUTRAL AXIS DEPTH, (k)
Exit For
ElseIf errorp < 0 Then
c1 = c
ElseIf errorp > 0 Then
c2 = c
End If

Next k

If m = min And (fi * totalmoment(m) >= mdesign) Then
ratio = 1

'EXIT FOR ITERATION FOR OPTIMUM REINFORCEMENT RATIO, (m)
Exit For
```

ElseIf m = max And (fi * totalmoment(m) <= mdesign) Then

ratio = "MAX."

'EXIT FOR ITERATION FOR OPTIMUM REINFORCEMENT RATIO, (m)

Exit For

ElseIf m = max Then

For t = min To (max - 1)

If (fi * totalmoment(t)) <= mdesign And (fi * totalmoment(t + 1)) > mdesign Then

ratio1 = t

ratio2 = t + 1

m = m + 1

GoTo KONTROL

End If

Next t

ElseIf m < max Then

m = m + 1

ratio1 = m

ratio2 = m

GoTo KONTROL

ElseIf m > max Then

errorm = ((fi * totalmoment(m) - mdesign) / mdesign) * 100

If limitm >= errorm And errorm >= (-limitm) Then

'EXIT FOR ITERATION FOR OPTIMUM REINFORCEMENT RATIO, (m)

Exit For

ElseIf errorm < 0 Then

ratio1 = ratio

ElseIf errorm > 0 Then

ratio2 = ratio

End If

End If

Next m

steelratio = ratio

End Function

****

***** PROCEDURE "steelstrain" TO CALCULATE EXTREME *****

***** TENSION STEEL STRAIN *****

****

Public Function steelstrain(n)

```
Dim fc, fy, ec, ey, elasmod, min, max, limitp, limitm, spacing As Double
Dim cover, d, pdesign, mdesign As Double
Dim c1, c2, c, ratio1, ratio2, ratio, pi, x, kalan, extr, fimax, fimin As Double
Dim nbar, areasteel, errorp, errorm, k1 As Double
Dim dist, area1, area2, area, alfa, cofgrav, cofgrav1 As Double
Dim forcesteel, momentsteel, totalmomentmin, totalmomentmax As Double
Dim forceconcrete, momentconcrete, totalforce As Double
Dim steelx(500), steely(500), strainsteel(500), totalmoment As Double
Dim i, k, j, m, t, kmin, kmax, jmin, jmax

pi = 3.14159265358979
fc = Cells(4, 16).Value
fy = Cells(4, 19).Value
cover = Cells(9, 16).Value
spacing = Cells(11, 19).Value
min = Cells(10, 16).Value
```

```
max = Cells(11, 16).Value
limitp = Cells(9, 19).Value
ec = Cells(7, 16).Value
elasmod = Cells(5, 19).Value
ey = Cells(6, 19).Value
ratio = Cells(21 + n, 43).Value
If fc <= 28 Then
k1 = 0.85
ElseIf (0.85 - (fc - 28) * 0.05 / 7) <= 0.65 Then
k1 = 0.65
ElseIf fc > 28 Then
k1 = 0.85 - (fc - 28) * 0.05 / 7
End If
d = 1000 * Cells(21 + n, 2).Value

'UNDER ZERO AXIAL LOAD RATIO
pdesign = 1
nbar = Int(pi * (d - 2 * cover) / spacing)
kalan = nbar Mod 2
If kalan = 1 Then
extr = (nbar + 1) / 2
ElseIf kalan = 0 Then
extr = nbar / 2 + 1
End If
steelx(1) = 0
steely(1) = d / 2 – cover

'ITERATION FOR FINDING COORDINATES OF REINFORCING STEEL, (i)
For i = 2 To nbar
steelx(i) = steelx(1) + Sin(2 * pi * (i - 1) / nbar) * steely(1)
steely(i) = Cos(2 * pi * (i - 1) / nbar) * steely(1)
```

```
Next i

areasteel = (pi * (d ^ 2) / 4) * (ratio / 100) / nbar
c1 = 0
c2 = 4 * d

'ITERATION FOR FINDING NEUTRAL AXIS DEPTH, (k)
For k = 1 To 10000
c = (c1 + c2) / 2
totalforce = 0
totalmoment = 0
'ITERATION FOR REINFORCING BAR STRESS, (j)
For j = 1 To nbar
If (d / 2) > steely(j) And steely(j) >= (d / 2 - c) Then
strainsteel(j) = ec * (1 - (d / 2 - steely(j)) / c)
If Abs(strainsteel(j)) >= (ey) Then
forcesteel = fy * areasteel
momentsteel = forcesteel * steely(j)
ElseIf (ey) > Abs(strainsteel(j)) Then
forcesteel = strainsteel(j) * elasmod * areasteel
momentsteel = forcesteel * steely(j)
End If
ElseIf (d / 2 - c) > steely(j) And steely(j) > (-d / 2) Then
strainsteel(j) = ec * (((c - d / 2) + steely(j)) / c)
If Abs(strainsteel(j)) >= (ey) Then
forcesteel = fy * areasteel * (-1)
momentsteel = forcesteel * steely(j)
ElseIf (ey) > Abs(strainsteel(j)) Then
forcesteel = strainsteel(j) * elasmod * areasteel
momentsteel = forcesteel * steely(j)
End If
End If
```

```
totalforce = totalforce + forcesteel
totalmoment = totalmoment + momentsteel

Next j

'RECTANGULAR STRESS BLOCK CALCULATION
If (k1 * c) <= (d / 2) Then
dist = d / 2 - k1 * c
x = 1 - 2 * k1 * c / d
alfa = Atn(-x / Sqr(-x * x + 1)) + 2 * Atn(1)
area1 = (d ^ 2) * alfa / 4
area2 = dist * d * Sin(alfa) / 2
area = area1 - area2
cofgrav = (area1 * d * Sin(alfa) / (3 * alfa) - area2 * 2 * dist / 3) / area
ElseIf d > (k1 * c) And (k1 * c) > (d / 2) Then
dist = k1 * c - d / 2
x = 2 * k1 * c / d - 1
alfa = Atn(-x / Sqr(-x * x + 1)) + 2 * Atn(1)
area1 = (d ^ 2) * alfa / 4
area2 = dist * d * Sin(alfa) / 2
area = pi * (d ^ 2) / 4 - (area1 - area2)
cofgrav1 = (area1 * d * Sin(alfa) / (3 * alfa) - area2 * 2 * dist / 3) / (area1 - area2)
cofgrav = (area1 - area2) * cofgrav1 / area
ElseIf (k1 * c) >= d Then
area = pi * (d ^ 2) / 4
cofgrav = 0
End If
forceconcrete = 0.85 * fc * area
momentconcrete = forceconcrete * cofgrav
totalforce = totalforce + forceconcrete
totalmoment = totalmoment + momentconcrete
errorp = ((totalforce) / pdesign) * 100
```

```
If limitp >= errorp And errorp >= (-limitp) Then

'EXIT FOR ITERATION FOR FINDING NEUTRAL AXIS DEPTH, (k)
Exit For
ElseIf errorp < 0 Then
c1 = c
ElseIf errorp > 0 Then
c2 = c
End If

Next k

steelstrain = strainsteel(extr)
End Function

*****************************************************************
***          PROCEDURE "nominalmoment" TO CALCULATE          ***
***                 NOMINAL MOMENT CAPACITY                  ***
*****************************************************************

Public Function nominalmoment(n, index)

Dim fc, fy, ec, ey, elasmod, min, max, limitp, limitm, spacing As Double
Dim cover, d, pdesign, mdesign As Double
Dim c1, c2, c, ratio1, ratio2, ratio, pi, x, kalan, extr, fimax, fimin As Double
Dim nbar, areasteel, errorp, errorm, k1 As Double
Dim dist, area1, area2, area, alfa, cofgrav, cofgrav1 As Double
Dim forcesteel, momentsteel, totalmomentmin, totalmomentmax As Double
forceconcrete, momentconcrete, totalforce As Double
Dim i, k, j, m, t, kmin, kmax, jmin, jmax
Dim steelx(500), steely(500), strainsteel(500), totalmoment As Double
```

```
pi = 3.14159265358979
fc = Cells(4, 16).Value
fy = Cells(4, 19).Value
cover = Cells(9, 16).Value
spacing = Cells(11, 19).Value
min = Cells(10, 16).Value
max = Cells(11, 16).Value
limitp = Cells(9, 19).Value
ec = Cells(7, 16).Value
elasmod = Cells(5, 19).Value
ey = Cells(6, 19).Value
ratio = Cells(21 + n, 43).Value
If index = 2 Then
fc = 1.5 * fc
fy = 1.25 * fy
ec = 0.01
ey = fy / elasmod
End If
If fc <= 28 Then
k1 = 0.85
ElseIf (0.85 - (fc - 28) * 0.05 / 7) <= 0.65 Then
k1 = 0.65
ElseIf fc > 28 Then
k1 = 0.85 - (fc - 28) * 0.05 / 7
End If
d = 1000 * Cells(21 + n, 2).Value
pdesign = 1000 * Cells(21 + n, 35).Value
nbar = Int(pi * (d - 2 * cover) / spacing)
steelx(1) = 0
steely(1) = d / 2 – cover
```

'ITERATION FOR FINDING COORDINATES OF REINFORCING STEEL, (i)

```
For i = 2 To nbar
steelx(i) = steelx(1) + Sin(2 * pi * (i - 1) / nbar) * steely(1)
steely(i) = Cos(2 * pi * (i - 1) / nbar) * steely(1)

Next i

areasteel = (pi * (d ^ 2) / 4) * (ratio / 100) / nbar
c1 = 0
c2 = 4 * d

'ITERATION FOR FINDING NEUTRAL AXIS DEPTH, (k)
For k = 1 To 10000
c = (c1 + c2) / 2
totalforce = 0
totalmoment = 0
'ITERATION FOR REINFORCING BAR STRESS, (j)
For j = 1 To nbar
If (d / 2) > steely(j) And steely(j) >= (d / 2 - c) Then
strainsteel(j) = ec * (1 - (d / 2 - steely(j)) / c)
If Abs(strainsteel(j)) >= (ey) Then
forcesteel = fy * areasteel
momentsteel = forcesteel * steely(j)
ElseIf (ey) > Abs(strainsteel(j)) Then
forcesteel = strainsteel(j) * elasmod * areasteel
momentsteel = forcesteel * steely(j)
End If
ElseIf (d / 2 - c) > steely(j) And steely(j) > (-d / 2) Then
strainsteel(j) = ec * (((c - d / 2) + steely(j)) / c)
If Abs(strainsteel(j)) >= (ey) Then
forcesteel = fy * areasteel * (-1)
momentsteel = forcesteel * steely(j)
ElseIf (ey) > Abs(strainsteel(j)) Then
```

```
forcesteel = strainsteel(j) * elasmod * areasteel
momentsteel = forcesteel * steely(j)
End If
End If
totalforce = totalforce + forcesteel
totalmoment = totalmoment + momentsteel

Next j

'RECTANGULAR STRESS BLOCK CALCULATION
If (k1 * c) <= (d / 2) Then
dist = d / 2 - k1 * c
x = 1 - 2 * k1 * c / d
alfa = Atn(-x / Sqr(-x * x + 1)) + 2 * Atn(1)
area1 = (d ^ 2) * alfa / 4
area2 = dist * d * Sin(alfa) / 2
area = area1 - area2
cofgrav = (area1 * d * Sin(alfa) / (3 * alfa) - area2 * 2 * dist / 3) / area
ElseIf d > (k1 * c) And (k1 * c) > (d / 2) Then
dist = k1 * c - d / 2
x = 2 * k1 * c / d - 1
alfa = Atn(-x / Sqr(-x * x + 1)) + 2 * Atn(1)
area1 = (d ^ 2) * alfa / 4
area2 = dist * d * Sin(alfa) / 2
area = pi * (d ^ 2) / 4 - (area1 - area2)
cofgrav1 = (area1 * d * Sin(alfa) / (3 * alfa) - area2 * 2 * dist / 3) / (area1 - area2)
cofgrav = (area1 - area2) * cofgrav1 / area
ElseIf (k1 * c) >= d Then
area = pi * (d ^ 2) / 4
cofgrav = 0
End If
forceconcrete = 0.85 * fc * area
```

```
momentconcrete = forceconcrete * cofgrav
totalforce = totalforce + forceconcrete
totalmoment = totalmoment + momentconcrete
errorp = ((totalforce - pdesign) / pdesign) * 100
If limitp >= errorp And errorp >= (-limitp) Then

'EXIT FOR ITERATION FOR FINDING NEUTRAL AXIS DEPTH, (k)
Exit For
ElseIf errorp < 0 Then
c1 = c
ElseIf errorp > 0 Then
c2 = c
End If

Next k

nominalmoment = totalmoment
End Function
```

****

*****   PROCEDURE "momentcurvature" TO OBTAIN   *****

*****   MOMENT CURVATURE RELATIONSHIP   *****

****

```
Public Function momentcurvature(n)

Dim fy, fsu, esh, esu, ey, fcc, rcc, rco, ecc, fco, eco, esp, ecu As Double
Dim coverrein, limitpp, coverun, pdesign, nbar As Double
Dim areasteel, d, incstrain, thick As Double
Dim dist, xx1, xx2, alfa1, alfa2, coor, unconstrain, x, unconstress As Double
Dim strr, length1, lengthcon, lengthun, constrain, constress As Double
Dim errorpp, kalan, extr, curv, pretotal, check As Double
```

```
Dim totalforce, totalmoment, forcesteel, momentsteel, unconforce As Double
Dim unconmoment, conforce, conmoment As Double
Dim momenty, curvy, momentult, curvult, momentyy As Double
Dim curvyy, count, energy, spacing, ratio As Double
Dim c1, c2, c, pi As Double
Dim i, k, j, m, t
Dim steelx(150), steely(150), strainsteel(150), moment(250) As Double
Dim curvature(250), steelextr(250), straincon(250) As Double

fy = Cells(4, 26).Value
fsu = Cells(5, 26).Value
ey = Cells(7, 26).Value
esh = Cells(8, 26).Value
esu = Cells(9, 26).Value
fcc = Cells(21 + n, 75).Value
rcc = Cells(21 + n, 78).Value
rco = Cells(21 + n, 81).Value
ecc = Cells(21 + n, 76).Value
fco = Cells(4, 23).Value
eco = Cells(5, 23).Value
esp = Cells(6, 23).Value
ecu = Cells(21 + n, 79).Value
pi = 3.14159265358979
momenty = 0
curvy = 0
count = 0
moment(0) = 0
curvature(0) = 0
steelextr(0) = 0
straincon(0) = 0
energy = 0
ratio = Cells(21 + n, 43).Value
```

```
spacing = Cells(11, 19).Value
coverrein = Cells(11, 23).Value
coverun = Cells(12, 23).Value
limitpp = Cells(12, 26).Value
pdesign = (Cells(21 + n, 35).Value) * 1000
d = (Cells(21 + n, 2).Value) * 1000
incstrain = Cells(11, 26).Value
thick = Cells(13, 23).Value
nbar = Int(pi * (d - 2 * coverrein) / spacing)
areasteel = (pi * (d ^ 2) / 4) * (ratio / 100) / nbar
steelx(1) = 0
steely(1) = d / 2 – coverrein

'ITERATION FOR FINDING COORDINATES OF REINFORCING STEEL, (t)
For t = 2 To nbar
steelx(t) = steelx(1) + Sin(2 * pi * (t - 1) / nbar) * steely(1)
steely(t) = Cos(2 * pi * (t - 1) / nbar) * steely(1)

Next t
'ITERATION FOR ULTIMATE CONCRETE CRUSHING STRAIN, (i)
For i = incstrain To (ecu + incstrain) Step incstrain
If check = 2 Then
GoTo skip1
End If
If i >= 0 And (2 * eco) >= i Then
x = i / eco
unconstress = fco * x * rco / (rco - 1 + x ^ rco)
unconforce = unconstress * pi * (d ^ 2 - (d - 2 * coverun) ^ 2) / 4
ElseIf i > (2 * eco) And esp >= i Then
strr = fco * 2 * rco / (rco - 1 + 2 ^ rco)
unconstress = strr - (i - 2 * eco) * strr / (esp - 2 * eco)
unconforce = unconstress * pi * (d ^ 2 - (d - 2 * coverun) ^ 2) / 4
```

```
ElseIf i > esp Then
unconforce = 0
End If
If ecu >= i Then
x = i / ecc
constress = fcc * x * rcc / (rcc - 1 + x ^ rcc)
conforce = constress * pi * ((d - 2 * coverun) ^ 2) / 4
ElseIf i > ecu Then
conforce = 0
End If
If i <= ey Then
forcesteel = i * 200000 * areasteel * nbar
ElseIf i <= esh And i > ey Then
forcesteel = fy * areasteel * nbar
ElseIf i > esh And esu >= i Then
forcesteel = (fsu - (fsu - fy) * (((esu - i) / (esu - esh)) ^ 2)) * areasteel * nbar
ElseIf i > esu Then
forcesteel = 0
End If
pretotal = forcesteel + conforce + unconforce
If (1.1 * pdesign) >= pretotal Then
check = 1
GoTo skip2
ElseIf pdesign < pretotal Then
check = 2
End If
skip1:
c1 = 0
c2 = 4 * d

'ITERATION FOR FINDING NEUTRAL AXIS DEPTH, (k)
For k = 1 To 10000
```

```
c = (c1 + c2) / 2
totalforce = 0
totalmoment = 0
forcesteel = 0
momentsteel = 0

'ITERATION FOR REINFORCING BAR STRESS, (j)
For j = 1 To nbar
If (d / 2 > steely(j)) And (steely(j) >= (d / 2 - c)) Then
strainsteel(j) = i * (c - (d / 2 - steely(j))) / (c - coverun)
If strainsteel(j) <= ey Then
forcesteel = strainsteel(j) * 200000 * areasteel
momentsteel = forcesteel * steely(j)
ElseIf strainsteel(j) <= esh And strainsteel(j) > ey Then
forcesteel = fy * areasteel
momentsteel = forcesteel * steely(j)
ElseIf strainsteel(j) > esh And esu >= strainsteel(j) Then
 forcesteel = (fsu - (fsu - fy) * (((esu - strainsteel(j)) / (esu - esh)) ^ 2)) * areasteel
momentsteel = forcesteel * steely(j)
ElseIf strainsteel(j) > esu Then
forcesteel = 0
momentsteel = 0
End If
ElseIf ((d / 2 - c) > steely(j)) And (steely(j) > (-d / 2)) Then
strainsteel(j) = i * (c - (d / 2 - steely(j))) / (c - coverun)
If Abs(strainsteel(j)) <= ey Then
forcesteel = strainsteel(j) * 200000 * areasteel
momentsteel = forcesteel * steely(j)
ElseIf Abs(strainsteel(j)) <= esh And Abs(strainsteel(j)) > ey Then
forcesteel = -fy * areasteel
momentsteel = forcesteel * steely(j)
ElseIf Abs(strainsteel(j)) > esh And esu >= Abs(strainsteel(j)) Then
```

```
        forcesteel = -(fsu - (fsu - fy) * (((esu - Abs(strainsteel(j))) / (esu - esh)) ^ 2)) *
        areasteel
momentsteel = forcesteel * steely(j)
ElseIf Abs(strainsteel(j)) > esu Then
forcesteel = 0
momentsteel = 0
End If
End If
totalforce = totalforce + forcesteel
totalmoment = totalmoment + momentsteel

Next j

conforce = 0
unconforce = 0
conmoment = 0
unconmoment = 0

'ITERATION FOR CONFINED AND UNCONFINED CONCRETE FORCES, (m)
For m = thick / 2 To c Step thick
If coverun >= (m + (thick / 2)) Then
dist = d / 2 - m
xx1 = dist * 2 / d
alfa1 = Atn(-xx1 / Sqr(-xx1 * xx1 + 1)) + 2 * Atn(1)
lengthun = Abs(Sin(alfa1) * d)
coor = d / 2 - m
unconstrain = i * (c - (d / 2) + coor) / (c - coverun)
If unconstrain >= 0 And (2 * eco) >= unconstrain Then
x = unconstrain / eco
unconstress = fco * x * rco / (rco - 1 + x ^ rco)
unconforce = unconstress * thick * lengthun
unconmoment = unconforce * coor
```

```
ElseIf unconstrain > (2 * eco) And esp >= unconstrain Then
strr = fco * 2 * rco / (rco - 1 + 2 ^ rco)
unconstress = strr - (unconstrain - 2 * eco) * strr / (esp - 2 * eco)
unconforce = unconstress * thick * lengthun
unconmoment = unconforce * coor
ElseIf unconstrain > esp Then
unconforce = 0
unconmoment = 0
End If
conforce = 0
conmoment = 0
ElseIf (m - (thick / 2)) >= coverun And (d - coverun) >= (m + (thick / 2)) Then
dist = d / 2 - m
xx1 = dist * 2 / d
xx2 = dist / (d / 2 - coverun)
alfa1 = Atn(-xx1 / Sqr(-xx1 * xx1 + 1)) + 2 * Atn(1)
alfa2 = Atn(-xx2 / Sqr(-xx2 * xx2 + 1)) + 2 * Atn(1)
length1 = Abs(Sin(alfa1) * d)
lengthcon = Abs(Sin(alfa2) * (d / 2 - coverun) * 2)
lengthun = length1 - lengthcon
coor = d / 2 - m
unconstrain = i * (c - (d / 2) + coor) / (c - coverun)
If unconstrain >= 0 And (2 * eco) >= unconstrain Then
x = unconstrain / eco
unconstress = fco * x * rco / (rco - 1 + x ^ rco)
unconforce = unconstress * thick * lengthun
unconmoment = unconforce * coor
ElseIf unconstrain > (2 * eco) And esp >= unconstrain Then
strr = fco * 2 * rco / (rco - 1 + 2 ^ rco)
unconstress = strr - (unconstrain - 2 * eco) * strr / (esp - 2 * eco)
unconforce = unconstress * thick * lengthun
unconmoment = unconforce * coor
```

```
ElseIf unconstrain > esp Then
unconforce = 0
unconmoment = 0
End If
constrain = unconstrain
If ecu >= constrain Then
x = constrain / ecc
constress = fcc * x * rcc / (rcc - 1 + x ^ rcc)
conforce = constress * thick * lengthcon
conmoment = conforce * coor
ElseIf constrain > ecu Then
conforce = 0
conmoment = 0
End If
ElseIf (d - coverun) <= (m - (thick / 2)) And d >= (m + (thick / 2)) Then
dist = d / 2 - m
xx1 = dist * 2 / d
alfa1 = Atn(-xx1 / Sqr(-xx1 * xx1 + 1)) + 2 * Atn(1)
lengthun = Abs(Sin(alfa1) * d)
coor = d / 2 - m
unconstrain = i * (c - (d / 2) + coor) / (c - coverun)
If unconstrain >= 0 And (2 * eco) >= unconstrain Then
x = unconstrain / eco
unconstress = fco * x * rco / (rco - 1 + x ^ rco)
unconforce = unconstress * thick * lengthun
unconmoment = unconforce * coor
ElseIf unconstrain > (2 * eco) And esp >= unconstrain Then
strr = fco * 2 * rco / (rco - 1 + 2 ^ rco)
unconstress = strr - (unconstrain - 2 * eco) * strr / (esp - 2 * eco)
unconforce = unconstress * thick * lengthun
unconmoment = unconforce * coor
ElseIf unconstrain > esp Then
```

unconforce = 0

unconmoment = 0

End If

conforce = 0

conmoment = 0

ElseIf (m - (thick / 2)) >= d Then

unconforce = 0

unconmoment = 0

conforce = 0

conmoment = 0

'EXIT FOR ITERATION FOR CONFINED AND UNCONFINED CONCRETE FORCES, (m)

Exit For

End If

totalforce = totalforce + conforce + unconforce

totalmoment = totalmoment + conmoment + unconmoment

Next m

errorpp = 100 * (totalforce - pdesign) / pdesign

If errorpp >= (-limitpp) And limitpp >= errorpp Then

'ITERATION FOR FINDING NEUTRAL AXIS DEPTH, (k)

Exit For

ElseIf errorpp < 0 Then

c1 = c

ElseIf errorpp > 0 Then

c2 = c

End If

Next k

```
kalan = nbar Mod 2
If kalan = 1 Then
extr = (nbar + 1) / 2
ElseIf kalan = 0 Then
extr = nbar / 2 + 1
End If
If Abs(strainsteel(extr)) > esu Then
Cells(21 + n, 82).Value = "Steel reached a tensile strain of " & esu & "."

'EXIT FOR ITERATION FOR ULTIMATE CONCRETE CRUSHING STRAIN, (i)
Exit For
ElseIf Abs(strainsteel(extr)) <= esu Then
count = count + 1
    Cells(21 + n, 82).Value = "Concrete reached a crushing strain of " & Round(ecu, 4) & "."
moment(count) = totalmoment / 1000000
curvature(count) = 1000 * i / (c - coverun)
steelextr(count) = strainsteel(extr)
straincon(count) = i * c / (c - coverun)
End If
If momenty = 0 Then
If Abs(steelextr(count)) >= ey And (Abs(straincon(count)) < eco) Then
    momenty = moment(count - 1) + ((moment(count) - moment(count - 1)) / (Abs(steelextr(count)) - Abs(steelextr(count - 1)))) * (ey - Abs(steelextr(count - 1)))
    curvy = curvature(count - 1) + ((curvature(count) - curvature(count - 1)) / (Abs(steelextr(count)) - Abs(steelextr(count - 1)))) * (ey - Abs(steelextr(count - 1)))
ElseIf Abs(steelextr(count)) < ey And (Abs(straincon(count)) >= eco) Then
    momenty = moment(count - 1) + ((moment(count) - moment(count - 1)) / (Abs(straincon(count)) - Abs(straincon(count - 1)))) * (eco - Abs(straincon(count - 1)))
```

```
        curvy = curvature(count - 1) + ((curvature(count) - curvature(count - 1)) /
        (Abs(straincon(count)) - Abs(straincon(count - 1)))) * (eco -
        Abs(straincon(count - 1)))
ElseIf Abs(steelextr(count)) >= ey And (Abs(straincon(count)) >= eco) Then
        momenty = moment(count - 1) + ((moment(count) - moment(count - 1)) /
        (Abs(steelextr(count)) - Abs(steelextr(count - 1)))) * (ey - Abs(steelextr(count
        - 1)))
        curvy = curvature(count - 1) + ((curvature(count) - curvature(count - 1)) /
        (Abs(steelextr(count)) - Abs(steelextr(count - 1)))) * (ey - Abs(steelextr(count
        - 1)))
End If
End If
        energy = energy + (moment(count) + moment(count - 1)) * (curvature(count)
        - curvature(count - 1)) / 2
skip2:

Next i

momentult = moment(count)
curvult = curvature(count)
Cells(21 + n, 83).Value = curvy
Cells(21 + n, 86).Value = momentult
Cells(21 + n, 87).Value = curvult
        curvyy = 2 * (energy - momentult * curvult / 2) / (momenty * curvult / curvy
        - momentult)
momentyy = momenty * curvyy / curvy
Cells(21 + n, 84).Value = momentyy
Cells(21 + n, 85).Value = curvy

End Function
```